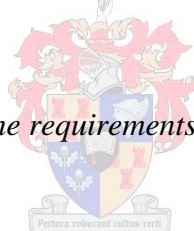


A study on the reversible photo-induced isomerisation of platinum(II) and palladium(II) complexes of the *N,N*-dialkyl-*N'*-acyl(aroyl)thioureas with reversed-phase HPLC separation from related rhodium(III), ruthenium(III) and iridium(III) complexes

A thesis submitted to

STELLENBOSCH UNIVERSITY

In fulfillment of the requirements for the degree of



MASTER OF SCIENCE

By

Henry Ane Nkabyo

Supervisor: Prof. Klaus Koch

April 2014

Declaration

By submitting this thesis electronically, I declare that the entirety of the work contained herein is my own, original work, that I am the owner of the copyright therefore (unless to the extent of explicitly otherwise states) and that I have not previously in its entirety or in part submitted it for obtaining any qualification.

April 2014

Acknowledgements

I hereby acknowledge the support of the following people throughout the course of this study:

- My supervisor Professor Klaus Koch for teaching, guidance, mentoring and support throughout my studies.
- The University of Stellenbosch PGM research group for their contributions, discussions and comments throughout the course of my studies.
- Mr Malcom Taylor for assistance with system setup during the study.
- Egmont Rohwer of the Laser Physics Institute for assistance with laser experiments.
- Stellenbosch University for support.
- My wife Cordelia for continuous encouragement and support.
- To God for granting me the strength to be able to successfully complete the studies.

List of Abbreviations

GC	Gas Chromatography
LC	Liquid Chromatography
HPLC	High Performance Liquid Chromatography
RP-HPLC	Reversed-phase High Performance Liquid Chromatography
NP-HPLC	Normal Phase High Performance Liquid Chromatography
HL	<i>N,N</i> -dialkyl- <i>N'</i> -acyl(aroyle)thiourea
H ₂ L	<i>N</i> -alkyl- <i>N'</i> -acyl(aroyle)thiourea
NMR	Nuclear Magnetic Resonance
IR	Infra-Red
UV-VIS	Ultra violet Visible
CT	Charge Transfer
MLCT	Metal-to-Ligand Charge Transfer
LMCT	Ligand-to Metal Charge Transfer
ILCT	Inter Ligand Charge Transfer
LLCT	Ligand-to-Ligand Charge Transfer
MeOH	Methanol
MeCN	Acetonitrile
Am	amine
ESI-MS	Electrospray Ionisation Mass Spectrometry
ODS	Octadecylsilane

Conference Proceedings

This work has been presented at the conference stated below:

SACI Inorg Conference, June 2013, Durban, Poster presented

Title: Photo-isomerisation of platinum(II) and palladium(II) *N,N*-dialkyl-*N'*-acylthioureas studied using reversed-phase HPLC.

Abstract

A series of *N,N*-dialkyl-*N'*-acyl(aryl)thioureas and associated complexes with platinum(II), palladium(II), rhodium(III), ruthenium(III) and iridium(III) have been synthesised and characterised by various techniques. In particular, *N,N*-diethyl-*N'*-benzoylthiourea forms relatively stable *cis*-[M(Lⁿ-S,O)₂] (M = Pt(II), Pd(II)) and *fac*-[M(Lⁿ-S,O)₂] (M = Rh(III), Ru(III)) complexes.

As a result of some favourable properties of the ligands, reversed-phase HPLC has been employed for the separation of the *cis*-[Pd(Lⁿ-S,O)₂], *cis*-[Pt(Lⁿ-S,O)₂], *fac*-[Rh(Lⁿ-S,O)₃], *fac*-[Ru(Lⁿ-S,O)₃], [Ir(Lⁿ-S,O)₃] complexes. For analytical recovery of these metals from aqueous solutions, a salt-induced pre-concentration and sample preparation method is used for Pt(II), Pd(II), Rh(III) and Ru(III) complexes with *N,N*-diethyl-*N'*-benzoylthiourea prior to their HPLC analysis. A series of *cis*-[Pd(Lⁿ-S,O)₂] complexes with different ligands are also well separated by reversed-phase HPLC showing that electron-donating ligand substituents have an effect on increasing the polarity and consequently the decreasing retention time of such complexes.

In acetonitrile solutions, the *cis*-[M(Lⁿ-S,O)₂] (M = Pt(II)/Pd(II)) complexes have been found to undergo a reversible photo-induced isomerisation upon irradiation with different light sources, while the *fac*-[M(Lⁿ-S,O)₂] (M = Rh(III) and Ru(III)) are unaffected when so illuminated. With reversed-phase HPLC separation of the *cis/trans* isomers, a novel setup involving simultaneous irradiation with a Hg UV lamp and separation, was developed to determine the extent of isomerisation by simply changing the coil length through which the sample flows, thereby varying the photon flux intensity for irradiation. With this apparatus, an increase in the extent of isomerisation is observed as the length of coil increases leading to a steady state in the amounts of *cis/trans* isomers in solution. Also, the presence of electron-donating methoxy substituents on the *N,N*-dialkyl-*N'*-acyl(aryl)thioureas is found to decrease the retention times of the resulting *cis*-[Pd(Lⁿ-S,O)₂] complexes relative to those of the *trans* complexes. The presence of three of these groups in *cis*-bis(*N,N*-diethyl-*N'*-3,4,5-trimethoxybenzoylthioureaato)palladium(II) is also felt in decreasing the extent of isomerisation as a function of the *trans/cis* peak area ratios determined by reversed-phase HPLC.

The qualitative rate at which both the forward ($cis-[M(L^n-S,O)_2] \rightarrow trans-[M(L^n-S,O)_2]$) as well as the reverse ($trans-[M(L^n-S,O)_2] \rightarrow cis-[M(L^n-S,O)_2]$) isomerisation occur have also been estimated by irradiation with the blue violet laser pointer ($\lambda = 405 \text{ nm}$). Upon irradiation, cis -bis(N,N -diethyl- N' -3,4,5-trimethoxythioureato)palladium(II) in acetonitrile is found to undergo the forward isomerisation process at a much higher rate than the Pt(II) analogue. The reverse isomerisation reactions occur at a relatively fast rate for $[Pd(L^6-S,O)_2]$, but much slower for $[Pt(L^6-S,O)_2]$, with the $[Pt(L^6-S,O)_2]$ complex showing the reversible formation of other photo-decomposition products.

The relative rates of both forward and reverse $cis/trans$ isomerisation processes are affected by the presence of different ligand substituents. Introducing electron-donating methoxy substituents on the ligands as in cis -bis(N,N -diethyl- N' -3,4,5-trimethoxybenzoylthioureato)palladium(II) is found to decrease the relative rate of the forward isomerisation reaction meanwhile the reverse reaction takes place at a much higher rate compared to cis -bis(N,N -diethyl- N' -benzoylthioureato)palladium(II). With a single methoxy group attached to the benzoyl moiety, a similar but slightly higher relative rate of $cis/trans$ isomerisation to that of cis -bis(N,N -diethyl- N' -benzoylthioureato)palladium(II) is obtained.

Opsomming

'n Reeks *N,N*-dialkiel-*N'*-asiel(aroïel)tioureas en geassosieerde komplekse met platinum(II), palladium(II), rhodium(III), ruthenium(III) en iridium(III) is gesintetiseer en gekarakteriseer met behulp van verskeie tegnieke. Daar is gevind dat *N,N*-diëtiel-*N'*-bensoïeltiourea relatief stabiele *cis*-[M(Lⁿ-S,O)₂] (M = Pt(II), Pd(II)) en *fac*-[M(Lⁿ-S,O)₂] (M = Rh(III), Ru(III)) komplekse form.

Die spesifieke eienskappe van hierdie ligande het die gebruik van omgekeerde-fase HPLC toegelaat vir die skeiding van die *cis*-[Pd(Lⁿ-S,O)₂], *cis*-[Pt(Lⁿ-S,O)₂], *fac*-[Rh(Lⁿ-S,O)₃], *fac*-[Ru(Lⁿ-S,O)₃] en [Ir(Lⁿ-S,O)₃] komplekse. Ten einde die analitiese herwinning van hierdie metale uit waterige oplossing te bewerkstellig is 'n soutgeïndusseeerde prekonsentrasie en monster bereidingsmetode gebruik vir die komplekse van Pt(II), Pd(II), Rh(III) en Ru(III) met *N,N*-diëtiel-*N'*-bensoïeltiourea voor HPLC analiese. 'n Reeks *cis*-[Pd(Lⁿ-S,O)₂] komplekse met verskeie ligande kan ook geskei word deur HPLC en toon dat elektrondonerende ligandsubstituentte die polariteit van sulke komplekse verhoog en gevolglik ook hul retensietyd verkort.

Daar is gevind dat die komplekse *cis*-[M(Lⁿ-S,O)₂] (M = Pt(II)/Pd(II)) in asetonitriël-oplossings 'n omkeerbare fotogeïndusseeerde isomerisasie ondergaan onder bestraling met verskillende ligbronne terwyl soortgelyke behandeling die *fac*-[M(Lⁿ-S,O)₂] (M = Rh(III) and Ru(III)) komplekse onveranderd laat. Ten einde die omgekeerde-fase HPLC skeiding van *cis/trans* isomere is 'n nuwe opstelling ontwikkel waarin monsters tegelyketyd met 'n Hg UV lamp bestraal en geskei kan word en waarmee die mate van isomerisasie bepaal kan word deur eenvoudig die lengte van die bestralingspad en sodoende die intensiteit van die fotonfluks te verander. Met hierdie apparaat is bepaal dat die mate van isomerisasie toeneem namate die bestralingspad waardeur die monster vloei verleng word voordat 'n konstante verhouding *cis/trans* isomere uiteindelik in die oplossing teenwoordig is. Verder is gevind dat die teenwoordigheid van elektrondonerende metoksiesubstituentte aan die *N,N*-dialkiel-*N'*-asiel(aroïel)tioureas die retensietye van hul *cis*-[Pd(Lⁿ-S,O)₂] komplekse verkort relatief tot die van ooreenstemmende *trans* komplekse. Die teenwoordigheid van drie sulke groepe in *cis*-bis(*N,N*-diëtiel-*N'*-3,4,5-trimetoksiebensoïeltioureato)palladium(II) word ook gevoel in die afname van die mate van isomerisasie as 'n funksie van die *trans/cis* piekareaverhouding soos bepaal deur omgekeerde-fase HPLC.

Die kwalitatiewe tempo waarteen die voorwaartse ($cis\text{-}[M(L^n-S,O)_2] \rightarrow trans\text{-}[M(L^n-S,O)_2]$) en terugwaartse ($trans\text{-}[M(L^n-S,O)_2] \rightarrow cis\text{-}[M(L^n-S,O)_2]$) isomerisasie plaasvind is ook bepaal met behulp van bestraling deur 'n blou-violet laser ($\lambda = 405 \text{ nm}$). Daar is gevind dat tydens bestraling die voorwaartse isomerisasieproses van $cis\text{-bis}(N,N\text{-diëtiel-}N'\text{-}3,4,5\text{-trimetoksie-tioureato})\text{palladium(II)}$ in asetonitriël teen 'n veel hoër tempo verloop in vergelyking met die van die Pt(II) analoog. Vir $[Pd(L^6-S,O)_2]$ vind die terugwaartse reaksies teen 'n relatief hoë tempo plaas, maar veel stadiger vir $[Pt(L^6-S,O)_2]$, met hierdie Pt(II) kompleks wat ook die omkeerbare vorming van ander fotodegradasieprodukte toon.

Die relatiewe tempos van beide die voorwaartse en terugwaartse $cis/trans$ isomerisasieprosesse word beïnvloed deur die teenwoordigheid van verskillende ligandsubstituentte. Daar is gevind dat toevoeging van elektrondonerende metoksiesubstituentte tot ligande, soos in $cis\text{-bis}(N,N\text{-diëtiel-}N'\text{-}3,4,5\text{-trimetoksie-bensoëltioureato})\text{palladium(II)}$, die relatiewe tempo van die voorwaartse isomerisasiereaksie verlaag, terwyl die terugwaartse reaksie teen 'n veel hoër tempo plaasvind in vergelyking met $cis\text{-bis}(N,N\text{-diëtiel-}N'\text{-bensoëltioureato})\text{palladium(II)}$. Met 'n enkele metoksiegroep geheg aan die bensoëlgedeelte word 'n soortgelyke, maar effens hoër tempo van $cis/trans$ isomerisasie as die van $cis\text{-bis}(N,N\text{-diëtiel-}N'\text{-bensoëltioureato})\text{palladium(II)}$ waargeneem.

Table of contents

Declaration	i
April 2014	i
Acknowledgements	ii
List of Abbreviations.....	iii
Conference Proceedings	iv
Abstract	v
Opsomming	vii
Table of contents	ix
List of Figures	xii
List of Tables.....	xviii
CHAPTER I: <i>General introduction, background and objectives of study</i>	1
1.1. General Introduction.....	1
1.2. Co-ordination of platinum group metals to <i>N,N</i> -dialkyl- <i>N'</i> -acyl(aroyl)thioureas.....	4
1.3. HPLC determination of metal complexes	8
1.4. Photo-isomerisation of d^8 metal complexes	11
1.4.1. Photochemistry of Pt and Pd complexes	11
1.4.2. Photo-induced isomerisation of platinum(II) and palladium(II) <i>N,N</i> -dialkyl- <i>N'</i> -acyl(aroyl)thioureas.....	14
1.4.3. Effect of ligands and solvents on rates of isomerisation	16
1.4.4. Mechanism of <i>cis/trans</i> isomerisation in d^8 metal complexes	18
1.5. Aims and objectives of this work.....	21
CHAPTER II: <i>Synthesis and characterisation of ligands, platinum(II), palladium(II), rhodium(III), ruthenium(III) and iridium(III) complexes</i>	22
2.1. Synthesis.....	22
2.1.1. Synthesis of Ligands	22

2.1.2. Synthesis of platinum(II), palladium(II), rhodium(III), ruthenium(III) and iridium(III) complexes with <i>N,N</i> -dialkyl- <i>N'</i> -acyl(aryl)thioureas.....	24
2.1.3. Experimental details for synthesis of Ligands and complexes	28
2.2. Characterisation.....	33
2.2.1. NMR Characterisation.....	33
2.2.2. Mass Spectrometry	40
2.2.3. IR spectroscopy	42
CHAPTER III: <i>Reversed-phase HPLC separation of platinum(II), palladium(II), rhodium(III), ruthenium(III) and iridium(III) complexes</i>	45
3.1. Introduction	45
3.2. Chromatographic conditions	46
3.3. Separation of <i>cis</i> -[Pt(L- <i>S,O</i>) ₂], <i>cis</i> -[Pd(L- <i>S,O</i>) ₂], <i>fac</i> -[Rh(L- <i>S,O</i>) ₃], [Ru(L- <i>S,O</i>) ₃] and [Ir(L- <i>S,O</i>) ₃].....	47
3.4. Effect of ligand structure on HPLC separation	50
3.5. A Preliminary investigation of a salt-induced pre-concentration method for the HPLC determination of Pt(II), Pd(II), Rh(III) and Ru(III) <i>N,N</i> -diethyl- <i>N'</i> -benzoylthiourea	53
3.6. Conclusions	55
CHAPTER IV: <i>Photo-induced isomerisation of palladium(II) and platinum(II) complexes</i> ..	57
4.1. Irradiation setup for <i>cis/trans</i> isomerisation.....	59
4.2. <i>cis/trans</i> isomerisation of palladium(II) and platinum(II) <i>N,N</i> -dialkyl- <i>N'</i> -acyl(aryl)thioureas.....	60
4.3. UV-VIS spectroscopy for monitoring <i>cis/trans</i> isomerisation.....	63
4.4. Photo-induced isomerisation of <i>cis</i> -[Pd(L ⁿ - <i>S,O</i>) ₂] complexes.....	65
4.5. Effect of nature of ligands on relative rate of isomerisation of <i>cis</i> -[Pd(L ⁿ - <i>S,O</i>) ₂] complexes.....	69
4.5.1. Ligand effect on relative rate of forward (<i>cis</i> → <i>trans</i>) isomerisation of [Pd(L ⁿ - <i>S,O</i>) ₂] complexes.....	70
4.5.2. Ligand effect on relative rate of reverse (<i>trans</i> → <i>cis</i>) isomerisation for [Pd(L ⁿ - <i>S,O</i>) ₂] complexes.....	74

4.6. Photo-induced Isomerisation of <i>cis</i> -[Pt(L ⁿ -S,O) ₂] complexes.....	77
4.7. Conclusions	80
4.8. Experimental section	81
4.8.1. General procedure	81
4.8.2. Preparation of acetate buffer for HPLC separation	82
CHAPTER V: <i>Conclusions, proposed isomerisation mechanism and future work</i>	83
5.1. Discussions and proposed mechanism of <i>cis/trans</i> isomerisation	83
5.2. General conclusion	86
5.3. Future work	88
References	89

List of Figures

Figure 1.1: Platinum supply by region for the year 2003.

Figure 1.2: Scheme showing the steps involved for the extraction of platinum group metals from mineral ores.

Figure 1.3: Representation of general structure of *N,N*-dialkyl-*N'*-acyl(aroyle)thioureas.

Figure 1.4: A scheme showing the proposed mechanism for deprotonation of the *N,N*-dialkyl-*N'*-acyl(aroyle)thioureas.

Figure 1.5: Structure of *cis*-[M(L-S,O)₂] (M = Pt(II) or Pd(II)) and *fac*-[Rh(L-S,O)₃].

Figure 1.6: Structures showing the conformations of *N*-alkyl-*N'*-acyl(aroyle)thioureas (H₂L) and *N,N*-dialkyl-*N'*-acyl(aroyle)thioureas (HL).

Figure 1.7: A Scheme showing the possible reactions of *N,N*-dialkyl-*N'*-acyl(aroyle)thioureas in acidic medium.

Figure 1.8: Entropy and enthalpy considerations for *cis-trans* isomerisation of platinum(II) complexes.

Figure 1.9: Simplified orbital and state diagrams representing the photo-induced electronic transitions for d⁸ complexes.

Figure 1.10: Crystal structure of bis(*N,N*-di(*n*-butyl)-*N'*-naphthoylethioureato)platinum(II).

Figure 1.11: Representation of the photo-induced isomerisation of *cis*-[M(L-S,O)₂] (M = Pt(II), Pd(II)) complexes in acetonitrile.

Figure 1.12: Proposed mechanism for the photo-isomerisation of *cis*-glycinato-platinum(II) complexes.

Figure 1.13: A scheme illustrating the consecutive displacement mechanism.

Figure 1.14: Schemes representing intramolecular and intermolecular mechanisms during photo-induced isomerisation.

Figure 2.1: Reaction scheme for the synthesis of *N,N*-dialkyl-*N'*-acyl(aroyle)thioureas.

Figure 2.2: Reaction scheme for synthesis of *cis*-[Pt(L³-S,O)₂], *cis*-[Pd(L³-S,O)₂] and *fac*-[Rh(L³-S,O)₃].

Figure 2.3: A reaction scheme for the synthesis of palladium(II) and platinum(II) *N,N*-dialkyl-*N'*-acyl(aroyle)thioureas.

Figure 2.4: Reaction scheme for synthesis of tris(*N,N*-diethyl-*N'*-benzoylthioureato)ruthenium(III) and tris(*N,N*-diethyl-*N'*-benzoylthioureato)iridium(III).

Figure 2.5: Possible resonance structures of *N*-pirrolidyl-*N'*-(2,2-dimethylpropanoyl)thiourea.

Figure 2.6: ¹H NMR spectrum of *N*-pirrolidyl-*N'*-(2,2-dimethylpropanoyl)thiourea (HL¹) in CDCl₃ and at 25 °C.

Figure 2.7: ¹H NMR spectrum of bis(*N*-pirrolidyl-*N'*-(2,2-dimethylpropanoyl)thioureato)palladium(II) in CDCl₃ and at 25 °C.

Figure 2.8: Numbering scheme used for *N,N*-diethyl-*N'*-benzoylthiourea and palladium(II) derivatives.

Figure 2.9: ESI-MS(+) spectrum of tris(*N,N*-diethyl-*N'*-benzoylthioureato)ruthenium(III) in acetonitrile.

Figure 2.10: ESI-MS(+) spectrum of tris(*N,N*-diethyl-*N'*-benzoylthioureato)iridium(III) in acetonitrile.

Figure 2.11: FT-IR spectrum of *N,N*-diethyl-*N'*-benzoylthiourea.

Figure 2.12: FT-IR spectrum of bis(*N,N*-diethyl-*N'*-benzoylthioureato)palladium(II).

Figure 3.1: Chromatogram representing the separation of a mixture of *cis*-[Pd(L³-S,O)₂], *cis*-[Pt(L³-S,O)₂], *fac*-[Rh(L³-S,O)₃] and [Ru(L³-S,O)₃] in acetonitrile; conditions: flow rate 1 ml min⁻¹, Column 5 μm, C₁₈ ODS 150 x 4.6 mm, mobile phase 90:10 (% v/v) acetonitrile:0.1M acetate buffer (pH 6), injection volume 20 μl, 262 nm detection.

Figure 3.2: Chromatogram representing the separation of peaks for $[\text{Ir}(\text{L}^3\text{-S},\text{O})_3]$ in acetonitrile; conditions: C_{18} ODS, 5 μm , 150 x 4.6 mm column; mobile phase 90:10 (% v/v) acetonitrile:0.1M acetate buffer (pH 6); flow rate 1 ml min^{-1} , 20 μl injection volume, 262 nm detection.

Figure 3.3: Chromatogram representing the separation of a mixture of *cis*- $[\text{Pt}(\text{L}^3\text{-S},\text{O})_2]$, *cis*- $[\text{Pd}(\text{L}^3\text{-S},\text{O})_2]$, *fac*- $[\text{Rh}(\text{L}^3\text{-S},\text{O})_3]$, $[\text{Ru}(\text{L}^3\text{-S},\text{O})_3]$ and $[\text{Ir}(\text{L}^3\text{-S},\text{O})_3]$ in acetonitrile; conditions: Column 5 μm , C_{18} ODS, 150 x 4.6 mm, mobile phase 90:10 (% v/v) acetonitrile:0.1M acetate buffer (pH 6); flow rate 1 ml min^{-1} ; 20 μl injection volume, 262 nm detection.

Figure 3.4: Chromatogram representing the separation of a mixture of *cis*- $[\text{Pd}(\text{L}^3\text{-S},\text{O})_2]$, *cis*- $[\text{Pt}(\text{L}^3\text{-S},\text{O})_2]$, *fac*- $[\text{Rh}(\text{L}^3\text{-S},\text{O})_3]$, $[\text{Ru}(\text{L}^3\text{-S},\text{O})_3]$ and $[\text{Ir}(\text{L}^3\text{-S},\text{O})_3]$ in methanol; conditions: Column 5 μm , C_{18} ODS 150 x 4.6 mm, mobile phase 85:15 (% v/v) methanol:0.1M acetate buffer (pH 6), flow rate 1 ml min^{-1} , 20 μl injection volume, 262 nm detection.

Figure 3.5: Chromatogram representing the reversed-phase HPLC separation of a mixture of acetonitrile solutions of *cis*- $[\text{Pd}(\text{L}^1\text{-S},\text{O})_2]$, *cis*- $[\text{Pd}(\text{L}^2\text{-S},\text{O})_2]$ and *cis*- $[\text{Pd}(\text{L}^3\text{-S},\text{O})_2]$ in the dark; conditions: GEMINI C_{18} 5 μm , 150 x 4.6 mm column, mobile phase 95:5 (% v/v) acetonitrile : 0.1M acetate buffer (pH 6) flow rate 1 ml min^{-1} , injection volume 20 μl .

Figure 3.6: Chromatogram representing the reversed-phase HPLC separation of acetonitrile solution of a mixture of *cis*- $[\text{Pd}(\text{L}^3\text{-S},\text{O})_2]$, *cis*- $[\text{Pd}(\text{L}^4\text{-S},\text{O})_2]$, *cis*- $[\text{Pd}(\text{L}^6\text{-S},\text{O})_2]$ and *cis*- $[\text{Pd}(\text{L}^7\text{-S},\text{O})_2]$ in the dark; conditions: GEMINI C_{18} 5 μm , 150 x 4.6 mm column, mobile phase 85:15 (% v/v) acetonitrile:0.1M acetate buffer (pH 6) flow rate 1 ml min^{-1} , injection volume 20 μl , 262 nm detection.

Figure 3.7: A salt-induced sample preparation scheme for pre-concentration of Pt(II), Pd(II), Rh(III) and Ru(III) *N,N*-diethyl-*N'*-benzoylthiourea in aqueous solutions.

Figure 3.8: Chromatogram obtained for separation of Pd(II), Pt(II), Rh(III) and Ru(III) complexes with *N,N*-diethyl-*N'*-benzoylthiourea after a salt-induced pre-concentration method; conditions: Column GEMINI C_{18} , 5 μm , 150 mm x 4.6

mm, mobile phase 90:10 (% v/v) acetonitrile:0.1 M acetate buffer (pH 6), flow rate 1 ml min⁻¹, 20 µl injection volume, 262 nm detection.

Figure 4.1: Simultaneous irradiation and determination setup used to study *cis/trans* isomerisation of *cis*-[M(Lⁿ-S,O)₂] complexes.

Figure 4.2: Chromatogram representing the separation of acetonitrile solutions of *cis*-[Pd(L⁶-S,O)₂] and *cis*-[Pt(L⁶-S,O)₂] in the dark; Conditions: C₁₈ ODS, 5 µm, 150 x 4.6 mm column; mobile phase 85:15 (% v/v) acetonitrile:0.1M acetate buffer (pH 6); flow rate 1 ml min⁻¹, 262 nm detection.

Figure 4.3: Chromatogram representing the separation of *cis* and *trans* complexes of [Pd(L⁶-S,O)₂] and [Pt(L⁶-S,O)₂] in acetonitrile upon irradiation with a Hg UV lamp; Conditions: C₁₈ ODS, 5 µm, 150 x 4.6 mm column; mobile phase 85:15 (% v/v) acetonitrile:0.1M acetate buffer (pH 6); flow rate 1 ml min⁻¹, 262 nm detection.

Figure 4.4: Electronic absorption spectrum obtained in the dark and after irradiation of *cis*-[Pd(L⁶-S,O)₂] in acetonitrile with a blue violet laser pointer (λ = 405 nm) at room temperature.

Figure 4.5: Electronic absorption spectrum in the dark and upon irradiation of a solution of [Pt(L⁶-S,O)₂] in acetonitrile with a blue violet laser (λ = 405 nm) and at room temperature.

Figure 4.6: Chromatogram representing the separation of *cis* and *trans* isomers of [Pd(L⁷-S,O)₂], [Pd(L⁶-S,O)₂], [Pd(L⁴-S,O)₂] and [Pd(L³-S,O)₂] in acetonitrile, upon irradiation with Hg UV lamp; Conditions: C₁₈ ODS, 5 µm, 150 x 4.6 mm column; mobile phase 85:15 (% v/v) acetonitrile:0.1M acetate buffer (pH 6); flow rate 1 ml min⁻¹.

Figure 4.7: Overlaid chromatograms representing the separation of *cis* and *trans* complexes of [Pd(L⁶-S,O)₂] in acetonitrile both in the dark and upon irradiation with a Hg UV lamp; conditions: GEMINI C 18 5µm, 150 x 4.6 mm, mobile phase 90:10 (% v/v) acetonitrile:0.1M acetate buffer (pH 6), flow rate 1 ml min⁻¹, injection volume 20 µl, 262 nm detection.

Figure 4.8: Plots of peak area for *cis* and *trans*-[Pd(L⁶-S,O)₂] in acetonitrile with length of coil upon irradiation with Hg UV lamp.

Figure 4.9: A plot of *trans/cis* peak area ratio with time for *cis*-[Pd(L⁶-S,O)₂] in acetonitrile upon irradiation with tungsten lamp.

Figure 4.10: Overlaid chromatograms representing the forward isomerisation of a solution of [Pd(L⁶-S,O)₂] in acetonitrile upon irradiation with a 405 nm blue violet laser; Conditions: GEMINI C18 ODS, 5 μm, 150 x 4.6 mm column; mobile phase 95:5 (% v/v) acetonitrile:0.1M acetate buffer (pH 6); 1 ml min⁻¹ flow rate.

Figure 4.11: Overlaid chromatograms representing the forward isomerisation of a solution of [Pd(L⁵-S,O)₂] in acetonitrile upon irradiation with a 405 nm wavelength laser; Conditions: GEMINI C18 ODS, 5 μm, 150 x 4.6 mm column; mobile phase 95:5 (% v/v) acetonitrile:0.1M acetate buffer (pH 6); 1 ml min⁻¹ flow rate.

Figure 4.12: Overlaid chromatograms representing the forward isomerisation of a solution of [Pd(L³-S,O)₂] in acetonitrile upon irradiation with a 405 nm wavelength laser; Conditions: GEMINI C₁₈ ODS, 5 μm, 150 x 4.6 mm column; mobile phase 95:5 (% v/v) acetonitrile:0.1M acetate buffer (pH 6); 1 ml min⁻¹ flow rate.

Figure 4.13: A plot of *trans/cis* peak area ratio vs time of irradiation for *cis*→*trans* isomerisation of [Pd(L³-S,O)₂], [Pd(L⁵-S,O)₂] and [Pd(L⁶-S,O)₂] in acetonitrile upon irradiation with blue violet laser pointer (λ = 405 nm).

Figure 4.14: Overlaid chromatograms representing changes in isomerisation for [Pd(L⁶-S,O)₂] when an irradiated acetonitrile solution of sample is allowed in the dark at 17.4 °C; conditions: GEMINI C 18 ODS 5 μm, 150 x 4.6 mm column, mobile phase 95:5 (% v/v) acetonitrile:0.1M acetate buffer (pH 6), flow rate 1 ml min⁻¹.

Figure 4.15: A plot of *trans/cis* peak area ratio against time in dark when a solution of [Pd(L⁶-S,O)₂] in acetonitrile is irradiated with a 405 nm blue violet laser and allowed to stay in the dark at different times at 17.4 °C.

Figure 4.16: Overlaid chromatograms representing the changes in peak areas for both *cis* and *trans* complexes of $[\text{Pd}(\text{L}^3\text{-S},\text{O})_2]$ in acetonitrile after irradiation with 405 nm blue violet laser and allowed to stay in the dark at 17.4 °C; conditions: GEMINI C 18 ODS 5 μm , 150 x 4.6 mm column, mobile phase 95:5 (% v/v) acetonitrile:0.1M acetate buffer (pH 6), flow rate 1 ml min⁻¹.

Figure 4.17: Variation of *trans/cis* peak area ratio with time for $[\text{Pd}(\text{L}^6\text{-S},\text{O})_2]$ after an acetonitrile solution of the complex is irradiated with a blue violet laser pointer (405 nm) and allowed for stay in the dark at 17.4 °C.

Figure 4.18: Overlaid chromatograms representing the reversed-phase HPLC separation of acetonitrile solution of *cis*- $[\text{Pt}(\text{L}^6\text{-S},\text{O})_2]$ and *trans*- $[\text{Pt}(\text{L}^6\text{-S},\text{O})_2]$ with increase in time of irradiation with blue violet laser pointer (405 nm).; conditions: GEMINI C 18 ODS, mobile phase 90:10 (% v/v) acetonitrile:0.1M acetate buffer (pH 6), flow rate 1 ml min⁻¹.

Figure 4.19: Overlaid chromatograms representing the changes in peak areas of *cis* and *trans* complexes of $[\text{Pt}(\text{L}^6\text{-S},\text{O})_2]$ when an acetonitrile solution of the *cis* complex was irradiated with a 405 nm laser and the allowed to stay in the dark at different time intervals; conditions: GEMINI C 18 ODS, mobile phase 95:5 (% v/v) acetonitrile:0.1M acetate buffer (pH 6), flow rate 1 ml min⁻¹.

Figure 5.1: Proposed mechanism for the photo-induced isomerisation of *cis*- $[\text{M}(\text{L-S},\text{O})_2]$ complexes in acetonitrile.

List of Tables

Table 1: Table showing the characteristic of various types of liquid chromatographic techniques.

Table 2: Table of a list of names, abbreviations and structures for the *N,N*-dialkyl-*N'*-acyl(aroyl)thioureas used for complex formation.

Table 3: Table of pK_a values of amine groups and chemical shifts for N-CH₂ protons in *N*-pirrolidyl-*N'*-(2,2-dimethyl-propanoyl)thiourea, *N,N*-dibutyl-*N'*-(2,2,-dimethyl-propanoyl)thiourea, *N*-piperidyl-*N'*-benzoylthiourea and *N,N*-diethyl-*N'*-benzoylthiourea in CDCl₃ and at 25 °C.

Table 4: ¹H NMR chemical shifts (in ppm) of *N,N*-diethyl-*N'*-benzoylthiourea and its Pd(II) derivatives, in CDCl₃ and at 25 °C.

Table 5: Table of FT-IR ν (N-H) and ν (C=O) stretches for different ligands and their respective complexes.

Table 6: Table showing the difference in wavelengths at maximum absorbance, retention times and peak areas of *cis* and *trans* complexes of [Pd(L³-*S,O*)₂], [Pd(L⁴-*S,O*)₂], [Pd(L⁵-*S,O*)₂] and [Pd(L⁶-*S,O*)₂] in acetonitrile upon irradiation with a Hg UV lamp.

Table 7: Table showing the changes in peak areas and relative rate of reverse isomerisation for [Pd(L⁶-*S,O*)₂] upon irradiation of an acetonitrile solution with a blue violet laser.

CHAPTER I

General introduction, background and objectives of study

1.1. General Introduction

The metals platinum, palladium, rhodium, ruthenium, iridium and osmium constitute the Platinum Group Metals (PGMs), whose co-ordination chemistry renders them useful in a wide range of applications. For the past decades, South Africa has been one of the world's leading producers of platinum and its associated metals, with mining of the metals carried out primarily in the Bushveld Complex. From this Complex, the mining is done from three main areas which include the Platreef, Chromitite reef, and also the Merensky reef from which a great majority of the metals were derived.¹

Other countries which contain deposits of the PGMs include Russia, China, Canada and the United States but these deposits are widespread in South Africa which produced more than 70% of the metals in 2003 as shown in Figure 1.1.² The precious metals are in very high demands for their potential uses. Some of the factors which could influence their demand include their production cost, market price, as well as the environmental considerations needed for their production. The metals are primarily used as catalytic converters in the automotive industry. Other uses are in dental alloys, electronic components, computer hard discs, and in fuel cells. Compounds of PGMs are also known for several uses especially in medicine. For example, platinum(II) diamines such as cisplatin has for long been established as a well suited drug for the treatment of cancer due to its potential anti-tumor activity.³ The *cis* isomer of this compound is anti-tumor active while the *trans* isomer is known to be inactive as a potential cancer chemotherapy agent.

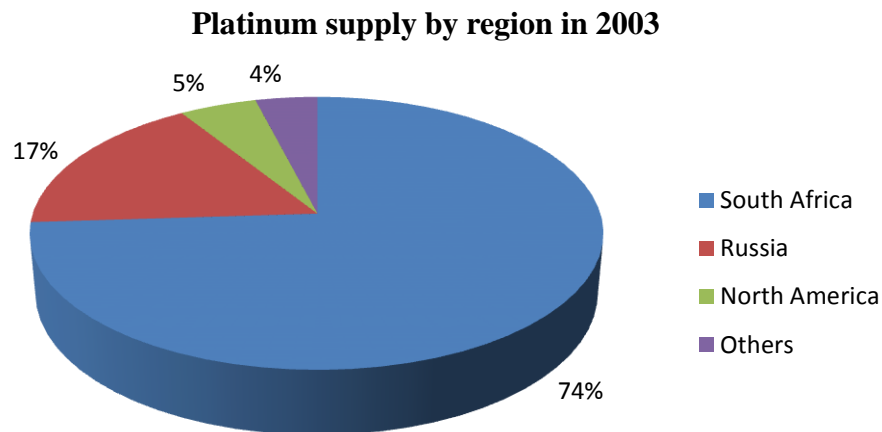


Figure 1.1. Platinum supply by region for the year 2003.²

Production of the platinum group metals is an expensive and a complex process and it involves a series of steps as illustrated in the flow diagram in Figure 1.2.⁴ During this process, the metal ions are converted to water soluble chloro anions thereby aiding their separation.

After the metals are extracted from ores, trace amounts of them could be remaining in industrial waste streams as water soluble species. This presents an environmental hazard as their soluble forms in water could have consequences on crops, fruit bearing plants which sometimes are consumable by humans. Added to this, because of their high value, introduction of the metals into process streams could lead to a huge loss in revenue for the mining industry. Hence adequate and reliable analytical techniques are needed for the determination of traces of PGMs in solution and for their recovery in aqueous solutions. This sometimes is difficult to carry out due to various factors some of which include the low reactivity of the metals, their chemical similarities, variable oxidation states and speciation due to the possibility of formation of various complexes in aqueous solutions.

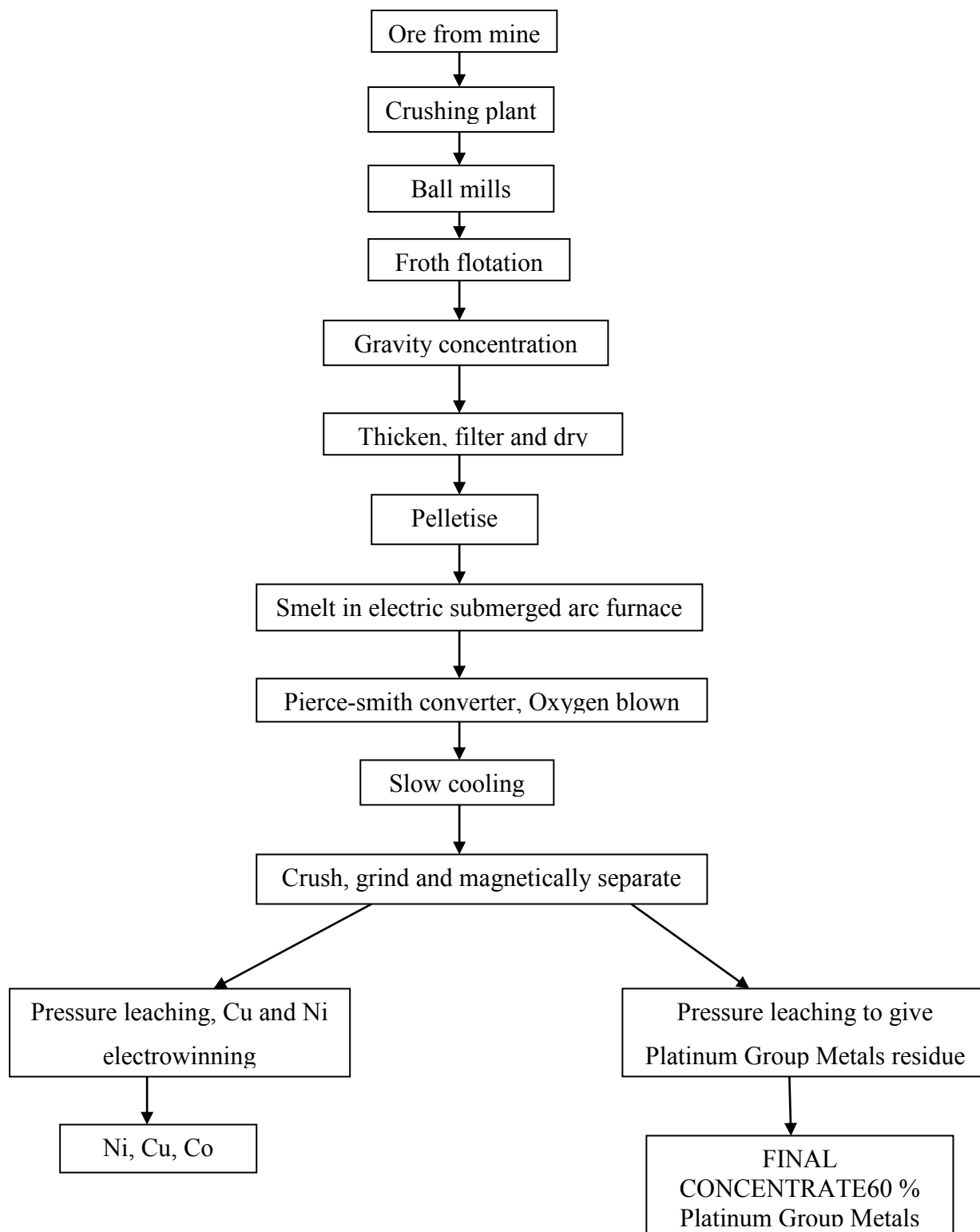


Figure 1.2. Scheme showing the steps involved for the extraction of platinum group metals from mineral ores.⁴

Newer techniques for the extraction, separation and recovery of the PGMs are needed and these should be able to separate the metals with high efficiency and such that a minimum amount of the metals is lost. Examples of separation techniques which have been used in the past include ion exchange, crystallisation, selective precipitation, solvent extraction and distillation.⁵ Another separation technique widely used for determination of the metals in trace amounts is by chromatography. Prior to a chromatographic separation of the PGMs, complex formation of their metal ions is usually carried out with the use of a suitable ligand of which the *N,N*-dialkyl-*N'*-acyl(aryl)thioureas are examples.

1.2. Co-ordination of platinum group metals to *N,N*-dialkyl-*N'*-acyl(aryl)thioureas

The ligands represented by Figure 1.3 are generally known as *N,N*-dialkyl-*N'*-acyl(aryl)thioureas or 3,3-dialkyl-1-acyl(aryl)thioureas (**HL**) and were first prepared by K. Nuecki⁶ in 1873. Since then, numerous derivatives of these ligands have been prepared by varying the nature of the alkyl or aryl groups,^{7,8} and some of the ligands have very interesting properties.

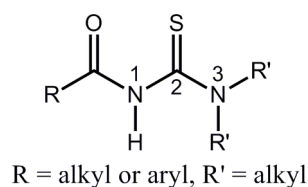


Figure 1.3. Representation of general structure of *N,N*-dialkyl-*N'*-acyl(aryl)thioureas.

These ligands co-ordinate to the platinum group metals through the sulfur and oxygen atoms and this occurs after deprotonation from the central nitrogen atom. Although the mechanism behind the ligand deprotonation is not yet known, it is thought to occur through the possible routes proposed in Figure 1.4, assisted by the presence of a base.

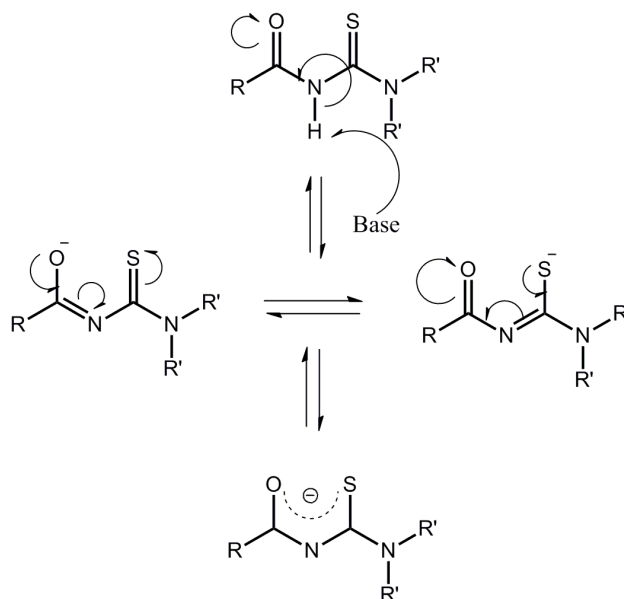


Figure 1.4. A scheme showing the proposed mechanism for deprotonation of the *N,N*-dialkyl-*N'*-acyl(aryl)thioureas.

Earlier studies by Beyer and Hoyer⁹ involved the determination of the acid and stability constants of some of the *N,N*-dialkyl-*N'*-acyl(aryl)thioureas such as *N,N*-di(2-hydroxyethyl)-*N'*-benzoylthiourea with some first and second row transition metal ions. The ligands have been reported by Koch *et al.*¹⁰ to co-ordinate to platinum(II) and palladium(II) metal ions through the sulfur and oxygen atoms forming predominantly stable *cis*-[M(Lⁿ-S,O)₂] (M = Pt(II), Pd(II)) complexes meanwhile with rhodium(III) similar co-ordination mode led to *fac*-[Rh(Lⁿ-S,O)₃] complex as shown in Figure 1.5. The mode of co-ordination in these complexes was confirmed from their resulting crystal structures determined.

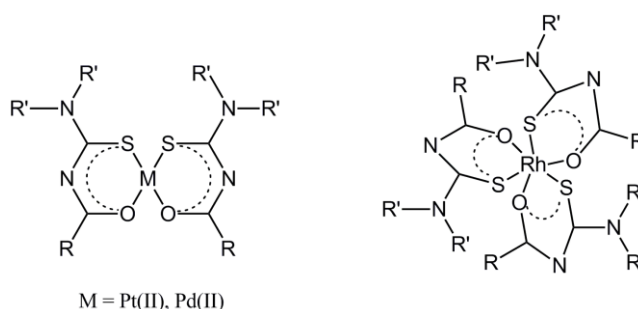


Figure 1.5. Structure of *cis*-[M(Lⁿ-S,O)₂] (M = Pt(II) or Pd(II)) and *fac*-[Rh(Lⁿ-S,O)₃].¹⁰

Some of the *N,N*-dialkyl-*N'*-benzoylthioureas such as *N,N*-diethyl-*N'*-*p*-chloro-benzoylthiourea have been found to co-ordinate to metal ions such as Co(II),¹¹ Zn(II),¹²

Cu(II),¹³ Ag(I),¹⁴ Hg(II)¹⁵ and Ni(II)^{16,17} also through the sulfur and oxygen atoms. Of the complexes resulting from such co-ordination, some are known to have very useful applications. For example, the bis(*N,N*-diethyl-*N'*-*p*-nitro-benzoylthioureato)copper(II) complex formed from co-ordination of *N,N*-diethyl-*N'*-*p*-nitro-benzoylthiourea to Cu(II) was found to enhance the antitumor activity tested.¹⁸ Apart from those of rhodium(III), facial complexes of these ligands with ruthenium(III) have also been reported. A crystal structure determination of an octahedral *tris*-(1,1-diethyl-3-benzoyl-thioureato)ruthenium(III) complex synthesised revealed that co-ordination of the metal center to the donor atoms of the ligands occur in a facial manner.¹⁹

Co-ordination of the *N,N*-dialkyl-*N'*-acyl(aryl)thioureas to platinum group metals is expected to be dependent on the acidity of the medium. The effect of acid on the ease of such complex formation with the *N,N*-dialkyl-*N'*-benzoylthioureas has previously been studied by Schuster and coworkers²⁰ under various pH conditions. Their results showed that the metals used formed complexes with ligands such as *N,N*-diethyl-*N'*-benzoylthiourea and *N,N*-di-*n*-butyl-*N'*-benzoylthiourea under the conditions used. The ease of complex formation with pH dependence was used for a solvent-solvent extraction and pre-concentration of the metals from acid solutions and also to separate the metals from each other and from other metals.²¹

Another group of ligands similar to the *N,N*-dialkyl-*N'*-acyl(aryl)thioureas are their mono-substituted analogues generally known as *N*-alkyl-*N'*-acyl(aryl)thioureas (**H₂L**). Co-ordination of this second group of ligands to transition metals is also possible but occurs only through the sulfur atom of the ligands. Complexes of Mn(II), Cu(II), Ni(II), Co(II), Zn(II), Hg(II), Pt(II) and Pd(II) with *N*-phenyl-*N'*-(2-phenolyl)thiourea formed after such co-ordination have been previously obtained and their biological activity on some category of bacteria also tested.²²

In the *N*-alkyl-*N'*-acyl(aryl)thioureas, there is a possibility of an intramolecular hydrogen bond linking the carbonyl and thiourea NH moieties (Figure 1.6).²³ This leads to structural and conformational differences between this group of ligands compared to the *N,N*-dialkyl-*N'*-acyl(aryl)thioureas. The intramolecular hydrogen bond causes 'locking' of the –C(O)NHC(S)NHR group in the *N*-alkyl-*N'*-acyl(aryl)thioureas giving rise to a structure with

a planar six-membered ring geometry, meanwhile a twisted conformation is formed for the *N,N*-dialkyl-*N'*-acyl(aryl)thioureas in which hydrogen bonding is absent.^{24,25}

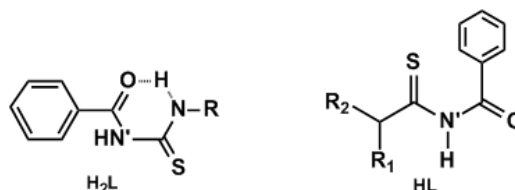


Figure 1.6. Structures showing the conformations of *N*-alkyl-*N'*-acyl(aryl)thioureas (H_2L) and *N,N*-dialkyl-*N'*-acyl(aryl)thioureas (HL).²³

This difference in conformation between the two groups of ligands have a consequence on the distribution of *cis/trans* isomers in a mixture when the ligands co-ordinate Pt(II) and Pd(II).²⁶ Unlike the *N,N*-dialkyl-*N'*-acyl(aryl)thioureas which co-ordinate to M(II) (M = Pt(II) or Pd(II)) metal ions to form *cis*-[M(Lⁿ-S,O)₂], co-ordination of the same metal ions to the *N*-alkyl-*N'*-acyl(aryl)thioureas results to a mixture of *cis*- and *trans*-[Pt(H_2L -S)₂Cl₂] complexes. The *cis*-[Pt(H_2L -S)₂Cl₂] complexes formed could undergo a solvent dependent isomerisation in solution to give a *cis/trans* mixture.

The water solubility of both the *N,N*-dialkyl-*N'*-acyl(aryl)thioureas and the *N*-alkyl-*N'*-acyl(aryl)thioureas can be enhanced by introducing more hydrophilic groups to the alkyl or aryl substituent. Some of these water soluble ligands and their complexes with Pt(II) and Pd(II) have been synthesised and the products formed were found to be different. The metal complexes with *N,N*-di(2-hydroxyethyl)-*N'*-benzoylthiourea formed mainly *cis* complexes whereas those having *N*-(2-hydroxyethyl)-*N'*-benzoylthiourea yielded a mixture of *cis* and *trans* isomers of the complex.²⁷

Complexes of Pt(II) with the *N,N*-dialkyl-*N'*-benzoylthioureas for example *N,N*-di(*n*-butyl)-*N'*-benzoylthiourea in CDCl₃ can undergo a reversible protonation under relatively acidic conditions.²⁸ Such complexes are stable when the chelating ligand is not protonated. However, when the complexes are protonated in the presence of concentrated HCl, the oxygen atom becomes a weaker donor compared to when it has a partial charge, when the complex is deprotonated. Such reactions could lead to the formation of a mixture of *cis* and *trans*

complexes of the type $[\text{Pt}(\text{HL-S})_2\text{Cl}_2]$ and could also involve a partial ring opening as illustrated in Figure 1.7 below.

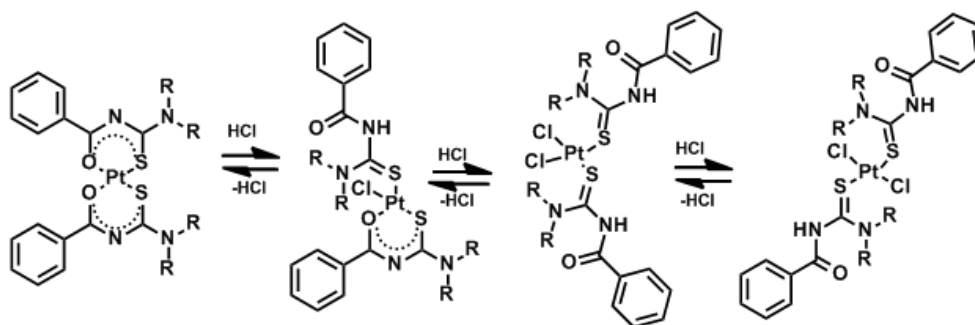


Figure 1.7. A Scheme showing the possible reactions of *N,N*-dialkyl-*N'*-acyl(aryl)thioureas in acidic medium.²⁸

Some of the Pt(II) complexes with the *N,N*-dialkyl-*N'*-acyl(aryl)thioureas are susceptible to oxidative addition with halogen molecules resulting to octahedral Pt(IV) complexes.²⁹ For example, in chloroform, Pt(II) complexes with the ligands *N,N*-diethyl-benzoylthiourea and *N,N*-di(*n*-butyl)-*N'*-benzoylthiourea are known to undergo a rapid oxidative addition with the halogens I_2 and Br_2 to their corresponding halogenated Pt(IV) complexes, meanwhile the use of a mono-dentate ligand such as *N*-propyl-*N'*-benzoylthiourea yield different products for both I_2 and Br_2 on attempted oxidative addition.

1.3. HPLC determination of metal complexes

Some of the techniques used for the determination of metal complexes include spectrophotometry, atomic absorption, neutron activation methods, inductively coupled plasma atomic emission and inductively coupled plasma mass spectrometry and chromatography.

The chromatographic techniques used can be grouped into Gas Chromatography (GC) and Liquid Chromatography (LC) and their use for determination depends on the nature of the analyte. A widely used form of liquid chromatography is High Performance Liquid Chromatography (HPLC) which is very efficient in separating mixtures of similar analytes within relatively shorter times. It also has the advantage of being highly sensitive, with the sample having a relatively smaller diffusion coefficient when in the mobile phase.³⁰

The various liquid chromatographic techniques which could be used for determination of metal complexes include normal phase (NP) HPLC, reversed-phase (RP) HPLC, ion pair chromatography and gel permeation/size exclusion chromatography. The characteristics of these techniques are summarised in Table 1.

Table 1. Table showing the characteristic of various types of liquid chromatographic techniques.

Types of Liquid Chromatography	Mobile phase	Stationary phase	Type of compounds separated
Normal phase	Non- polar	Polar	Compounds insoluble in water, Organic isomers
Reversed phase	Polar	Apolar	Neutral, weak acids, weak bases
Ion-pair	Polar	Apolar	Neutral, weak acids, weak bases
Size exclusion	Aqueous or organic	Porous polymers or silica	Polymers, peptides, proteins, nucleic acids

In normal phase chromatography, the stationary phase is hydrophilic thus having a high affinity for hydrophilic molecules in the mobile phase, meanwhile hydrophobic molecules pass through the column and are eluted first. Also, the hydrophilic molecules can be eluted from the column by increasing the polarity of the solution in the mobile phase.

Reversed-phase chromatography functions by a different mode in that it uses a hydrophobic stationary phase and hence hydrophobic molecules in the polar mobile phase tend to be retained in the hydrophobic stationary phase, while hydrophilic molecules in the mobile phase pass through the column and are eluted first. Hydrophobic molecules can be eluted from the column by decreasing the polarity of the mobile phase using an organic solvent which reduces hydrophobic interactions.

For separation of metal complexes, samples are better retained the less water soluble they are and the separation of highly non-polar analytes require the use of non-aqueous eluents. This implies that a good choice on the mobile phase used during normal and reversed-phase chromatography could greatly enhance the selectivity and subsequent separation and determination of the metal complexes. The mobile phase composition is therefore of great importance and separation under isocratic conditions is usually initiated with a much higher amount of organic component in the mobile phase.

Buffers are sometimes used as part of the mobile phase composition especially during ion-exchange and reversed-phase chromatography. This is done so as to maintain the analyte molecule in a single undissociated form for compounds which are ionic or easily ionisable.³⁰ Irrespective of whether the analyte is basic or acidic, the choice of pH of the buffer should be such that it favours the molecules in the analyte remaining intact in one single form. For this reason, a buffer of pH 2 units lower than the pK_a is preferred for an acidic analyte as it causes the analyte to remain undissociated, whereas with pH 2 units higher anionic species are formed. A buffer with pH 2 units higher than the pK_a is needed to keep a basic analyte intact during a chromatographic separation.

Several reports on the analysis of PGMs as complexes using reversed-phase HPLC have been published.³¹⁻³⁶ Different HPLC methods using different columns have been also used to evaluate the separation of Pt, Pd, Ir and Rh after the formation of 8-hydroxyquinolate chelates³⁷ without necessarily having to eliminate the excess reagent used, meanwhile other studies involved the use of *N*-heterocyclic azodyes.³⁸ Reagents such as 1-(2-Pyridylazo)-naphthol^{39,40} and 4-(2-thiazolylazo)-resorcinol⁴¹ have also been used to form complexes with some PGMs prior to their determination and separation by reversed-phase HPLC.

Another type of chromatographic technique which has widely been used in the past for the determination of metal complexes is ion-exchange chromatography. This is mostly used for anionic complexes despite its disadvantage of having a lower sensitivity. Ion-exchange chromatography has been established to be useful in the separation of PGMs from base metals⁴² and for determination as well as quantification of some platinum complex anionic species.⁴³

The work done on the reversed-phase HPLC separation for most of the PGMs after complex formation with the *N,N*-diakyl-*N'*-acyl(aryl)thioureas by Koch *et al.*¹⁰ involved complex formation of ligands such as *N*-pirrolidyl-*N'*-(2,2-dimethylpropanoyl)thiourea with Pt(II), Pd(II) and Rh(III). The hydrophilic nature of such ligands led to a reversed-phase HPLC separation of the resulting *cis*-[Pd(L-S,O)₂], *cis*-[Pt(L-S,O)₂] and *fac*-[Rh(L-S,O)₃] complexes but did not involve similar complexes with Ru(III) and Ir(III). With a salt-induced sample preparation method established as useful for pre-concentration of these complexes prior to their HPLC separation, detection limits for trace amounts of the metals were also established. The possibility to render such metal complexes separable due to the hydrophilic nature of the ligands is the basis for this current study and a reversed-phase HPLC separation of similar complexes with Pt(II), Pd(II) as well as Rh(III), Ru(III) and Ir(III) will be carried out as will be discussed later.

1.4. Photo-isomerisation of d⁸ metal complexes

1.4.1. Photochemistry of Pt and Pd complexes

Transition metals near the end of the transition series are capable of forming square planar complexes. These complexes can exist as *cis/trans* isomers under certain conditions one of which is by irradiation with a suitable light source. Some of these square planar complexes include those of d⁸ ions such as Rh^I, Ir^I, Pd^{II}, Pt^{II}, and Au^{III} although most work from previous studies indicate that of these metal ions, only Pt(II) and Pd(II) are most likely to form *cis/trans* isomers.⁴⁴

A variety of techniques have been used to monitor the *cis/trans* isomerisation of these metal complexes after irradiation with a suitable light source. Some of these techniques include Nuclear Magnetic Resonance Spectroscopy (NMR),^{45,46} High Performance Liquid Chromatography,⁴⁷ UV-VIS spectroscopy,⁴⁸ IR spectroscopy,⁴⁹ and dipole moment measurements.^{50,51} Monitoring the transformations involved using these methods could sometimes lead to determination of the rates of *cis/trans* isomerisation. Measurement of the rates of photochemical processes such as photo-induced isomerisation is usually done either indirectly by determining the intensity of light to obtain quantum yields,^{52,53} or directly from laser induced fluorescence spectroscopy to measure associated fluorescent lifetimes.⁵⁴

Palladium(II) complexes are known to be kinetically more labile to *cis/trans* isomerisation than the corresponding platinum complexes, hence the *trans* geometry is more likely to be formed for the palladium complexes. For the formation of geometric isomers of some of these complexes, it is generally known that the *cis* isomers are enthalpy-favoured while the formation of the *trans* analogues is entropy-favoured as illustrated in Figure 1.8.⁴⁴ The stability of the resulting *cis* or *trans* isomers for both the platinum(II) and palladium(II) complexes is determined by changes in metal center, ligand, solvent and temperature.

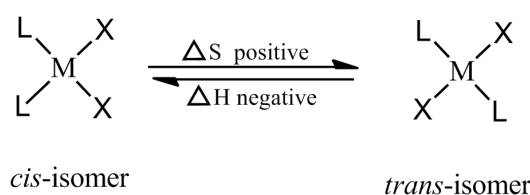


Figure 1.8. Entropy and enthalpy considerations for *cis/trans* isomerisation of platinum(II) complexes.⁴⁴

In order to understand the photochemistry accompanying the kinetics of *cis/trans* isomerisation in square planar complexes, it is important to consider the properties of the excited electronic state of the molecules. Irradiation with light in the visible and UV regions may lead to light absorption by the molecules. The absorbed radiation may possess sufficient energy to cause a change in the electronic state, vibrational and rotational motion of the molecules. In the metals complexes, there exists a variety of electronic states and different transitions may occur between the ground and excited states. The various possible electronic transitions in the square planar d^8 complexes are shown in Figure 1.9. The ground state in these complexes could be excited to either a singlet or triplet excited state through d-d metal transitions, charge transfer (MLCT or LMCT) transitions or *intra*-ligand ($\pi-\pi^*$) transitions.

Transitions such as d-d type occur from bonding or non-bonding to anti-bonding orbitals. This leads to the weakening of the metal-ligand bonds since there is a significant increase in electronic repulsion along the metal-ligand sigma bonding axis. Because d-d transitions are forbidden transitions, their absorption bands are usually weak transitions leading to low values of molar extinction coefficients and low energies. This results in the fact that d-d transitions are not generally observed in the electronic absorption spectra of some complexes. Whenever these transitions are possible in a metal complex, they could have a significant

effect on the photochemical properties of the complex due to their short lived nature in solution compared to the other types of transition.⁵⁵

Charge transfer (CT) transitions can be mainly classified as either metal to ligand (MLCT) or ligand to metal (LMCT) depending on the movement of charges. Unlike d-d transitions, these are high energy transitions and have higher values of molar extinction coefficient. Usually, excitations involving MLCT could involve low-lying transition states which could be associated with a radiative or non-radiative excited state decay.⁵⁵ The decay constant for these processes will depend on the excited state lifetime and the quantum yields.

Also possible are *intra*-ligand transitions also known as π - π^* transitions. Absorption bands resulting from these transitions could vary in energy depending on the type of metal and its oxidation state.

The difference in energy between the electronic states involved in the three groups of transitions discussed could determine the photo-stability of a metal complex upon irradiation. This energy difference would depend on the polarity of the solvent, the nature of the metal center and the groups attached to the ligands as will be discussed later during this study (Chapter V, page 83).

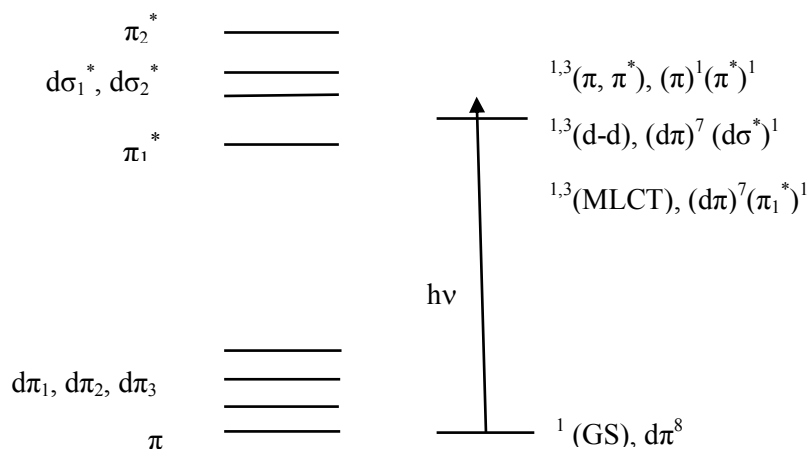


Figure 1.9. Simplified orbital and state diagrams representing the photo-induced electronic transitions for d^8 complexes.⁵⁵

1.4.2. Photo-induced isomerisation of platinum(II) and palladium(II) *N,N*-dialkyl-*N'*-acyl(aryl)thioureas

The photochemistry of the Pt(II) and Pd(II) complexes with *N,N*-dialkyl-*N'*-acyl(aryl)thioureas is an area of study which has not been explored to a great extent. Understanding the factors affecting rate of the photo-induced isomerisation for these complexes and their associated mechanism could possibly lead to isolation of *trans*-[M(Lⁿ-S,O)₂] complexes from corresponding *cis*-[M(Lⁿ-S,O)₂] complexes. With the limited reports so far on a possible and direct route to obtain such *trans*-[M(Lⁿ-S,O)₂] complexes, understanding the factors governing the photo-stability of the *cis*-[M(Lⁿ-S,O)₂] complexes is of great importance. In 1994, the first *trans*-[Pt(L-S,O)₂] (L = *N,N*-di(*n*-butyl)-*N'*-naphthoylthiourea) (Figure 1.10) complex was isolated by Koch *et al.*⁵⁶ which is still the only authentic *trans* complex of Pt(II) with the *N,N*-dialkyl-*N'*-acyl(aryl)thioureas known to date, out of more than 25 related crystal structures reported.⁵⁷

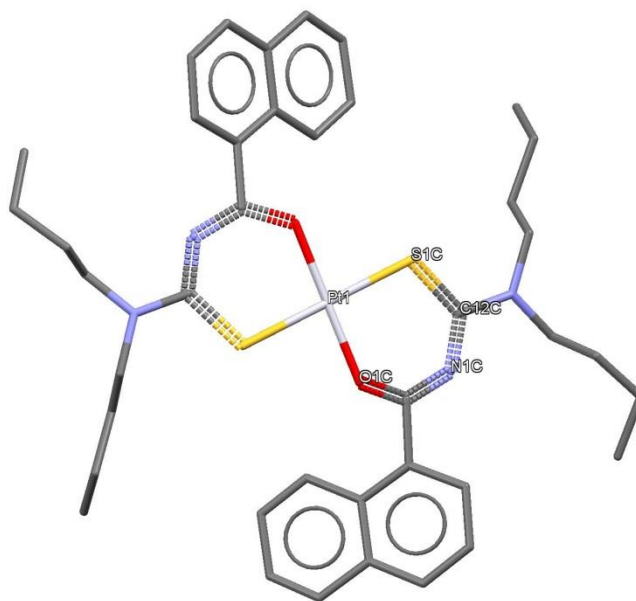


Figure 1.10. Crystal structure of *trans*-bis(*N,N*-di(*n*-butyl)-*N'*-naphthoylthiourea)platinum(II).⁵⁷

Later on, it was found that the key to obtaining the *trans*-[M(Lⁿ-S,O)₂] complexes is by a photo-induced isomerisation of the *cis*-[M(Lⁿ-S,O)₂] complexes in acetonitrile solution.⁵⁸ The *cis*-[M(Lⁿ-S,O)₂] complexes in acetonitrile were shown to undergo a reversible *cis/trans*

isomerisation induced by the presence of yellow, blue and white light used for irradiation. This easily yielded the *trans*-[M(Lⁿ-S,O)₂] complexes as illustrated in Figure 1.11 with monitoring of the *cis/trans* isomerisation done using reversed-phase HPLC. The extent of *cis/trans* isomerisation was found to be dependent on the photon flux intensity of radiation as well as the solvent used. Also it was concluded that a radiation of wavelength *ca.* < 450 nm was necessary for the *cis/trans* isomerisation to occur, and that the reverse process (*trans*→*cis*) which is temperature dependent occurs spontaneously in the dark.

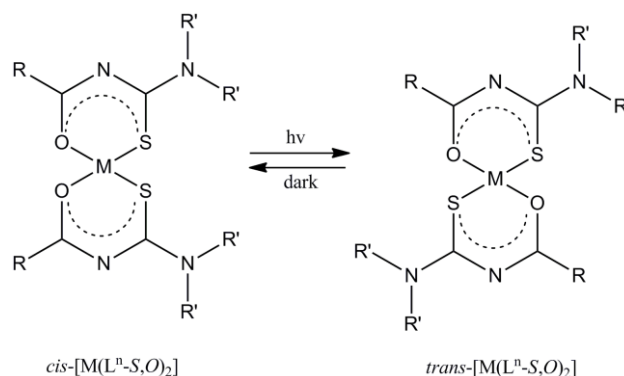


Figure 1.11. Representation of the photo-induced isomerisation of *cis*-[M(Lⁿ-S,O)₂] (M = Pt(II), Pd(II)) complexes in acetonitrile, L = *N,N*-diethyl-*N'*-3,4,-trimethoxybenzoylthiourea.⁵⁸

Since then, there has been little work on the *cis/trans* isomerisation on the *cis*-[M(Lⁿ-S,O)₂] complexes and the mechanism by which such reactions occur is still poorly understood. By using suitable techniques such as reversed-phase HPLC, NMR or UV-VIS spectroscopy for monitoring such processes, a kinetic study on the rates of *cis/trans* isomerisation could be carried out. With the kinetic studies, factors such as a change in ligand structure, metal centre and solvent could also be varied, and their effect on the rates of isomerisation could be used to give an idea on how the mechanism of isomerisation occurs. The *cis/trans* isomerisation of these complexes may occur *via* a variety of pathways which would depend among other factors on solvents and co-ordinating ligands and predicting the mechanism by which such reactions occur could be complicated. As a result, products from isomerisation and the isomerisation conditions require careful investigation in order to establish the appropriate reaction pathways and to determine the mechanism of isomerisation.

Balzani and coworkers⁵⁹ have carried out a similar investigation on the *cis/trans* isomerisation of some platinum(II) complexes but using glycine ligands. They found that *cis*-

bis(glycinato)platinum(II) complexes when irradiated yields the *trans* isomer in a reversible isomerisation process which was proposed to occur through a pseudo tetrahedral mechanism such as that illustrated in Figure 1.12. They also came to a conclusion that the forward reaction which is photo-induced occurs through an intramolecular twist mechanism, with the assumption that the formation of a tetrahedral intermediate occurs from the triplet excited state of the complex.⁶⁰ In a similar study, quantum yields of *ca.* 0.13 were obtained when such platinum(II) complexes were irradiated with light in the near UV.⁶¹

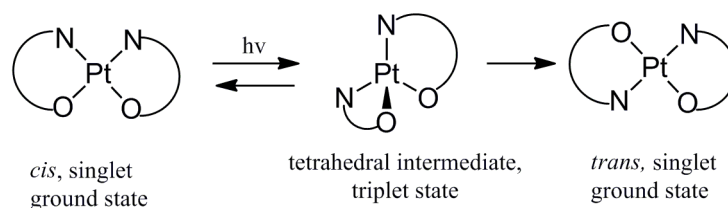


Figure 1.12. Proposed mechanism for the photo-isomerisation of *cis*-bis(glycinato)platinum(II) complexes.⁶⁰

1.4.3. Effect of ligands and solvents on rates of isomerisation

The extent of a variety of photochemical reactions in square planar platinum group metal complexes would possibly depend on the extent to which their electronic state energies are affected by factors such as the nature of solvent and ligand involved. In these complexes, the absorption spectra and energies for transitions involving MLCT should vary with change of solvent due to the change in radial distribution during these transitions.⁵⁵ On the other hand, *intra*-ligand ($\pi - \pi^*$) transitions are expected not to be affected by changes in the solvent since the transitions lack dipole character.

Anbalagan and Srivastava⁶² have reported that the nature of a variety of diimine ligands could possibly affect the extent to which some photo-oxidation reactions occur. Such reactions involved a singlet molecular oxygen ($^1\text{O}_2$) as an intermediate and ligand-to-ligand charge transfer (LLCT) bands were found to arise from the Pd(II) and Pt(II) α -diimine complexes. The resulting mononuclear and dinuclear complexes were investigated using molecular-oxygen-saturated DMF solutions and were found to be capable of generating $^1\text{O}_2$ in the presence of light. The extent of generating the molecular oxygen intermediate was found to be dependent on the nature of the metal ion, the nature of the α -diimine ligand used, and also on

the extent to which the square planarity of the complexes was kept intact. There were certain absorption bands resulting from the LLCT in these complexes which were found to depend strongly on the polarity of the solvent used. The energy of such bands decreased when the α -diimine was changed from 2,2'-bipyridine to 2,2'-biquinoline.

Different solvents and ligands used have also been shown by Gonzalo *et al.*⁶³ to affect the rate of photo-reduction in copper(II) 1,3-diketonates. The quantum yields in these reactions increased with an increase in the number of CF₃ groups in the ligands, and also as the hydrogen-atom-donating ability of the alcohol solvent increased. Photochemical reactions such as photo-induced ligand exchange which are associated with breaking of metal-ligand bonds are also known to be affected by the nature of ligand and solvents. Meyer and coworkers⁶⁴ have shown that the photo-stability of ruthenium polypyridyl complexes to such photo-induced ligand exchange reactions decreases with an increase in the use of strong ligands or co-ordinating solvents such as acetonitrile.

Several reports on the *cis/trans* isomerisation of platinum group metal complexes in which the processes depend on nature of the co-ordinating ligands and solvents have been published.^{65,66,67,68} In some substituted metal complexes, the *cis* isomer tends to be more favoured by the presence of two organic (R) groups as substituents ([MR₂L₂]), whereas the *trans* isomer is more favoured when only one of such organic groups is present ([MRXL₂]).⁶⁹ This could be due to the fact that in the case where two organic groups are present in the [MR₂L₂] complex, the two ligands (L) may end up being opposite to each other. This may result to *trans* effect in the complexes being weakened as the ligands would be able compete for the same metal center and hence the *cis* isomer is favoured.⁶⁹ Steric effects of ligands coordinated to the metal center could also play a role to determine which isomer is favoured to the other. Hence solutions of complexes of the type [PdCl₂(PR₃)₂] (R = alkyl or aryl) in chloroform upon *cis/trans* isomerisation are known for the extra stability imparted on the *cis* isomer of the complex when aryl substituents are present.⁷⁰ When smaller alkyl groups such as ethyl, propyl and butyl are present, the formation of the *trans* isomer of the complex is favoured.

There are however, limited reports on how variation of ligands or solvent medium would affect the photochemical *cis/trans* isomerisation of Pt(II) or Pd(II) with chelating ligands such

as the *N,N*-dialkyl-*N'*-acyl(aryl)thioureas ($[M(L^n-S,O)_2]$ ($M = Pt(II), Pd(II)$) except for that published by Koch *et al.*^{56,58} In such complexes, a dipole could be created in the excited state which could lead to their greater stability relative to the ground state in the presence of a solvent with higher dielectric constant.⁵⁸ Since the *trans*- $[M(L^n-S,O)_2]$ complexes should have a square planar geometry, they are expected to have a zero dipole moment whereas the *cis*- $[M(L^n-S,O)_2]$ complexes would have a non-zero dipole moment. Hence in the presence of a solvent with high dielectric constant, the *cis*- $[M(L^n-S,O)_2]$ complexes should be more stable than the *trans*- $[M(L^n-S,O)_2]$ complexes. The use of highly polar solvents such as acetonitrile could further stabilise the *trans*- $[M(L^n-S,O)_2]$ complexes relative to the stability of the *cis*- $[M(L^n-S,O)_2]$ complexes.⁵⁸

1.4.4. Mechanism of *cis/trans* isomerisation in d^8 metal complexes

Several mechanisms have been proposed for the *cis/trans* isomerisation of square planar metal complexes which are based on whether the process occurs spontaneously or if it is catalysed. Catalysed *cis/trans* isomerisation mechanisms can be classified into Consecutive Displacement Mechanism and the Pseudorotation Mechanism.

The Consecutive displacement mechanism which was first tentatively proposed in 1934⁷¹ proceeds through a trigonal bipyramidal intermediate and involves only stereospecific ligand substitution steps as shown in Figure 1.13, where L is a neutral ligand attached to the Pt center. The ligand L is first attached to the Pt center in the *cis* complex to form a trigonal bipyramidal intermediate (A). It then replaces the halide ion (X^-) in the complex to form $[PtXL_3]^+X^-$ after which another trigonal bipyramidal intermediate B is formed. This then leads to dissociation of the ligand molecule to give the *trans* complex. In these reactions, the *trans* effect of the ligand either stabilises the trigonal bipyramidal intermediate through the influence of π acceptor properties or destabilises the M-X bond. A Pseudorotation isomerisation mechanism is different from the consecutive displacement mechanism in that it does not involve the step for the formation of an ionic intermediate.

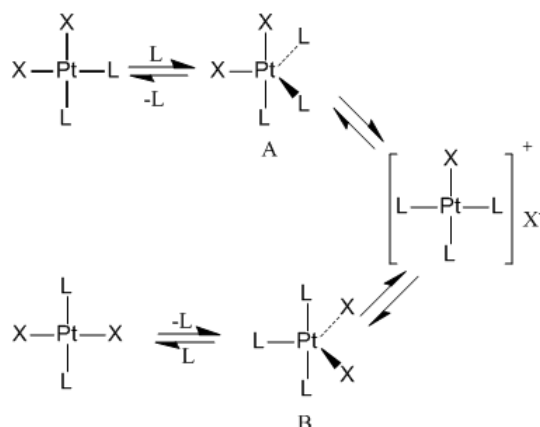


Figure 1.13. A scheme illustrating the consecutive displacement mechanism.

Earlier studies carried out by Cooper and Powell⁷² showed that complexes of the form $[\text{PdCl}_2(\text{Me}_2\text{RP})_2]$ ($\text{R} = o\text{-tolyl}, \alpha\text{-naphthyl}$) could undergo *cis/trans* isomerisation *via* a consecutive displacement mechanism with the formation of a $[\text{PdCl}(\text{Me}_2\text{-}o\text{-tolylP})_2\text{L}]^+$ intermediate. The rate of *cis/trans* isomerisation of these complexes in chloroform was found to depend on the type of ligand present. The rates of isomerisation were initially slow as a result of the bulky nature of the R groups, and much slower when PPh_3 ligands were used. In a later study, Louw⁷³ argued the fact that the *cis/trans* isomerisation of complexes of the form MX_2L_2 occur *via* a consecutive displacement mechanism as was earlier proposed. This argument was based partly on the observation that no reaction occurred when excess Cl^- was added to $[\text{PtCl}(\text{PEt}_3)_3]^+$ in a MeOH/n-hexane/chloroform mixture, as was expected for a consecutive displacement mechanism to take place. Instead, Louw suggested that the reaction occurred by a Pseudorotation mechanism involving a distorted five-co-ordinate intermediate in which the catalyst used occupies a unique position. Louw's conclusions were however contradicted later by Cooper and Powell⁷⁴ whose results showed that the isomerisation of the same compounds actually could occur *via* a consecutive displacement mechanism.

Other studies by Louw⁷⁵ also showed that a Pseudorotation mechanism was involved in iodide-catalysed isomerisation and phosphine-catalysed isomerisation in polar and non-polar systems for compounds of the type PtX_2L_2 ($\text{X} = \text{halide}, \text{L} = \text{phosphine}$). The reactions were shown to possibly occur by a consecutive displacement mechanism in the case where one of the halide groups in the compound was replaced by another group which has a strong *trans* effect such as alkyl or aryl. Catalysed *cis/trans* isomerisation of palladium complexes of the

form $[\text{PdX}_2(\text{am})_2]$ (am = amine), have also been proposed to occur *via* a consecutive displacement mechanism.⁷⁶

Isomerisation reactions may also occur spontaneously without the need of a catalyst and examples of these are by a direct geometry change and that involving a dissociative mechanism. For a direct geometry change mechanism, a change in geometry takes place for the intermediate of the tetrahedral complex involved. A dissociative mechanism is linked to ligand substitution with the arguments similar to those between the consecutive displacement and Pseudorotation mechanisms previously discussed.

With the studies carried out so far on the photo-induced *cis/trans* isomerisation of *cis*- $[\text{M}(\text{L}^n\text{-S},\text{O})_2]$ complexes,^{56,58} the mechanisms by which these reactions would occur is still poorly understood. Such photochemically induced *cis/trans* isomerisation reactions could occur either by an intramolecular or an intermolecular mechanism.⁷⁷ The possible pathways by which these two mechanisms could occur are shown in Figure 1.14. The first step which represents an intramolecular mechanism could either occur by an intramolecular “twisting” or may involve the breaking of a metal-ligand bond. Intermolecular mechanisms could involve co-ordination of a ligand or a solvent and may be associative or dissociative.

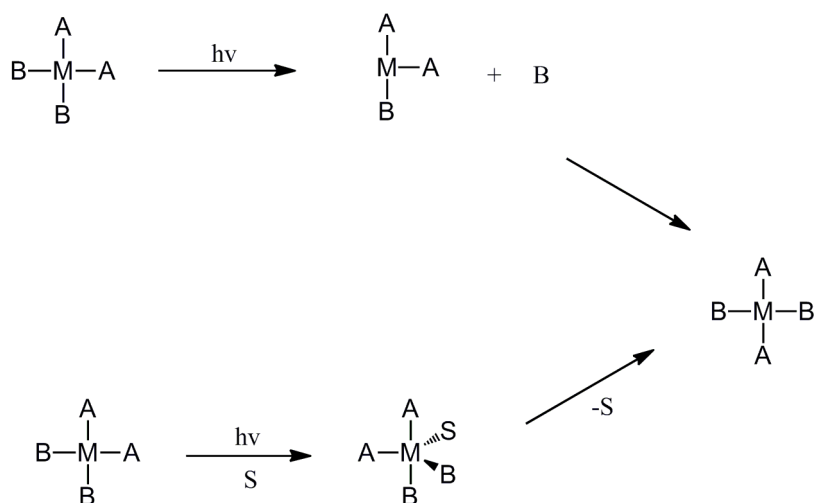


Figure 1.14. Schemes representing intramolecular and intermolecular mechanisms during photo-induced isomerisation, S = solvent.⁷⁷

1.5. Aims and objectives of this work

Reports from previous studies show the synthesis of some hydrophilic *N,N*-dialkyl-*N'*-acyl(aryl)thioureas and their corresponding *cis*-[Pt(Lⁿ-S,O)₂], *cis*-[Pd(Lⁿ-S,O)₂] and *fac*-[Rh(Lⁿ-S,O)₃] complexes and also the use of reversed-phase HPLC for separation of the complexes.¹⁰ While the Pt(II) complexes with monodentate ligands are expected to undergo *cis/trans* isomerisation readily, the same cannot be said for these chelating *N,N*-dialkyl-*N'*-acyl(aryl)thioureas and only few examples of such reactions for complexes with these ligands are known.^{56,58,60}

In view of this, the present study involves the extension of this method for the separation and recovery of the other platinum group of metals Ru(III) and Ir(III) as well as to investigate the ligand effects on the rates of isomerisation for *cis*-[Pt(Lⁿ-S,O)₂] and *cis*-[Pd(Lⁿ-S,O)₂] in an attempt to be able to successfully trap and isolate the *trans*-[M(Lⁿ-S,O)₂] complexes formed and to understand the mechanism of isomerisation.

The specific objectives of this study are:

1. To synthesise and characterise a series of *cis*-[M(Lⁿ-S,O)₂] (M = Pt(II), Pd(II)) and *fac*-[M(Lⁿ-S,O)₃] (M = Rh(III), Ru(III) and Ir(III)) complexes.
2. To evaluate the use of reversed-phase HPLC for the separation of a mixture of *cis*-[Pt(L³-S,O)₂], *cis*-[Pd(L³-S,O)₂], *fac*-[Rh(L³-S,O)₃], *fac*-[Ru(L³-S,O)₃] and *fac*-[Ir(L³-S,O)₃] complexes synthesised.
3. To use a salt induced pre-concentration method for preparation of aqueous acidic solution of Pt(II), Pd(II), Rh(III) and Ru(III) prior to HPLC analysis.
4. To investigate the photo-induced isomerisation of *cis*-[M(Lⁿ-S,O)₂] (M = Pt(II), Pd(II)) complexes using different setups.
5. To determine the effect of ligand substituents on relative rates of *cis*→*trans* and *trans*→*cis* of isomerisation for the [M(Lⁿ-S,O)₂] (M = Pt(II), Pd(II)) complexes.

CHAPTER II

Synthesis and characterisation of ligands, platinum(II), palladium(II), rhodium(III), ruthenium(III) and iridium(III) complexes

In this chapter, the synthesis of a variety of *N,N*-dialkyl-*N'*-acyl(aryl)thiourea ligands together with their *cis*-[M(Lⁿ-S,O)₂] (M = Pt(II), Pd(II)) and *fac*-[M(Lⁿ-S,O)₃] (M = Rh(III), Ru(III) or Ir(III)) complexes is described. The ligands were synthesised according to a slightly modified procedure used by Douglass and Dains⁷⁸ which involves a simple two-step procedure. The ligands and complexes were characterised by a variety of techniques including ¹H and ¹³C NMR spectroscopy, IR spectroscopy and mass spectrometry, the results of which are discussed here.

2.1. Synthesis

2.1.1. Synthesis of Ligands

Some of the properties of the *N,N*-dialkyl-*N'*-acyl(aryl)thioureas include their relatively hydrophilic nature and their solubility in water-miscible organic solvents such as acetonitrile and methanol. These properties depend on the structure of the ligands and the nature of the alkyl or aryl substituents and hence can be varied selectively. The properties impart the ability to separate a solution of the uncharged complexes of the ligands using reversed-phase HPLC. This was taken into consideration when selecting the ligands synthesised in this work by introducing either electron-donating or withdrawing groups into the ligand structure. Table 2 gives a list of ligands that were selected during this study with their structures together with the abbreviations used throughout this study.

Table 2. Table of a list of names, abbreviations and structures for the *N,N*-dialkyl-*N'*-acyl(aroyl)thioureas used for complex formation.

Name and abbreviation	Structure
<i>N</i> -pirrolidyl- <i>N'</i> -(2,2-dimethylpropanoyl)thiourea (HL¹)	
<i>N,N</i> -dibutyl- <i>N'</i> -(2,2-dimethylpropanoyl)thiourea (HL²)	
<i>N,N</i> -diethyl- <i>N'</i> -benzoylthiourea (HL³)	
<i>N</i> -piperidyl- <i>N'</i> -benzoylthiourea (HL⁴)	
<i>N,N</i> -diethyl- <i>N'</i> - <i>p</i> -methoxy-benzoylthiourea (HL⁵)	
<i>N,N</i> -diethyl- <i>N'</i> -3,4,5-trimethoxybenzoylthiourea (HL⁶)	
<i>N,N</i> -diethyl- <i>N'</i> - <i>p</i> -chloro-benzoylthiourea (HL⁷)	

Of the ligands selected, *N*-pirrolidyl-*N'*-(2,2-dimethylpropanoyl)thiourea (**HL**¹), *N,N*-dibutyl-*N'*-(2,2-dimethylpropanoyl)thiourea (**HL**²) and *N,N*-diethyl-*N'*-benzoylthiourea (**HL**³) were synthesised while other ligands were donated already synthesised by previous members of our group.

Generally, the ligands were obtained by a two-step synthetic procedure in which an appropriate acid chloride was reacted with anhydrous potassium thiocyanate in the first step in a solution of anhydrous acetone. The second step requires addition of an appropriate secondary amine in anhydrous acetone to the mixture to yield the desired ligand as shown in Figure 2.1. Dry conditions were needed, requiring anhydrous acetone and an atmosphere of nitrogen during both steps of the synthesis, to avoid moisture in the reaction mixture which could have led to hydrolysis of the acid chloride to a carboxylic acid.

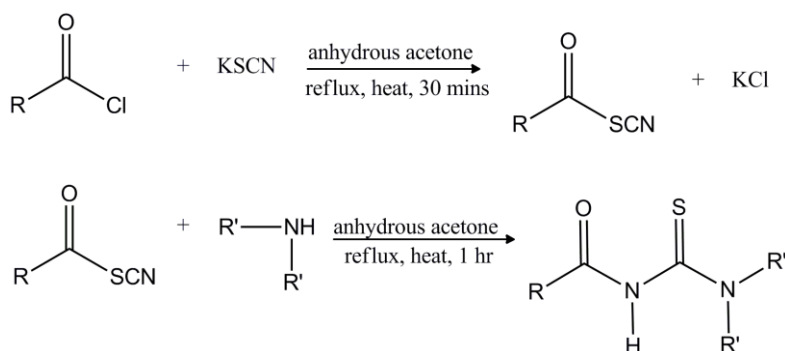


Figure 2.1. Reaction scheme for the synthesis of *N,N*-dialkyl-*N'*-acyl(aroyl)thioureas.

2.1.2. Synthesis of platinum(II), palladium(II), rhodium(III), ruthenium(III) and iridium(III) complexes with *N,N*-dialkyl-*N'*-acyl(aroyl)thioureas

The ease of complex formation of metals with the *N,N*-dialkyl-*N'*-acylthioureas varies from one metal to the other. The divalent Pt(II) and Pd(II) metal ions are expected to co-ordinate much easily compared to trivalent Rh(III), Ru(III) and Ir(III) ions which would mostly require heating conditions for complex formation to take place. Some of the challenges which could be involved during complex formation of ligands with platinum group of metals include the fact that the metals can exist in more than one oxidation states⁷⁹ and that in aqueous media, they could form many different species.⁸⁰ Thus during synthesis, different reaction yields

were obtained for all the complexes depending on the metal oxidation state and the medium used.

The metal complexes of Pt(II), Pd(II) and Rh(III) were synthesised according to literature procedures¹⁰ as shown schematically in Figure 2.2. This required adding a slight excess of two mole equivalents of the required ligands in an acetonitrile/water mixture to one equivalent of the Pt(II) or Pd(II) salts or three mole equivalent of the ligands to one mole equivalent of a solution of Rh(III) salt in the presence of sodium acetate. The reactions of Pt(II) and Pd(II) with the ligands were much faster and occurred on stirring at room temperature while Rh(III) complexes were formed only on heating under reflux for 8 hours. The same procedure was used to synthesise Pt(II) and Pd(II) complexes with both the *N,N*-dialkyl-*N'*-acylthioureas and *N,N*-dialkyl-*N'*-aroylthioureas.

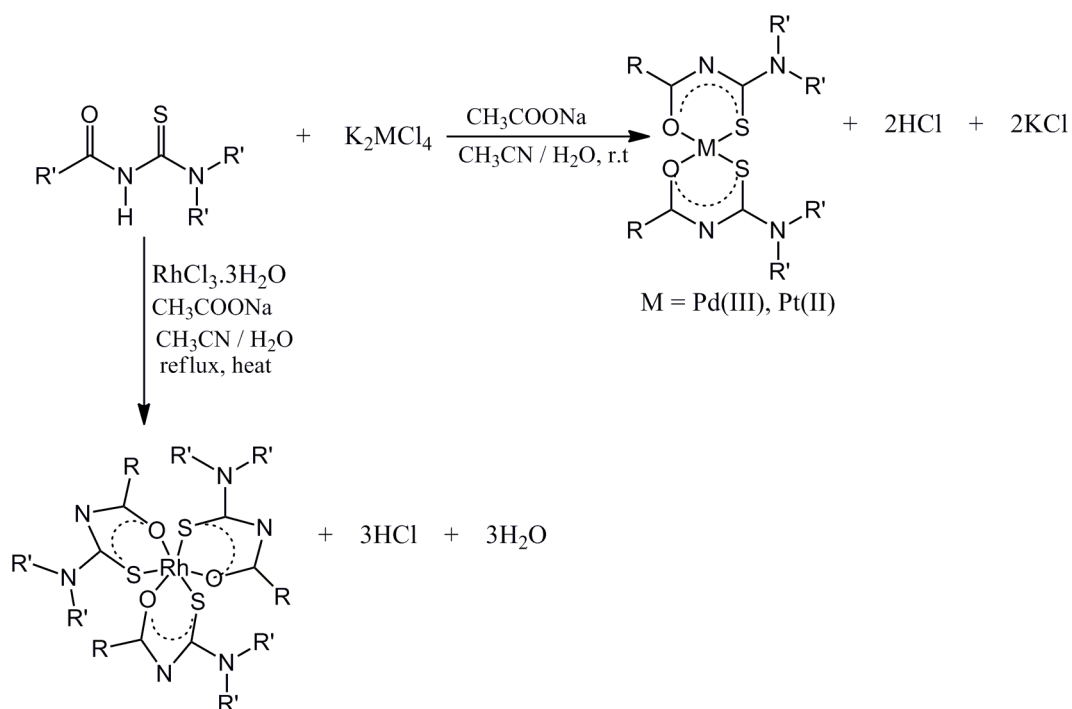


Figure 2.2. Reaction scheme for synthesis of *cis*-bis(*N,N*-diethyl-*N'*-benzoylthioureato)platinum(II), *cis*-bis(*N,N*-diethyl-*N'*-benzoylthioureato)palladium(II) and *fac*-tris(*N,N*-diethyl-*N'*-benzoylthioureato)rhodium(III).

During the synthesis, sodium acetate was used to deprotonate the N-H group, facilitating complex formation. Although the detailed mechanism for this reaction is not known, it is suggested that the initial step could involve the deprotonation of the uncharged ligand in the presence of sodium acetate to form an anionic form of the ligand. The anionic form of the *N,N*-dialkyl-*N'*-acyl(aroyl)thioureas is significantly more nucleophilic than the uncharged

form of this class of ligands. In the presence of M(II)/M(III) halide ions, the $[M(L^n-S,O)_2]$ or $[M(L^n-S,O)_3]$ complexes are readily formed as shown in Figure 2.3. In reference to the crystal structures previously determined for the Pt(II), Pd(II) and Rh(III) complexes synthesised,¹⁰ it is assumed that co-ordination of these metal ions to the ligands result to *cis*- $[Pt(L^n-S,O)_2]$, *cis*- $[Pd(L^n-S,O)_2]$ and *fac*- $[Rh(L^n-S,O)_3]$ complexes respectively and this assumption will be used for the remaining part of the study.

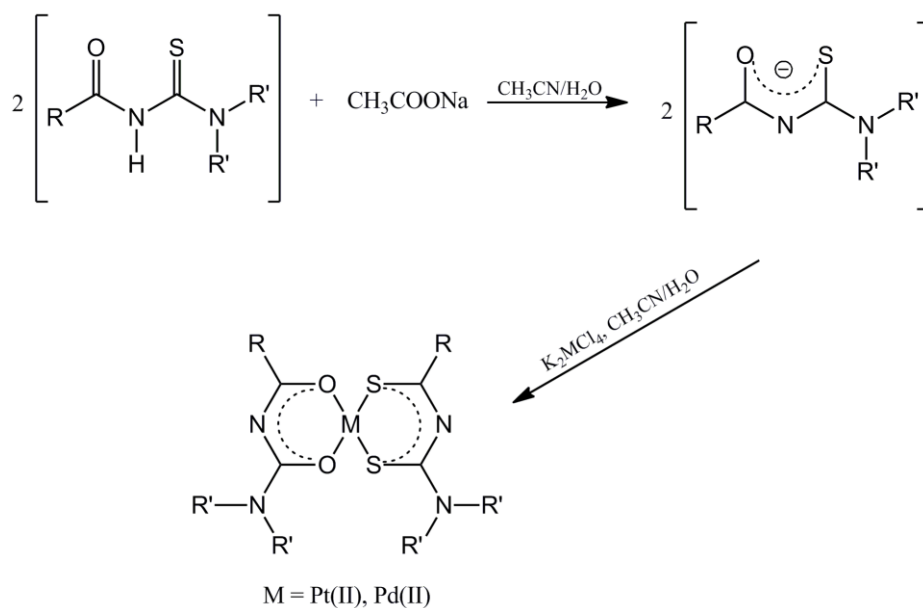


Figure 2.3. Reaction scheme for the synthesis of palladium(II) and platinum(II) *N,N*-dialkyl-*N'*-acyl(aryl)thiureas.

A synthesis of ruthenium(III) complex with *N*-pyrrolidyl-*N'*-(2,2-dimethylpropanoyl)thiourea and *N,N*-dibutyl-*N'*-(2,2-dimethylpropanoyl)thiourea using the procedure described above, yielded products which could not be isolated under the conditions used. However, the use of more hydrophobic ligands such as *N,N*-diethyl-*N'*-benzoylthiourea (**HL**³) resulted in the isolation of the corresponding $[Ru(L^3-S,O)_3]$ and $[Ir(L^3-S,O)_3]$ complexes using methanol as a suitable solvent, from which these complexes could be isolated in reasonable yields.

The complexes tris(*N,N*-diethyl-*N'*-benzoylthioureato)ruthenium(III) and tris(*N,N*-diethyl-*N'*-benzoylthioureato)iridium(III) were synthesised according to the scheme shown in Figure 2.4, a procedure which has previously been used by Schuster and coworkers²¹ under slightly acidic conditions of pH 2-4. This required addition of a slight excess of three mole equivalents of the ligand in methanol to one mole equivalent of an acetic acid/acetate buffer solution (pH 2) of the Ru(III) or Ir(III) salts used.

Alternatively, tris(*N,N*-diethyl-*N'*-benzoylthioureato)ruthenium(III) was also synthesised using a similar procedure described earlier for the preparation of *cis*-[M(Lⁿ-*S,O*)₂] (M = Pt(II), Pd(II)) and *fac*-[Rh(Lⁿ-*S,O*)₃] complexes but using methanol as a suitable solvent. Hence in the presence of sodium acetate in methanol and by heating to reflux, a slight excess of three mole equivalents of a solution of the *N,N*-diethyl-*N'*-benzoylthiourea was added to one mole of a solution of RuCl₃·3H₂O to give [Ru(L³-*S,O*)₃]. With this alternative route however, a slightly lower reaction yield (66.4 %) was obtained compared to the previous route when the reaction was carried out in a slightly acidic medium (67 % yield). Higher reaction yields were also obtained for the *cis*-[M(Lⁿ-*S,O*)₂] (M = Pt(II), Pd(II)) complexes compared to corresponding *fac*-[M(Lⁿ-*S,O*)₃] (M = Rh(III), Ru(III), Ir(III)) complexes. Although the detailed reason for these differences in yield was not studied further, it is likely due to the possible hydrolysis of RuCl₃·3H₂O when dissolved, to give soluble forms of precursor complexes such as [RuCl₃(OH)_n(H₂O)_{3-n}] in the formation of [Ru(L³-*S,O*)₃] and [Ir(L³-*S,O*)₃]. Thus the direct reaction of the *N,N*-dialkyl-*N'*-acyl(aro)ylthioureas with such solutions does not possibly give only one product hence lower yields are obtained. In the synthesis of *cis*-[M(Lⁿ-*S,O*)₂] (M = Pt(II), Pd(II)) complexes from their respective salts, hydrolysis of the PtCl₄²⁻ or PdCl₄²⁻ could be slow, resulting to only one product and hence higher yields.

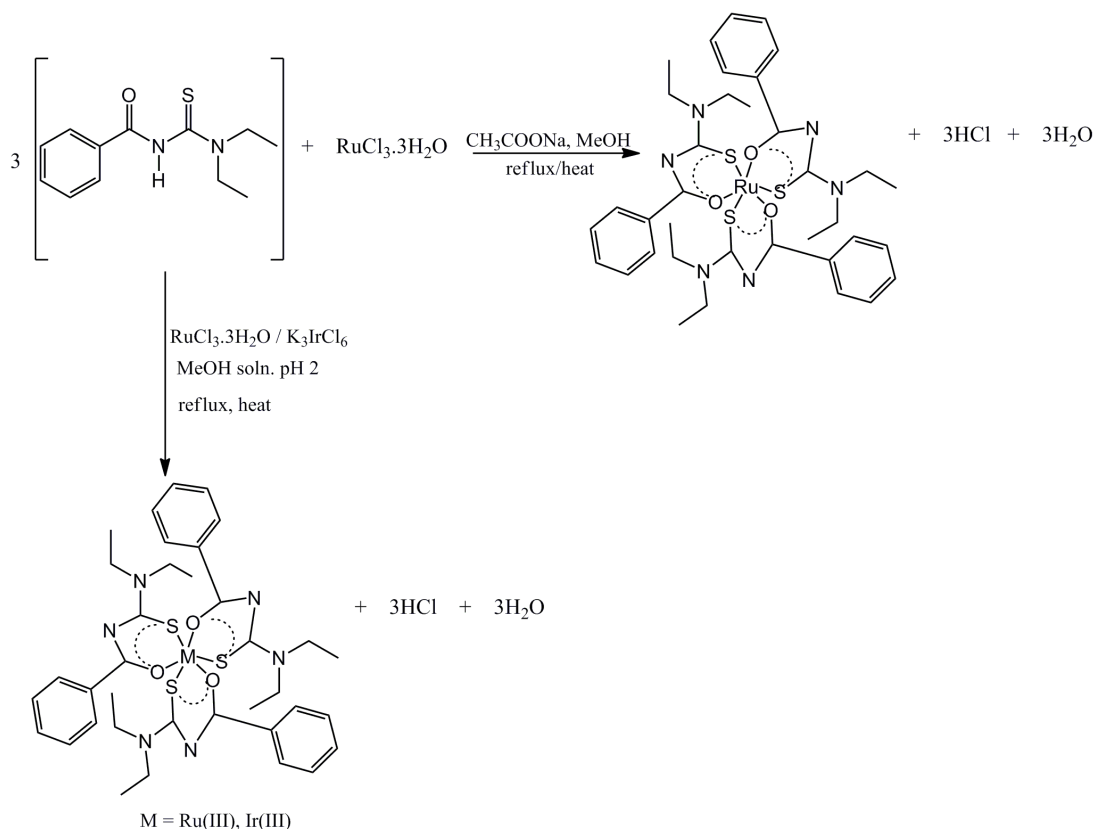


Figure 2.4. Reaction scheme for synthesis of tris(*N,N*-diethyl-*N'*-benzoylthioureato)ruthenium(III) and tris(*N,N*-diethyl-*N'*-benzoylthioureato)iridium(III).

2.1.3. Experimental details for synthesis of Ligands and complexes

2.3.3.1. Ligands

The ligands *N*-pirrolidyl-*N'*-(2,2-dimethylpropanoyl)thiourea (**HL**¹), *N,N*-dibutyl-*N'*-(2,2-dimethylpropanoyl)thiourea (**HL**²) and *N,N*-diethyl-*N'*-benzoylthiourea (**HL**³) were synthesised by dissolving 0.03 mole of potassium thiocyanate in 50 ml anhydrous acetone to which a solution of 0.03 mole of the appropriate acyl chloride in anhydrous acetone was added drop-wise. The mixture was heated to reflux for 30 minutes and then allowed to cool to room temperature. To this, 0.03 mole of the appropriate secondary amine dissolved in anhydrous acetone was added slowly. The resulting mixture was heated to reflux for a further 30 minutes, then allowed to cool to room temperature and poured into 100 ml of distilled water. This mixture was allowed to stand in fumehood overnight and the resulting crystals were obtained by re-crystallisation from an acetone/water mixture.

***N*-pirrolidyl-*N'*-(2, 2-dimethylpropanoyl)thiourea (HL¹)**

Colourless crystals; (5.31 g, 2.5 mmol, 81% yield); m.p. 136-137°C; IR (ATR, cm⁻¹): ν (N-H) 3274.95 cm⁻¹ (br, sh), ν (C=O) 1675.52 cm⁻¹ (vs); ¹H NMR (400 MHz, CDCl₃) δ 7.88 (s, 1H, N-H), 3.70 (dt, 4H, N-(CH₂)), 1.98 (unresolved, 4H, CH₂), 1.26 (s, 9H, CH₃); ¹³C NMR (400 MHz, CDCl₃) δ 24.82, 25.48, 28.67, 41.87, 50.35, 168.37, 185.18.

***N, N*-dibutyl-*N'*-(2, 2-dimethylpropanoyl)thiourea (HL²)**

Colourless crystals; (5.78 g, 2.14 mmol, 71.9% yield); m.p. 88-90°C; IR (ATR, cm⁻¹): ν (N-H) 3284.69 cm⁻¹ (br, sh), ν (C=O) 1651.09 cm⁻¹ (vs); ¹H NMR (400 MHz, CDCl₃) δ 7.65 (s, 1H, N-H), 3.64 (dt, 4H, CH₂), 1.66 (unresolved, 4H, CH₂), 1.32 (unresolved, 4H, CH₂), 1.24 (s, 9H, CH₃), 0.92 (p, 6H, CH₃); ¹³C NMR (400 MHz, CDCl₃) δ 13.79, 20.22, 28.43, 29.49, 29.82, 41.64, 51.31, 52.53, 184.99.

***N, N*-diethyl-*N'*-benzoylthiourea (HL³)**

Colourless crystals; (6.3 g, 2.7 mmol, 86.3% yield); m.p. 98-100°C; IR (ATR, cm⁻¹): ν (N-H) 3258.84 cm⁻¹ (br, sh), ν (C=O) 1649.35 cm⁻¹ (vs); ¹H NMR (600 MHz, CDCl₃) δ 8.34 (s, 1H, N-H), 7.82 (d, 2H, Ar-H), 7.56 (t, 1H, Ar-H), 7.46 (t, 2H, Ar-H), 3.81 (d, 4H, N-CH₂), 1.32 (t, 6H, CH₃); ¹³C NMR (600 MHz, CDCl₃) δ 11.32, 13.14, 47.54, 50.58, 129.25, 131.68, 134.11, 137.89, 164.23, 179.97.

***N*-piperidyl-*N'*-benzoylthiourea (HL⁴)**

m.p. 130-134 °C; ¹H NMR (600 MHz, CDCl₃) δ 1.71 (unresolved, 6H, CH₂), 3.87 (d, 4H, CH₂), 7.47 (t, 2H, Ar-H), 7.57 (unresolved, 1H, Ar-H), 7.83 (dd, 2H, Ar-H), 8.42 (s, 1H, N-H); ¹³C NMR (600 MHz, CDCl₃) δ 23.86, 25.24, 52.77, 127.77, 128.86, 132.57, 132.94, 163.13, 178.17.

***N, N*-diethyl-*N'*-*p*-methoxy-benzoylthiourea (HL⁵)**

m.p. 134-145 °C; ¹H NMR (600 MHz, CDCl₃) δ 1.27 (unresolved, 6H, CH₃), 3.57 (unresolved, 2H, CH₂), 3.84 (s, 3H, Ar-H), 6.93 (d, 2H, Ar-H), 8.21 (s, 1H, N-H); ¹³C NMR (600 MHz, CDCl₃) δ 11.28, 12.95, 47.66, 51.44, 114.17, 124.97, 130.00, 163.57, 179.93.

***N, N*-diethyl-*N'*-3,4,5-trimethoxybenzoylthiourea (HL⁶)**

m.p. 143-145 °C; ^1H NMR (600 MHz, CDCl_3) δ 1.31 (unresolved, 6H, CH_3), 3.55 (unresolved, 2H, CH_2), 3.85 (s, 3H, CH_3), 3.87 (s, 6H, CH_3), 7.05 (s, 2H, Ar-H), 8.82 (s, 1H, N-H); ^{13}C NMR (600 MHz, CDCl_3) δ 11.41, 13.30, 47.71, 56.38, 60.91, 105.23, 127.36, 142.05, 153.12, 163.34, 179.62.

2.3.3.2. Platinum(II), palladium(II) and rhodium(III) complexes

The synthetic procedures for the Pt(II), Pd(II) and Rh(III) complexes of all the ligands used were carried out as follows: a mixture was made containing 2 mole equivalents (for Pt(II) and Pd(II)) or 3 mole equivalents (for Rh(III)) of the ligands and with similar mole equivalents of sodium acetate dissolved in 10 ml of water and 15 ml of acetonitrile. To this mixture, a solution containing 1 mole equivalent of either K_2PtCl_4 , K_2PdCl_4 or $\text{RhCl}_3 \cdot 3\text{H}_2\text{O}$ dissolved in 10 ml of acetonitrile and 15 ml of water was added drop-wise. For Pt(II) and Pd(II) constant stirring of the mixture at room temperature was required while for the Rh(III) complexes, the mixture was heated under reflux for 6 hours. The reaction mixture was then allowed to cool to room temperature followed by the addition of 100 ml of distilled. The precipitates obtained were then placed in a refrigerator overnight and centrifugation afforded the solid complexes which were dried in vacuum.

2.3.3.3. Ruthenium(III) and iridium(III) complexes

The synthetic procedures for the tris(*N,N*-diethyl-*N'*-benzoylthiourea) ruthenium(III) and tris(*N,N*-diethyl-*N'*-benzoylthiourea) iridium(III) were done as follows:

Solutions of Ru(III) or Ir(III) were made by dissolving 0.15 mmol of $\text{RuCl}_3 \cdot 3\text{H}_2\text{O}$ or K_3IrCl_6 in 15 ml acetate buffer (pH 2). These were then added drop-wise to a refluxed mixture containing 0.5 mmol *N,N*-diethyl-*N'*-benzoylthiourea dissolved in methanol and the resulting mixture was heated for about 8 hours followed by cooling to room temperature. The precipitates formed were isolated by centrifugation and dried under vacuum.

Alternatively, 0.15 mmol of a solution of $\text{RuCl}_3 \cdot 3\text{H}_2\text{O}$ in a methanol/water (50:50 % v/v) was added drop-wise to a solution containing 0.5 mmol of *N,N*-diethyl-*N'*-benzoylthiourea. The resulting mixture was heated for 6 hours under reflux after which it was allowed to cool to room temperature. The reddish brown (for ruthenium) and orange (for iridium) precipitates obtained were washed with distilled water, centrifuged and dried under vacuum.

Bis(*N*-pirrolidyl-*N'*-2,2-dimethylpropanoylthioureato)palladium(II) [Pd(L¹-S,O)₂]

Yellow solid; (0.23 g, 0.43 mmol, 85.2% yield); m.p. 218-219°C; IR (ATR, cm⁻¹): ν (C=O) 1513.36 cm⁻¹(w); ¹H NMR (400 MHz, CDCl₃) δ 3.4 (dt, 4H, N-CH₂), 2.1 (m, 4H, CH₂), 1.6 (d, 4H, CH₂), 1.2 (d, 9, CH₃); ¹³C NMR (400 MHz, CDCl₃) δ 24.82, 25.84, 28.62, 41.81, 50.43, 168.37, 185.23.

Bis(*N,N*-dibutyl-*N'*-2,2-dimethylpropanoylthioureato)palladium(II) [Pd(L²-S,O)₂]

Yellow solid; (0.251 g, 0.39 mmol, 81.2% yield); m.p. 132-134°C; IR (ATR, cm⁻¹): ν (C=O) 1589.33 cm⁻¹(w); ¹H NMR (400 MHz, CDCl₃) δ 3.8 (m, 4H, CH₂), 1.8 (m, 2H, CH₂), 1.6 (m, 2H, CH₂), 1.3 (m, 4H, CH₂), 1.2 (s, 9H, CH₃), 0.9 (dt, 6H, CH₃); ¹³C NMR (400 MHz, CDCl₃) δ 13.79, 13.89, 20.22.

Bis(*N,N*-diethyl-*N'*-benzoylthioureato)palladium(II) [Pd(L³-S,O)₂]

Yellow solid; (0.106 g, 0.18 mmol, 88.3% yield); m.p. 159-163°C; IR (ATR, cm⁻¹): ν (C=O) 1583.74 cm⁻¹ (w); ¹H NMR (400 MHz, CDCl₃) δ 8.26 (d, 2H, Ar-H), 7.50 (unresolved, 1H, Ar-H), 7.44 (unresolved, 2H, Ar-H), 3.85 (m, 4H, N-CH₂), 3.50 (q, 4H, CH₂), 1.33 (unresolved, 4H, CH₂), 1.23 (t, 6H, CH₃); ¹³C NMR (400 MHz, CDCl₃) δ 12.63, 13.14, 15.28, 46.07, 47.22, 65.86, 127.95, 129.69, 131.45, 137.10, 170.64, 171.12.

Bis(*N,N*-diethyl-*N'*-benzoylthioureato)platinum(II) [Pt(L³-S,O)₂]

Orange yellow solid; (0.03 g, 0.045 mmol, 62.5% yield); m.p. 170-174°C; IR (ATR, cm⁻¹): ν (C=O) 1587.41 cm⁻¹ (w); ¹H NMR (600 MHz, CDCl₃) δ 8.28 (unresolved, 2H, Ar-H), 7.53 (unresolved, 1H, Ar-H), 7.46 (unresolved, 2H, Ar-H), 3.80 (q, 4H, CH₂), 3.50 (q, 4H, CH₂), 1.23 (t, 6H, CH₃); ¹³C NMR (600 MHz, CDCl₃) δ 12.46, 13.18, 15.28, 45.92, 47.00, 65.85, 128.07, 129.38, 131.36, 137.60, 167.03, 168.45.

Bis(*N*-piperidyl-*N'*-benzoylthioureato)palladium(II) [Pd(L⁴-S,O)₂]

Yellow solid, (0.062 g, 0.0103 mmol, 82.7% yield); m.p. 130-134°C; IR (ATR, cm⁻¹): ν (C=O) 1583.89 cm⁻¹(w); ¹H NMR (600 MHz, CDCl₃) 1.72 (unresolved, 6H, CH₂), 4.11 (unresolved, 4H, CH₂), 7.41 (t, 2H, Ar-H), 7.48 (t, 1H, Ar-H), 8.23 (unresolved, 2H, Ar-H);

^{13}C NMR (600 MHz, CDCl_3) δ 24.50, 26.09, 48.62, 51.05, 127.91, 129.72, 131.47, 131.14, 171.09, 171.39.

Bis(*N,N*-diethyl-*N*-*p*-methoxy-benzoylthioureato)palladium(II) [$\text{Pd}(\text{L}^5\text{-S,O})_2$]

Orange yellow solid (0.069 g, 0.1087 mmol, 86.5% yield); m.p. 138-140°C; IR (ATR, cm^{-1}): ν (C=O) 1579.25 cm^{-1} (w); ^1H NMR (600 MHz, CDCl_3) δ 1.33 (dt, 6H, CH_3), 3.84 (unresolved, 4H, CH_2), 3.87 (s, 3H, O- CH_3), 7.29 (unresolved, 2H, Ar-H), 7.03 (unresolved, 2H, Ar-H); ^{13}C NMR (600 MHz, CDCl_3) δ 12.61, 13.13, 46.15, 47.25, 55.21, 114.34, 117.81, 122.09, 128.76, 138.57.

Bis(*N,N*-diethyl-*N'*-3,4,5-trimethoxybenzoylthioureato)palladium(II) [$\text{Pd}(\text{L}^6\text{-S,O})_2$]

Yellow solid; (0.081 g, 0.0107 mmol, 85.3% yield); m.p. 198 – 202 °C; IR (ATR, cm^{-1}): ν (C=O) 1589.40 cm^{-1} (w); ^1H NMR (300 MHz, CDCl_3) δ 1.28 (t, 6H, CH_3), 1.32 (t, 6H, CH_3), 3.82 (q, 4H, CH_2), 3.83 (s, 12H, CH_3), 6.85 (t, 2H, Ar-H), 7.44 (d, 4H, Ar-H); ^{13}C NMR (300 MHz, CDCl_3) δ 12.26, 13.10, 46.21, 47.27, 55.35, 103.88, 107.45, 139.17, 160.25, 169.97, 171.18.

Bis(*N,N*-diethyl-*N'*-3,4,5-trimethoxybenzoylthioureato)platinum(II) [$\text{Pt}(\text{L}^6\text{-S,O})_2$]

Orange yellow solid; (0.057 g, 0.01 mmol, 69.5% yield); m.p. 218 – 221 °C, ^1H NMR (600 MHz, CDCl_3) δ 1.29 (t, 6H, CH_3), 1.30 (t, 6H, CH_3), 3.83 (q, 4H, CH_2), 3.87 (s, 12H, CH_3), 3.88 (s, 6H, CH_3), 7.56 (s, 4H, Ar-H); ^{13}C NMR (600 MHz, CDCl_3) δ 12.44, 13.09, 30.84, 46.01, 47.06, 107.45, 132.89, 141.61, 152.62, 166.88, 167.89.

Bis(*N,N*-diethyl-*N'*-*p*-chloro-benzoylthioureato)palladium(II) [$\text{Pd}(\text{L}^7\text{-S,O})_2$]

Orange yellow solid; (0.072 g, 0.112 mmol, 88.9% yield); m.p. 179-181°C; IR (ATR, cm^{-1}): ν (C=O) 1577.73 cm^{-1} (w); ^1H NMR (600 MHz, CDCl_3) δ 1.30 (dt, 6H, CH_3), 3.83 (q, 4H, CH_2), 7.38 (unresolved, 2H, Ar-H), 8.14 (unresolved, 2H, Ar-H); ^{13}C NMR (600 MHz, CDCl_3) δ 12.60, 13.09, 46.10, 47.31, 128.20, 130.97, 135.56, 137.69, 169.59, 171.22.

Tris(*N,N*-diethyl-*N'*-benzoylthioureato)rhodium(III) [$\text{Rh}(\text{L}^3\text{-S,O})_3$]

Yellow solid; (0.082 g, 0.1 mmol, 67% yield); m.p. 202-206°C; ^1H NMR (600 MHz, CDCl_3) δ 8.5 (m, 2H, Ar-H), 7.6 (m, 1H, Ar-H), 7.4 (m, 2H, Ar-H), 3.6 (dd, 4H, CH_2), 1.52 (t, 6H,

CH₃), ¹³C NMR (600 MHz, CDCl₃) δ 12.07, 12.60, 45.12, 45.74, 126.85, 129.04, 130.16, 138.10, 171.35.

Tris(*N,N*-diethyl-*N'*-benzoylthioureato)ruthenium(III) [Ru(L³-S,O)₃]

Reddish brown solid; (0.073 g, 0.09 mmol, 66.4% yield); m.p. 304-308°C; IR (ATR, cm⁻¹): ν (C=O) 1584.64 cm⁻¹ (w); MS-ESI(+): *m/z* [M+H]⁺ = 808.2, *m/z* [M+Na]⁺ = 830.2.

Tris(*N,N*-diethyl-*N'*-benzoylthioureato)iridium(III) [Ir(L³-S,O)₃]

Orange yellow solid; (0.043 g, 0.048 mmol, 62.3% yield); m.p. 158-160°C; IR (ATR, cm⁻¹): ν (C=O) 1583.95 cm⁻¹ (w); MS-ESI (+): *m/z* [M + H]⁺ = 899.2.

2.2. Characterisation

2.2.1. NMR Characterisation

The ¹H NMR spectra of all the *N,N*-dialkyl-*N'*-acyl(aryl)thioureas synthesised are characteristic of two distinct signals for the methylene N-(CH₂)₂ protons of the alkyl substituents.⁸¹ As seen in the ¹H NMR spectra of *N*-pyrrolidyl-*N'*-(2,2-dimethylpropanoyl)thiourea (Figure 2.6), the resonances of these methylene protons bonded to the nitrogen of the thioamide group appear as two separate signals at 3.83 ppm and 3.57 ppm with a well resolved triplet in each signal. The occurrence of two separate resonances is as a result of magnetic inequivalence of the CH₂ protons caused by a restricted rotation around the C-N bond between the thiocarbonyl group and the amine nitrogen. This leads to a partial double character hence the possibility of the ligand to exist in two forms as shown in Figure 2.5.

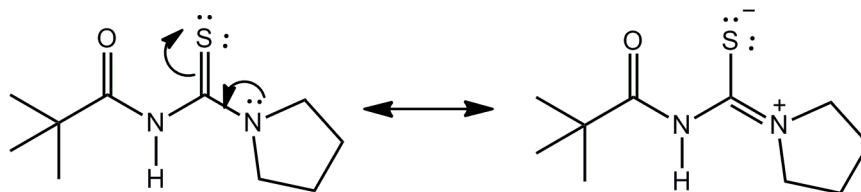


Figure 2 5. Possible resonance structures of *N*-pyrrolidyl-*N'*-(2,2-dimethylpropanoyl)thiourea caused by restricted rotation.

Similar observations in the signals for the N-CH₂ protons are observed in the ¹H NMR spectra of all the other ligands including those with the benzoyl moiety (HL³, HL⁴, HL⁵, HL⁶ and HL⁷). For this group of ligands, no significant difference is observed in the chemical shifts of the N-H signal including *N,N*-diethyl-*N'*-*p*-chloro-benzoylthiourea in which the chloro substituent on the aryl moiety is expected to have an inductive effect. The resonances of the aromatic protons in *N,N*-diethyl-*N'*-*p*-methoxy-benzoylthiourea are shifted upfield compared to those of *N,N*-diethyl-*N'*-benzoylthiourea. This shift is attributed to the presence of the electron-donating methoxy substituents on the aryl moiety of the ligand.

The chemical shifts of the N-CH₂ protons appear to be influenced by the nature of the amine substituent and these chemical shifts values correlate with the different pK_a values of the amine group attached as shown in Table 3. For ligands with similar acyl or aroyl groups attached, the chemical shifts are observed to decrease slightly as the pK_a value of amine group attached decreases. Hence both the dibutylamine (pK_a 11.27) in HL² and the diethylamine groups (pK_a 11.09) in HL³ have lower chemical shifts in the N-CH₂ protons compared to the pyrrolidine (pK_a 11.27) in HL¹ and piperidine groups (pK_a 11.22) in HL⁴ respectively.

Table 3. Table of pK_a values of amine groups and chemical shifts for N-CH₂ protons in *N*-pyrrolidyl-*N'*-(2,2-dimethylpropanoyl)thiourea, *N,N*-dibutyl-*N'*-(2,2,-dimethylpropanoyl)thiourea, *N*-piperidyl-*N'*-benzoylthiourea and *N,N*-diethyl-*N'*-benzoylthiourea in CDCl₃ and at 25 °C.

Ligand	pK _a	Chemical shift / ppm
HL ¹	11.27	3.70
HL ²	11.25	3.64
HL ³	11.09	3.81
HL ⁴	11.22	3.88

The ^1H NMR spectra of the metal complexes have similar features to those of the respective ligands with some exceptions. One of these is the disappearance of the signal for the N-H proton in the spectra of the complexes which is present in that of the free ligand. Figures 2.6 and 2.7 show the ^1H NMR spectra of *N*-pirrolidyl-*N'*-(2,2-dimethylpropanoyl)thiourea and bis(*N*-pirrolidyl-*N'*-(2,2-dimethylpropanoyl)thioureato)palladium(II) respectively. By comparison of both spectra, it is evident the N-H (δ 7.85 ppm) signal which is present in spectrum of the free ligand disappears in that of the *cis*-[Pd(L¹-S,O)₂] complex. This disappearance in the signal for the N-H protons confirms ligand deprotonation.⁸¹

Also the two sets of triplets for the N-CH₂ protons which appeared to be well separated in the spectrum of the free ligand (δ 3.83 and 3.57 ppm) are closer to each other centered at δ 3.69 ppm for bis(*N*-pirrolidyl-*N'*-(2,2-dimethylpropanoyl)thioureato)palladium(II) and this shift is also characteristic of complex formation.⁸¹ The fact that these signals are still separated to some extent indicates that there is still some degree of restricted rotation across the C-N bond even in the complexes.

The ^1H NMR spectra of the ligands and their respective *cis*-[Pd(Lⁿ-S,O)₂], *cis*-[Pt(Lⁿ-S,O)₂] and *fac*-[Rh(L³-S,O)₃] complexes showed similar characteristics to those of *N*-pirrolidyl-*N'*-(2,2,-dimethylpropanoyl)thiourea and the corresponding *cis*-[Pd(L¹-S,O)₂] complex (Appendix I). The fact that all the metal complexes show essentially the same chemical shifts for all the protons of the same ligand suggests that the proton electronic environments in these complexes are not largely affected by the changes in metal center.

Table 4 gives a summary of the chemical shifts for the assigned protons of *N,N*-diethyl-*N'*-benzoylthiourea (HL³), its corresponding *cis*-[Pd(L³-S,O)₂] complex and those of other derivatives of the ligand. Differences can be observed for the chemical shifts of the protons in the aromatic region of the ligand. The *ortho* protons (H3 and H3') appear to be more deshielded and hence are shifted more downfield compared to the *meta* and *para* protons (H1, H1' and H2). This shift is caused by magnetic anisotropy of π bonds of the carbonyl group attached to the aryl ring. After complex formation resulting to bis(*N,N*-diethyl-*N'*-benzoylthioureato)palladium(II), a slight decrease in chemical shift is observed for the *meta* and *para* protons, meanwhile the *ortho* protons appear to be more deshielded than in the free ligand.

The presence of electron-donating methoxy substituents in bis(*N,N*-diethyl-*N'*-*p*-methoxy-benzoylthioureato)palladium(II) appears to induce a greater shielding effect on the *ortho* protons (H1 and H1') than in the *meta* protons (H3 and H3'), hence the *meta* protons are shifted more downfield compared to the *ortho* protons. Compared to those in bis(*N,N*-diethyl-*N'*-benzoylthioureato)palladium(II), these protons are however more upfield which could mean that the magnetic anisotropic effect of the carbonyl group is greater compared to the electron-donating effect of the methoxy substituent. Similar observations are made for the protons *meta* to the *p*-methoxy group (H3 and H3') in bis(*N,N*-diethyl-*N'*-3,4,5-trimethoxy-benzoylthioureato)palladium(II).

The ¹H NMR spectra of other ligands and complexes are listed in Appendix I and show similar features to that discussed so far. The ¹H NMR spectra of tris(*N,N*-diethyl-*N'*-benzoylthioureato)ruthenium(III) and tris(*N,N*-diethyl-*N'*-benzoylthioureato)iridium(III) showed broad signals due to the paramagnetic nature of these complexes.

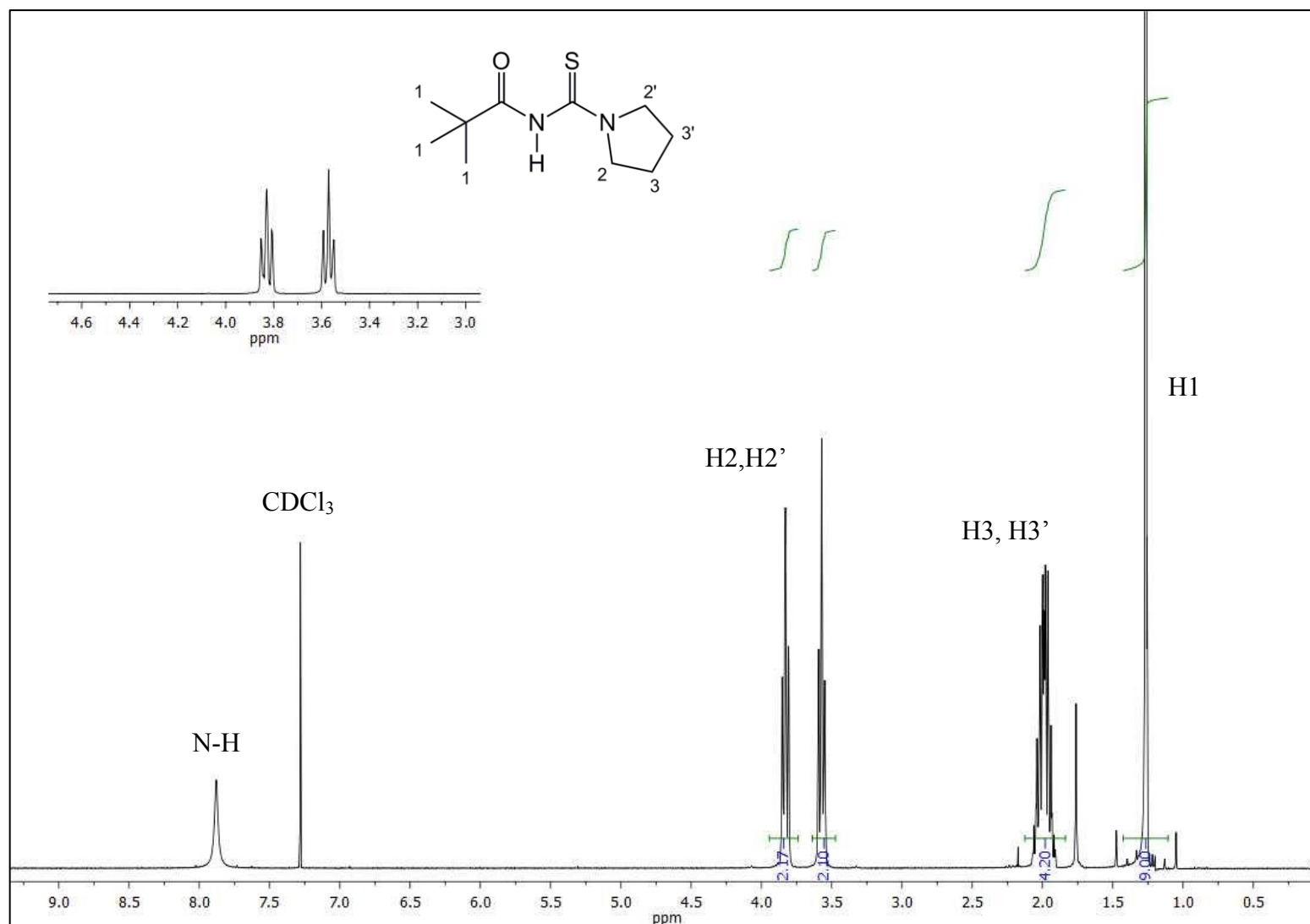


Figure 2 6. ^1H NMR spectrum of *N*-pyrrolidyl-*N'*-(2,2-dimethylpropanoyl)thiourea (HL¹) in CDCl_3 and at 25°C.

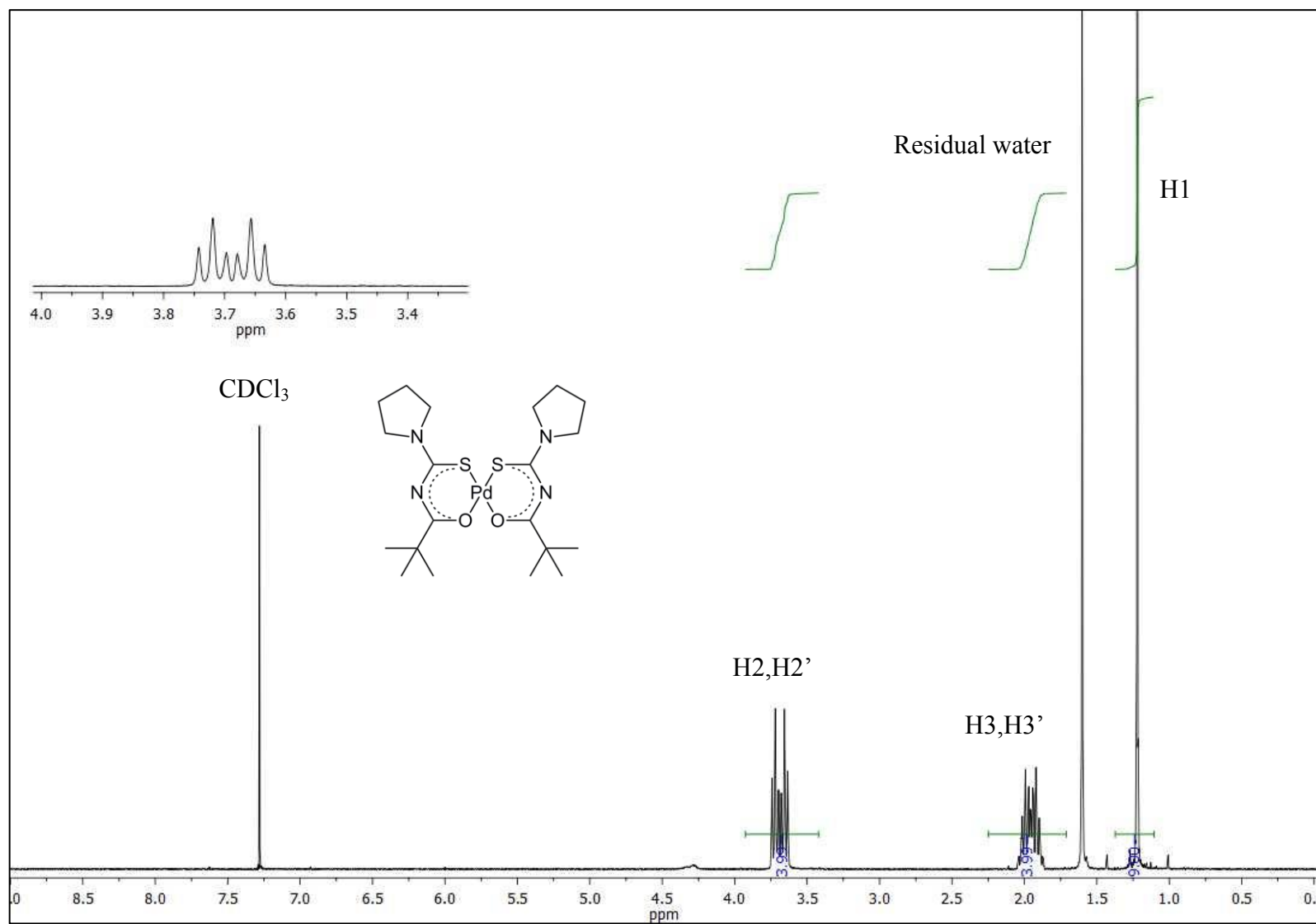


Figure 2.7. ^1H NMR spectrum of bis(*N*-pyrrolidyl-*N'*-(2,2-dimethylpropanoyl)thioureato)palladium(II) in CDCl_3 and at 25°C .

Table 4. ^1H NMR chemical shifts (in ppm) of *N,N*-diethyl-*N'*-benzoylthiourea and its Pd(II) derivatives, in CDCl_3 and at 25°C .

Compound	H1 + H1'	H2	H3 + H3'	H7 + H7'	H8 + H8'	N-H
HL^3	7.46	7.56	7.82	3.81	1.32	8.34
<i>cis</i> -[Pd(L ³ -S,O) ₂]	7.44	7.50	8.26	3.85	1.33	-
<i>cis</i> -[Pd(L ⁵ -S,O) ₂]	7.03	-	7.29	3.84	1.31	-
<i>cis</i> -[Pd(L ⁶ -S,O) ₂]	-	-	7.56	3.79	1.32	-
<i>cis</i> -[Pd(L ⁷ -S,O) ₂]	7.38	-	8.14	3.83	1.30	-

**Figure 2.8.** Numbering scheme used for *N,N*-diethyl-*N'*-benzoylthiourea and palladium(II) derivatives.

2.2.2. Mass Spectrometry

Electrospray Ionisation Mass Spectrometry (ESI-MS) in the positive mode was used for the characterisation of $[\text{Ru}(\text{L}^3\text{-S},\text{O})_3]$ and $[\text{Ir}(\text{L}^3\text{-S},\text{O})_3]$ as both complexes produced broad signals when characterised by ^1H and ^{13}C NMR spectroscopy. These broad signals are as a result of the paramagnetic nature of Ru(III) and Ir(III) respectively in these complexes.

For their ESI-MS analysis, solutions of $[\text{Ru}(\text{L}^3\text{-S},\text{O})_3]$ and $[\text{Ir}(\text{L}^3\text{-S},\text{O})_3]$ in acetonitrile were prepared and then converted into a gas by vacuum after which they were bombarded with electrons in the spectrometer leading to fragmentations into their various ionic species. With the spectra obtained, characterisation of species of both complexes was aided by comparison between the isotopic distribution patterns in the observed spectrum and that which was simulated.

The mass spectrum of $[\text{Ru}(\text{L}^3\text{-S},\text{O})_2]$ as shown in Figure 2.9 indicate the presence of the molecular ion at m/z 808.2. Since ruthenium has eleven naturally occurring isotopes, the observed isotopic distribution pattern for the complex shows eleven peaks which is consistent with the pattern observed in the simulated analogue (see Appendix III). The most abundant isotope at m/z 808.2 corresponds to the molecular ion $[\text{}^{101}\text{Ru}(\text{L}^3\text{-S},\text{O})_3 + \text{H}]^+$. The mass spectrum also shows a variety of additional peaks centered at m/z 830.0 corresponding to sodium adducts of substitution product $[\text{}^{101}\text{Ru}(\text{L}^3\text{-S},\text{O})_3 + \text{Na}]^+$.

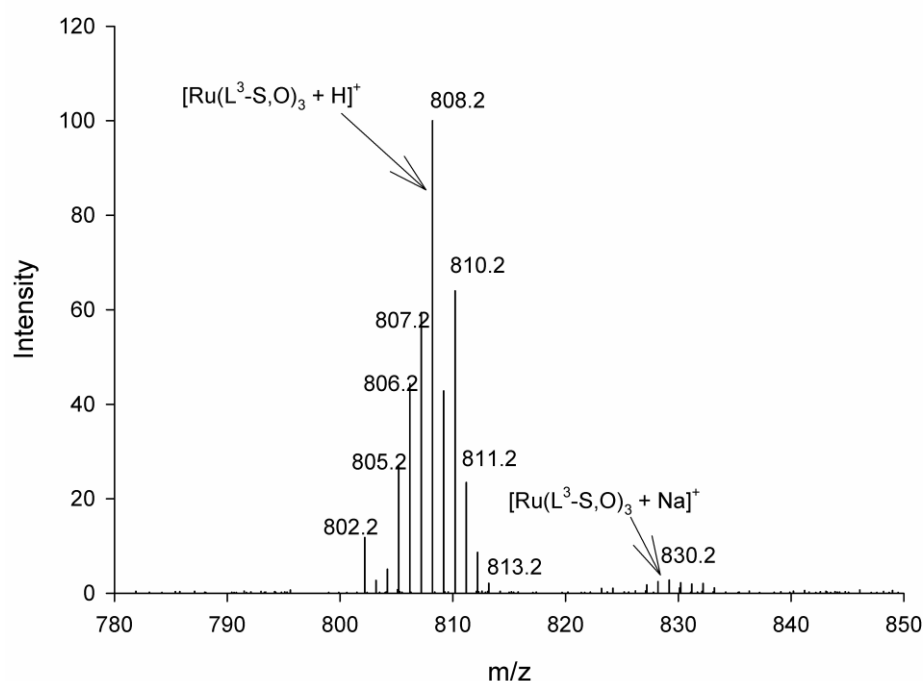


Figure 2.9. ESI-MS(+) spectrum of tris(*N,N*-diethyl-*N'*-benzoylthioureato)ruthenium(III) in acetonitrile.

For $[\text{Ir}(\text{L}^3\text{-S,O})_3]$, the mass spectrum showed the formation of the molecular ion at m/z 899.2 as shown in Figure 2.10. Similar to the case of the $[\text{Ru}(\text{L}^3\text{-S,O})_3]$, the isotopic distribution pattern of the observed spectrum for $[\text{Ir}(\text{L}^3\text{-S,O})_3]$ correlates well to the pattern for the simulated spectrum (see Appendix III) with six peaks observed. Also observed in the spectrum are major and unassigned peaks centered at m/z 883.2 and it could be suggested that these major peaks may be due to the formation of clusters of the Ir(III) complex as it is possible that the complex could undergo fragmentation due to its relative instability in solution. The simulated spectrum for this group of unassigned peaks correlates with a structure relating to the loss of an oxygen atom with a decrease in mass unit of 16. This could mean that fragmentation of the Ir(III) complex may lead to breaking of the Ir-O bond in the complex and subsequent loss of the oxygen atom from which clusters may be formed.

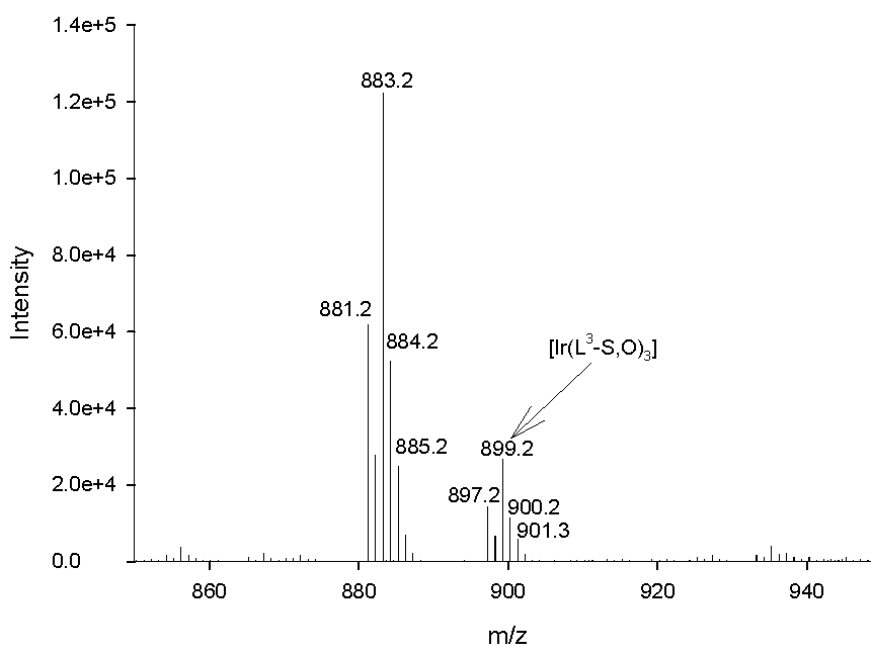


Figure 2.10. ESI (+)-MS spectrum of tris(*N,N*-diethyl-*N'*-benzoylthioureato)iridium(III) in acetonitrile.

2.2.3. IR spectroscopy

The ligands *N,N*-dialkyl-*N'*-acylthioureas give rise to two characteristic bands in their FT-IR spectra which include: ν (N-H) stretching bands of the secondary amine and ν (C=O) of the carbonyl moiety at stretching frequency ranges of 3200-3284 cm^{-1} and 1648-1690 cm^{-1} respectively.¹⁸ These main characteristic bands can be seen in the FT-IR spectra of *N,N*-diethyl-*N'*-benzoylthiourea in Figure 2.11 and Table 5. The band at 3258.84 cm^{-1} is attributed to the ν (N-H) vibrational frequency while that at 1649.35 cm^{-1} is due to the carbonyl stretching frequency. These characteristic bands were also observed in the FT-IR spectra of all the other ligands (See Appendix II).

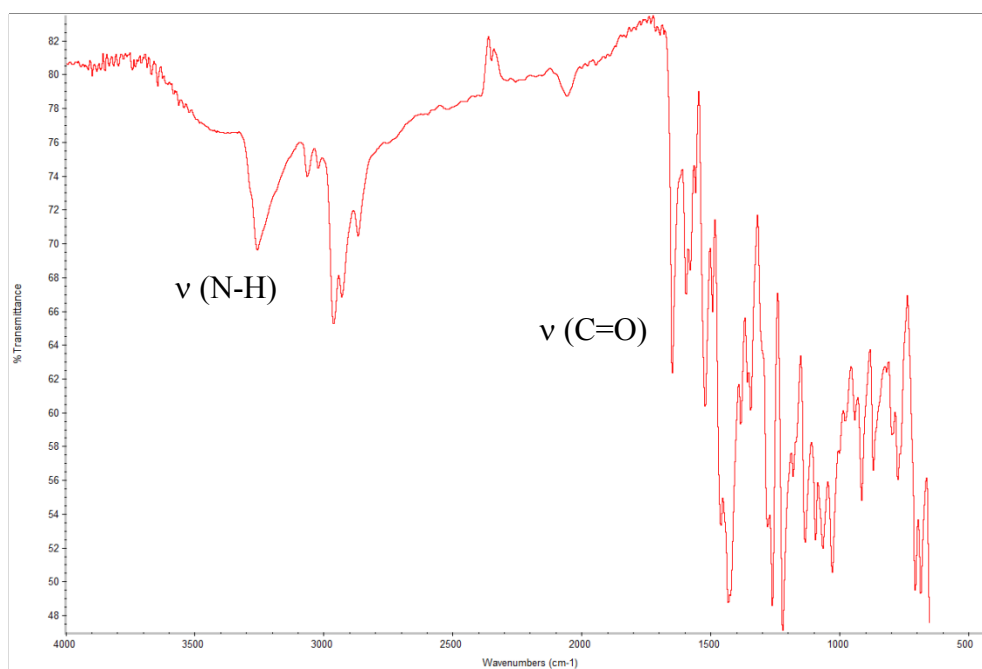


Figure 2.11. FT-IR spectrum of *N,N*-diethyl-*N'*-benzoylthiourea.

However complex formation with metal ions leads to the loss of the N-H proton, hence the FT-IR spectra of corresponding complexes of these ligands are expected to be without the ν (N-H) band and an almost disappearance or a shift to either lower or higher wavenumbers for the ν (C=O) stretch.⁸¹ After complex formation, the vibrational frequencies corresponding to the carbonyl groups in the free ligands are expected to shift to lower or higher values as a result of a decrease in double bond character of these groups.

The FT-IR spectrum (Figure 2.12 and Table 5) of *cis*-[Pd(L³-S,O)₂] shows the disappearance of the ν (N-H) band which was observed for the ligand HL³ at 3258.84 cm⁻¹, and an almost disappearance of the ν (C=O) stretch at 1583.71 cm⁻¹. Note that this value (1583.71 cm⁻¹) for the ν (C=O) stretch in *cis*-[Pd(L³-S,O)₂] is less than that observed for the free ligand (1649.35 cm⁻¹). This shift confirms that the ligand *N,N*-diethyl-*N'*-benzoylthiourea is co-ordinated to Pd(II) in the resulting complex and occurs due to a decrease in double bond character of the carbonyl group in the complex.

The loss of the ν (N-H) band and an apparent loss or a shift for the ν (C=O) band was also observed in the FT-IR spectra of all the other complexes synthesised (see Appendix II). Table 5 shows the stretching frequencies for the ν (N-H) and ν (C=O) bands of some of the ligands and also the changes in wavenumbers for these bands after complex formation with the

corresponding metal ions. From the table, it can be seen that the ν (N-H) band present in each of the ligands disappears and that a shift to lower wavenumbers for the ν (C=O) also occurs after complex formation.

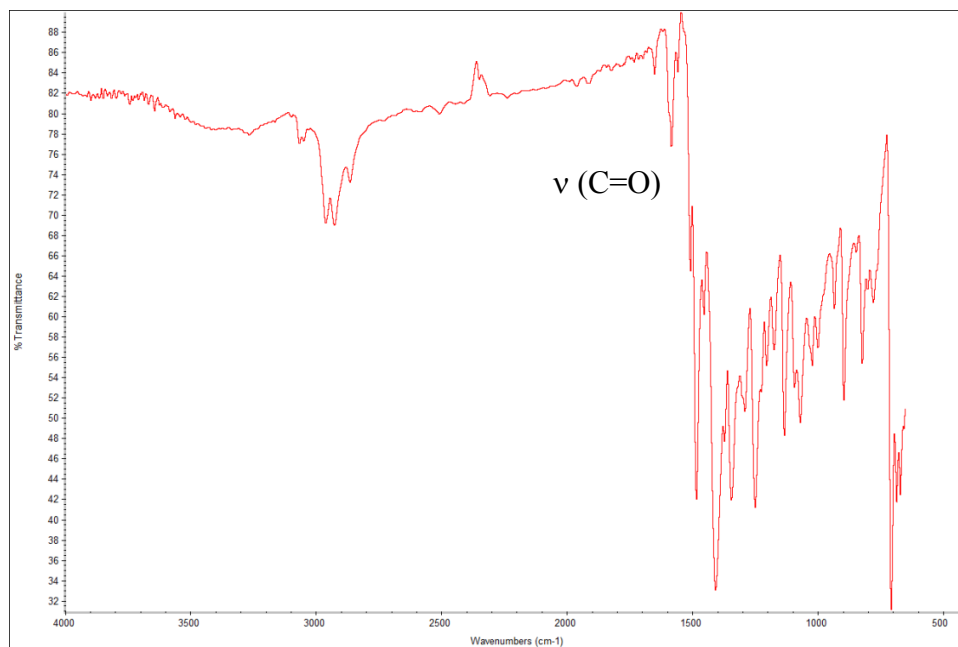


Figure 2.12. FT-IR spectrum of bis-(*N,N*-diethyl-*N'*-benzoylthioureato)palladium(II).

Table 5. Table of FT-IR ν (N-H) and ν (C=O) stretches for different ligands and their respective complexes.

Compound	ν (N-H) / cm^{-1}	ν (C=O) / cm^{-1}
HL ¹	3274.94	1675.52
<i>cis</i> -[Pd(L ¹ -S,O) ₂]	-	1513.36
HL ²	3284.69	1651.09
<i>cis</i> -[Pd(L ² -S,O) ₂]	-	1589.33
HL ³	3258.84	1649.35
<i>cis</i> -[Pd(L ³ -S,O) ₃]	-	1583.74
<i>cis</i> -[Pt(L ³ -S,O) ₃]	-	1587.41
[Ru(L ³ -S,O) ₃]	-	1584.64
[Ir(L ³ -S,O) ₃]	-	1583.95

CHAPTER III

Reversed-phase HPLC separation of platinum(II), palladium(II), rhodium(III), ruthenium(III) and iridium(III) complexes

3.1. Introduction

As was discussed in chapter 2, the *N,N*-dialkyl-*N'*-acyl(aryl)thioureas form stable and uncharged complexes such as *cis*-[Pt(L³-S,O)₂], *cis*-[Pd(L³-S,O)₂], *fac*-[Rh(L³-S,O)₃] and [Ru(L³-S,O)₃]. These complexes tend to be relatively soluble in organic solvents such as acetonitrile and methanol. Also, the fact that the ligand substituents could be varied provides a possibility for their separation of a series of complexes with the same metal center but different ligands by reversed-phase chromatography.

In this chapter, a reversed-phase HPLC separation will be carried out on the *cis*-[Pt(Lⁿ-S,O)₂], *cis*-[Pd(Lⁿ-S,O)₂], *fac*-[Rh(Lⁿ-S,O)₃], [Ru(Lⁿ-S,O)₃] and [Ir(Lⁿ-S,O)₃] complexes synthesised, and also for a series of *cis*-[Pd(Lⁿ-S,O)₂] complexes with different ligands. Studies on the separation of iridium complexes such as Ir(IV) oxinates from similar complexes of other metals by both normal and reversed-phase HPLC showed that such iridium complexes are unstable and form more than one peak in the chromatogram.³⁸ This was explained to be due to a spontaneous reduction to give Ir(III) oxinate since the redox process between these iridium species could be affected by pH and duration of the sample in acidic medium. For this reason, compared to the other complexes, some difficulties were anticipated for the separation and determination of the [Ir(L³-S,O)₃] complex synthesised. The choice of ligand and the chromatographic conditions used play a significant role for reversed-phase chromatographic separation of these metal complexes as these could lead to different interactions of the analyte with the stationary phase and hence would affect retention times.

3.2. Chromatographic conditions

Some of the chromatographic conditions which play a major role during determination and separation include the mobile phase composition, nature of stationary phase, flow rate and column dimension as was discussed in Chapter 1. In this study, binary mobile phases containing a mixture of either acetonitrile or methanol and a 0.1M acetate buffer were used in order to achieve a good separation. Methanol was sometimes selected as an alternative solvent due to its compatibility with reverse-phase columns and the solubility of the complexes in this solvent. Methanol has a greater polarity but lower elution power than acetonitrile during reversed-phase HPLC separations.

Usually in reversed-phase HPLC mode, these organic solvents are combined with water, with pH control provided by a buffer. The composition of the organic phase relative to that of water or aqueous buffer determines the extent to which peaks are separated and resolved during gradient elution. For this, it is always preferable to begin a separation using greater than 10% of the organic solvent in the total mixture composition relative to that of water or the buffer used so as to prevent the breakdown of the C₁₈ alkyl chains of the stationary phase used which also slows down its rate of attaining equilibrium with the organic solvent.³⁰

Adjusting the composition of the organic component in a binary mobile phase may have great effect towards improving resolution and separation. However, in some cases several components of the system may need to be altered. This may include a change in the organic solvent used, a change in the stationary phase used or optimisation of flow rate, particle size and column dimensions for the reversed-phase column used.

In this study the separation of the metal complexes under isocratic conditions was obtained through a mobile phase of acetonitrile/methanol:0.1M acetate buffer (90:10, % v/v) while in some cases, the composition was altered to 85:15 (% v/v) or 95:5 (% v/v) of the mixture, to obtain a better separation. The other chromatographic conditions were set as described below:

Column: LUNA or GEMINI C₁₈, 5 µm, 150 mm x 4.6 mm.

Mobile phase: 90:10 (% v/v) acetonitrile/methanol:0.1M acetate buffer (pH 6)

Flow rate: 1.0 ml min⁻¹

Injection Volume: 20 μ l

Detection: UV at 262 nm

3.3. Separation of *cis*-[Pt(L³-S,O)₂], *cis*-[Pd(L³-S,O)₂], *fac*-[Rh(L³-S,O)₃], [Ru(L³-S,O)₃] and [Ir(L³-S,O)₃]

For the reversed-phase separation of the metal complexes, 250 mg/L of solutions of each of the complexes *cis*-[Pd(L³-S,O)₂], *cis*-[Pt(L³-S,O)₂], *fac*-[Rh(L³-S,O)₃], [Ru(L³-S,O)₃] and [Ir(L³-S,O)₃] in both acetonitrile and methanol were prepared and 20 μ l of each were separately injected onto the HPLC column. Subsequently, 20 μ l of an aliquot of a mixture of these complexes was then injected onto the column for separation.

A chromatogram of a standard mixture of the four complexes *cis*-[Pt(L³-S,O)₂], *cis*-[Pd(L³-S,O)₂], *fac*-[Rh(L³-S,O)₃] and [Ru(L³-S,O)₃] in acetonitrile solutions is shown in Figure 3.1. This shows that all four complexes are well separated in acetonitrile with the retention order Rh < Ru < Pt < Pd. The closely retained *cis*-[Pt(L³-S,O)₂] and *cis*-[Pd(L³-S,O)₂] suggests the structural similarity between these two square planar complexes.

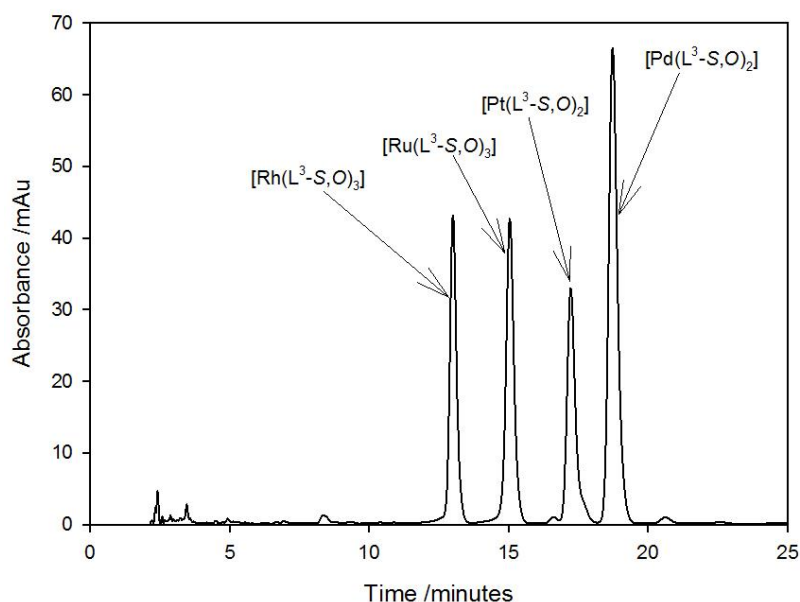


Figure 3.1. Chromatogram representing the separation of a mixture of *cis*-[Pd(L³-S,O)₂], *cis*-[Pt(L³-S,O)₂], *fac*-[Rh(L³-S,O)₃] and [Ru(L³-S,O)₃] in acetonitrile; conditions: flow rate 1 ml min⁻¹, Column 5 μ m, C₁₈ ODS 150 x 4.6mm, mobile phase 90:10 (%v/v) acetonitrile:0.1M acetate buffer (pH 6), injection volume 20 μ l, 262 nm detection.

In the separation of $[\text{Ir}(\text{L}^3\text{-S},\text{O})_3]$ dissolved in acetonitrile, two major peaks represented by (a) and (b) as well as other smaller additional peaks were observed as shown in Figure 3.2. The additional peaks could have resulted from the instability in solution of the Ir(III) complex in acetonitrile solvent used. The two major peaks (a) and (b) were found to have different absorbance profiles from their UV-VIS absorbance profiles (see Appendix IV) obtained from a diode array photometric detector, suggesting that they result from different species in solution. Although these two major peaks (a) and (b) have not yet been fully assigned, it is suggested that the peaks could have resulted from the spontaneous oxidation of the Ir(III) to Ir(IV) in solution. Since K_3IrCl_6 was initially used as a starting material for obtaining the Ir(III) complex, the expected complex to be formed was $[\text{Ir}^{\text{III}}(\text{L-S},\text{O})_3]$ and could possibly result in peak (b). However, if oxidation of this complex were to take place, the Ir(IV) complex formed is expected to be charged and could be of the form $[\text{Ir}^{\text{IV}}(\text{L-S},\text{O})_3]^+$. This charged Ir(IV) complex would possibly be less retained than the $[\text{Ir}^{\text{III}}(\text{L-S},\text{O})_3]$ and hence could have resulted in peak (a).

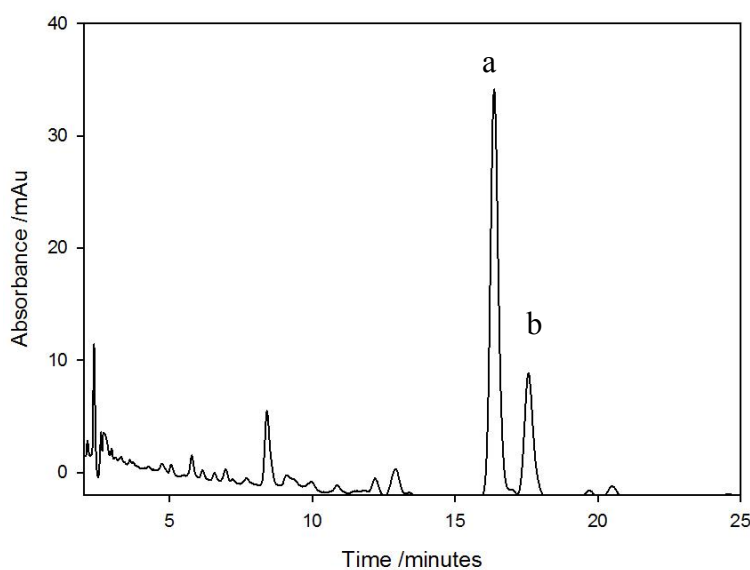


Figure 3.2. Chromatogram representing the separation of peaks for $[\text{Ir}(\text{L}^3\text{-S},\text{O})_3]$ in acetonitrile; conditions: C_{18} ODS, 5 μm , 150 x 4.6 mm column; mobile phase 90:10 (% v/v) acetonitrile:0.1M acetate buffer (pH 6); flow rate 1 ml min^{-1} , 20 μl injection volume, 262 nm detection.

When 20 μl of an aliquot of a mixture of all five complexes in acetonitrile was injected onto the column, a good separation was still obtained for *cis*- $[\text{Pt}(\text{L}^3\text{-S},\text{O})_2]$, *cis*- $[\text{Pd}(\text{L}^3\text{-S},\text{O})_2]$, *fac*- $[\text{Rh}(\text{L}^3\text{-S},\text{O})_3]$ and $[\text{Ru}(\text{L}^3\text{-S},\text{O})_3]$. An overlap in peaks was obtained leading to poor separation for the complexes $[\text{Rh}(\text{L}^3\text{-S},\text{O})_3]$ and $[\text{Ir}(\text{L}^3\text{-S},\text{O})_3]$ as these were both retained at

ca. 25 minutes (Figure 3.3). This similar retention times of the octahedral Rh(III) and Ir(III) complexes illustrates their expected structural similarity. The peaks for these two complexes were still poorly separated even after increasing the amount of 0.1M acetate buffer in the mobile phase to 20%. Except for $[\text{Ir}(\text{L}^3\text{-S},\text{O})_3]$, the other four complexes were inert enough to give adequate resolution and separation of peaks in all the mobile phases used.

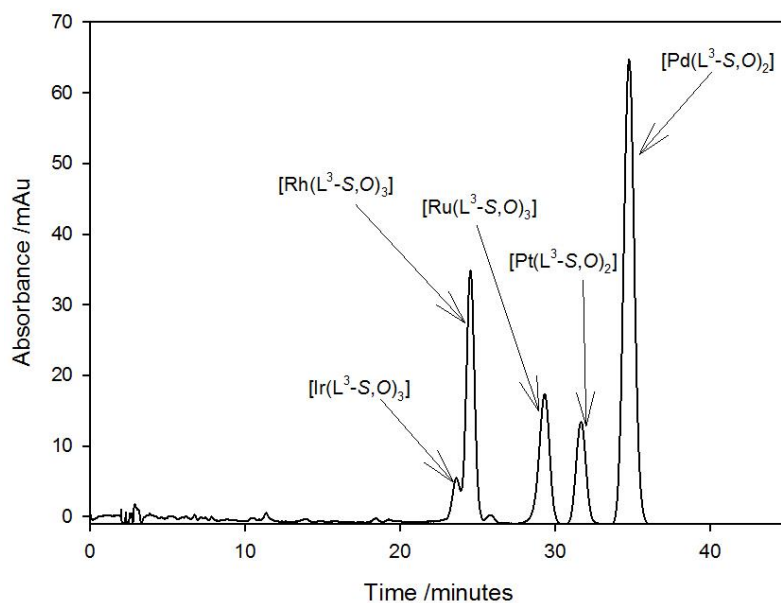


Figure 3.3. Chromatogram representing the separation of a mixture of $\text{cis-}[\text{Pt}(\text{L}^3\text{-S},\text{O})_2]$, $\text{cis-}[\text{Pd}(\text{L}^3\text{-S},\text{O})_2]$, $\text{fac-}[\text{Rh}(\text{L}^3\text{-S},\text{O})_3]$, $[\text{Ru}(\text{L}^3\text{-S},\text{O})_3]$ and $[\text{Ir}(\text{L}^3\text{-S},\text{O})_3]$ in acetonitrile; conditions: Column $5\ \mu\text{m}$, C_{18} ODS, $150 \times 4.6\ \text{mm}$, mobile phase 90:10 (% v/v) acetonitrile:0.1M acetate buffer (pH 6); flow rate $1\ \text{ml}\ \text{min}^{-1}$; $20\ \mu\text{l}$ injection volume, 262 nm detection.

A better separation was obtained for all five complexes when they were dissolved in methanol and with the methanol solvent used in the mobile phase instead of acetonitrile. As shown in Figure 3.4, the complexes were better separated with the same elution order and similar retention times as to when acetonitrile was used. Hence the use of methanol clearly improves the separation of the metal complexes. In both acetonitrile and methanol, $[\text{Ir}(\text{L}^3\text{-S},\text{O})_3]$ has the shortest retention time compared to the other four complexes and the elution order was $\text{Ir} < \text{Rh} < \text{Ru} < \text{Pt} < \text{Pd}$ in both solvents. The separation of the peaks was enhanced by increasing the percentage of 0.1M acetate buffer in the mobile phase using a 85:15 (v/v %) methanol: 0.1M acetate buffer mixture.

As can be seen in Figure 3.4, additional smaller peaks arise closer to the $[\text{Ru}(\text{L}^3\text{-S},\text{O})_3]$ and $[\text{Rh}(\text{L}^3\text{-S},\text{O})_3]$ peaks when the complexes are dissolved in methanol. It is suggested that these peaks are due to the *mer* isomers of these octahedral complexes. The *mer* isomers of these

complexes could spontaneously be formed by isomerisation of their respective *fac* complexes when dissolved in methanol. Due to the difficulty of obtaining a single peak in both solvents for the $[\text{Ir}(\text{L}^3\text{-S},\text{O})_3]$ complex, the attempts to include Ir(III) complexes in the later part of this study was abandoned until the reason for their poor separations is better understood.

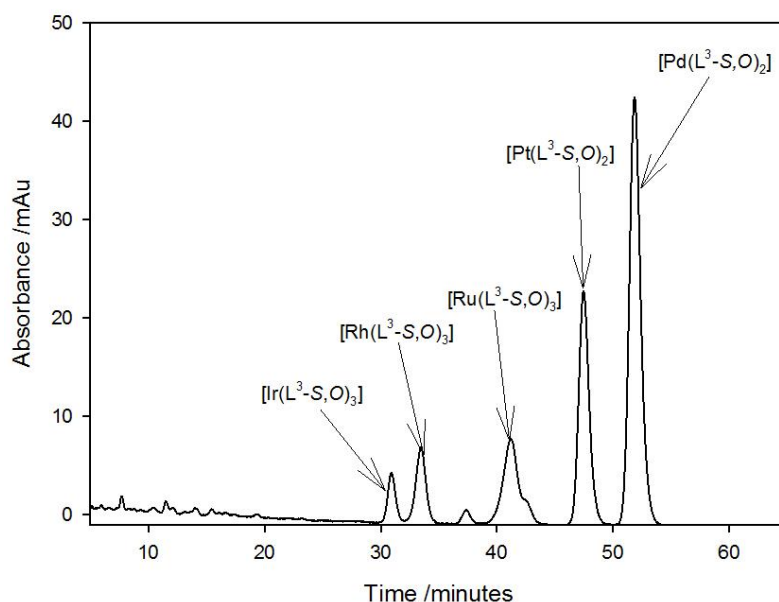


Figure 3.4. Chromatogram representing the separation of a mixture of *cis*- $[\text{Pd}(\text{L}^3\text{-S},\text{O})_2]$, *cis*- $[\text{Pt}(\text{L}^3\text{-S},\text{O})_2]$, *fac*- $[\text{Rh}(\text{L}^3\text{-S},\text{O})_3]$, $[\text{Ru}(\text{L}^3\text{-S},\text{O})_3]$ and $[\text{Ir}(\text{L}^3\text{-S},\text{O})_3]$ in methanol; conditions: Column $5\mu\text{m}$, C_{18} ODS 150×4.6 mm, mobile phase 85:15 (% v/v) methanol:0.1M acetate buffer (pH 6), flow rate 1 ml min^{-1} , $20\mu\text{l}$ injection volume, 262 nm detection.

3.4. Effect of ligand structure on HPLC separation

With the same metal center, changing the ligand structure is expected to have an effect on the polarity of the complex and hence their retention times by HPLC separation. Ligands having long chains or electron-withdrawing substituents tend to be less polar and are more strongly retained onto the apolar stationary phase of the C_{18} column used while those with substituents having stronger electron-donating ability are expected to be relatively more polar and elute faster under similar chromatographic conditions.

In this study, the effect of ligand structure of both the *N,N*-dialkyl-*N'*-acylthioureas and the *N,N*-dialkyl-*N'*-aroylthioureas on the separation of a series of *cis*- $[\text{Pd}(\text{L}^n\text{-S},\text{O})_2]$ complexes was investigated. With respect to structural differences of the two ligands *N*-pirrolidyl-*N'*-(2,2-dimethylpropanoyl)thiourea (**HL**¹) and *N,N*-dibutyl-*N'*-(2,2-dimethylpropanoyl)thiourea

(**HL**²), although both ligands have a tertiary butyl group attached to the carbonyl moiety, *cis*-[Pd(L²-S,O)₂] with longer butyl substituents is expected to be more hydrophobic compared to *cis*-[Pd(L¹-S,O)₂] which has a pyrrolidine ring attached. The other group consists of three ligands *N,N*-diethyl-*N'*-benzoylthiourea (**HL**³), *N,N*-diethyl-*N'*-3,4,5-trimethoxybenzoylthiourea (**HL**⁶) and *N,N*-diethyl-*N'*-*p*-chloro-benzoylthiourea (**HL**⁷) each having a phenyl ring attached to the carbonyl moiety and ethyl groups attached to the thioamide moiety. Of the complexes formed from these ligands, *cis*-[Pd(L⁶-S,O)₂] with electron-donating methoxy groups attached to the phenyl ring is expected to be more polar while *cis*-[Pd(L⁷-S,O)₂] with an electron-withdrawing chloro substituent is expected to be less polar. Attaching a piperidine ring to the thioamide moiety in *N*-piperidyl-*N'*-benzoylthiourea (**HL**⁴) is expected to decrease the polarity of the resulting *cis*-[Pd(L⁴-S,O)₂] complex compared to that of *cis*-[Pd(L³-S,O)₂].

To investigate the effect of ligand structure on the separation of *cis*-[Pd(L^{*n*}-S,O)₂] complexes, a 200 mg/L solution of the complexes *cis*-[Pd(L¹-S,O)₂], *cis*-[Pd(L²-S,O)₂], *cis*-[Pd(L³-S,O)₂], *cis*-[Pd(L⁴-S,O)₂], *cis*-[Pd(L⁶-S,O)₂] and *cis*-[Pd(L⁷-S,O)₂] in acetonitrile were prepared. Firstly, a 20 µl of an aliquot of a mixture of *cis*-[Pd(L¹-S,O)₂], *cis*-[Pd(L²-S,O)₂] and *cis*-[Pd(L³-S,O)₂] was injected for HPLC analysis resulting to the chromatogram in Figure 3.5.

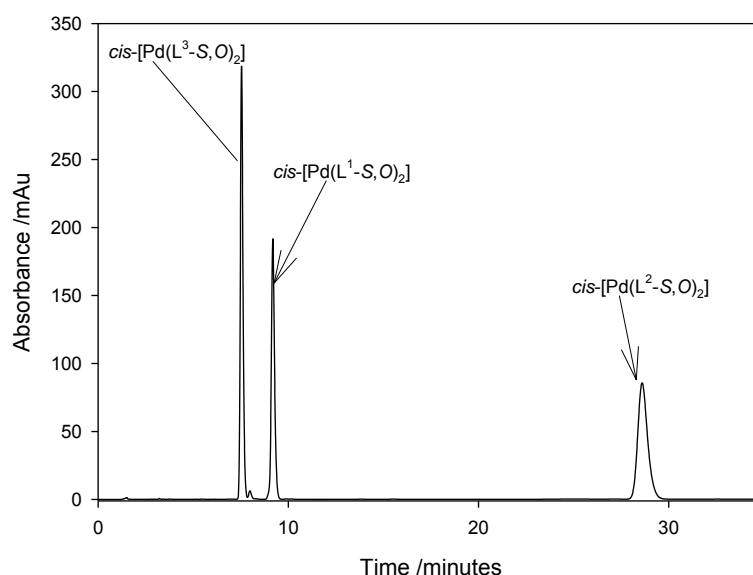


Figure 3.5. Chromatogram representing the reversed-phase HPLC separation of a mixture of acetonitrile solutions of *cis*-[Pd(L¹-S,O)₂], *cis*-[Pd(L²-S,O)₂] and *cis*-[Pd(L³-S,O)₂] in the dark; conditions: GEMINI C₁₈ 5 µm, 150 x 4.6 mm column, mobile phase 95:5 (% v/v) acetonitrile:0.1M acetate buffer (pH 6) flow rate 1 ml min⁻¹, injection volume 20 µl.

It can be clearly seen that $cis\text{-}[\text{Pd}(\text{L}^2\text{-S},\text{O})_2]$ is more retained onto the column than $cis\text{-}[\text{Pd}(\text{L}^1\text{-S},\text{O})_2]$. This suggests that the two longer butyl groups attached to the thiocarbonyl moiety in $cis\text{-}[\text{Pd}(\text{L}^2\text{-S},\text{O})_2]$ reduces the hydrophilicity of this complex compared to the effect of the pyrrolidine ring attached to $cis\text{-}[\text{Pd}(\text{L}^1\text{-S},\text{O})_2]$. The complex $cis\text{-}[\text{Pd}(\text{L}^3\text{-S},\text{O})_2]$ with a benzoyl moiety and also with ethyl groups attached to the thiocarbonyl moiety is less retained than $cis\text{-}[\text{Pd}(\text{L}^1\text{-S},\text{O})_2]$ as well as $cis\text{-}[\text{Pd}(\text{L}^2\text{-S},\text{O})_2]$.

When 20 μl of an aliquot of a mixture of $cis\text{-}[\text{Pd}(\text{L}^3\text{-S},\text{O})_2]$, $cis\text{-}[\text{Pd}(\text{L}^4\text{-S},\text{O})_2]$, $cis\text{-}[\text{Pd}(\text{L}^6\text{-S},\text{O})_2]$ and $cis\text{-}[\text{Pd}(\text{L}^7\text{-S},\text{O})_2]$ was injected for HPLC analysis, a good separation was also obtained for these complexes as shown in the chromatogram in Figure 3.6.

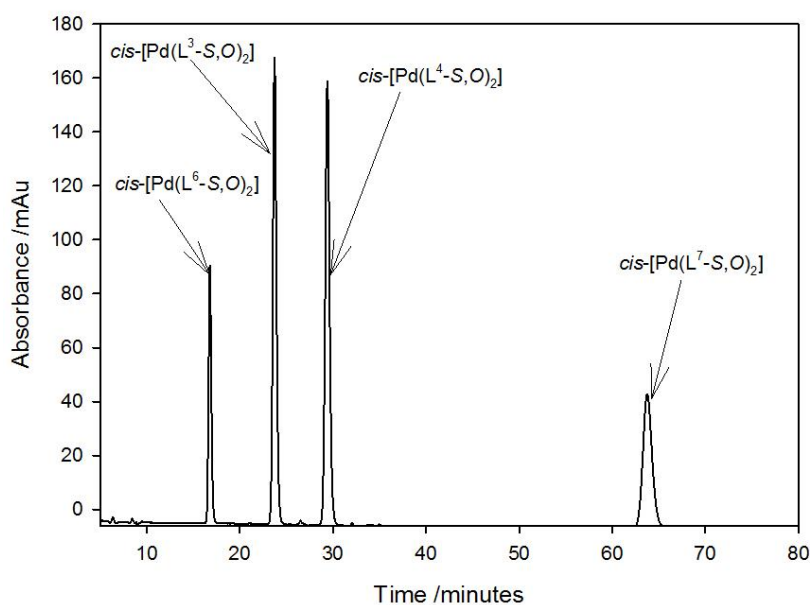


Figure 3.6. Chromatogram representing the reversed-phase HPLC separation of acetonitrile solution of a mixture of $cis\text{-}[\text{Pd}(\text{L}^3\text{-S},\text{O})_2]$, $cis\text{-}[\text{Pd}(\text{L}^4\text{-S},\text{O})_2]$, $cis\text{-}[\text{Pd}(\text{L}^6\text{-S},\text{O})_2]$ and $cis\text{-}[\text{Pd}(\text{L}^7\text{-S},\text{O})_2]$ in the dark; conditions: GEMINI C₁₈ 5 μm , 150 x 4.6 mm column, mobile phase 85:15 (% v/v) acetonitrile:0.1M acetate buffer (pH 6) flow rate 1 ml min^{-1} , injection volume 20 μl , 262 nm detection.

It can be seen that the presence of the chloro substituent appears to relatively decrease the polarity of $cis\text{-}[\text{Pd}(\text{L}^7\text{-S},\text{O})_2]$, hence this complex was only eluted after an hour. The piperidine ring attached to the benzoyl moiety appears to increase the polarity of $cis\text{-}[\text{Pd}(\text{L}^4\text{-S},\text{O})_2]$ and hence it is less retained compared to $cis\text{-}[\text{Pd}(\text{L}^7\text{-S},\text{O})_2]$.

Both $cis\text{-}[\text{Pd}(\text{L}^3\text{-S},\text{O})_2]$ and $cis\text{-}[\text{Pd}(\text{L}^6\text{-S},\text{O})_2]$ elute earlier compared to the other two complexes presumably due to the increase in polarity of the complexes by the presence of

these electron-donating methoxy groups. It can also be seen from the chromatogram that *cis*-[Pd(L⁶-S,O)₂] with three methoxy groups attached to the benzoyl moiety elutes faster than *cis*-[Pd(L³-S,O)₂] with no group attached to the phenyl ring.

It should be noted that in Figures 3.5 and 3.6, additional small peaks are observed closer to some of the main peaks. For example in Figure 3.6, an additional smaller peak is observed closer to the main peak for *cis*-[Pd(L³-S,O)₂] at $t_R=28$ minutes. The smaller peaks observed are tentatively assigned to be due to the various *trans* isomers of the complexes involved. This could be formed from a possible photo-induced isomerisation of the *cis* complexes in the presence of light, as will be explained further in the next Chapter.

3.5. A Preliminary investigation of a salt-induced pre-concentration method for the HPLC determination of Pt(II), Pd(II), Rh(III) and Ru(III) *N,N*-diethyl-*N'*-benzoylthiourea

In section 3.3 a good separation was obtained when a mixture of the complexes *cis*-[Pt(L³-S,O)₂], *cis*-[Pd(L³-S,O)₂], *fac*-[Rh(L³-S,O)₃] and [Ru(L³-S,O)₃] was directly injected onto the column for HPLC analysis. It is also possible to use an alternative sample preparation method which pre-concentrates the metal complexes prior to injection for HPLC separation. A variety of sample preparation methods for metal complexes have been used before their separation by HPLC.^{82,83} One of these is a salt-induced separation technique developed by Mueller and Lovett⁸⁴ which has an advantage that metal complexes are pre-concentrated in an acetonitrile layer before separation is carried out. In this method, the metal complexes are formed in an aqueous-acetonitrile mixture and on addition of a saturated sodium chloride solution, the aqueous and acetonitrile phases are separated into two layers. The latter is then extracted and directly injected for HPLC analysis.

Koch *et al.*¹⁰ have also used this method for pre-concentration of Pt(II) and Pd(II) in aqueous solution after which the complexes formed were separated using reversed-phase HPLC. They also showed that the salt-induced phase separation is facilitated by the presence of acid. An increase in peak area was observed in the chromatogram for Pt(II) and Pd(II) with increase in concentration of acid during the pre-concentration process. As a result, narrow and sharp peak areas were obtained for HCl concentrations between 0.1M to 0.5M, while peak broadening

was obtained when 2M to 5M HCl was used. This peak broadening was attributed to the possible formation of additional protonated species on separation.

In this study, a salt-induced water-acetonitrile phase separation was used in the treatment of aqueous mixture of Pt(II), Pd(II) with an extension to Rh(III) and Ru(III). A flow diagram for the procedure used during the process is shown in Figure 3.7 below.

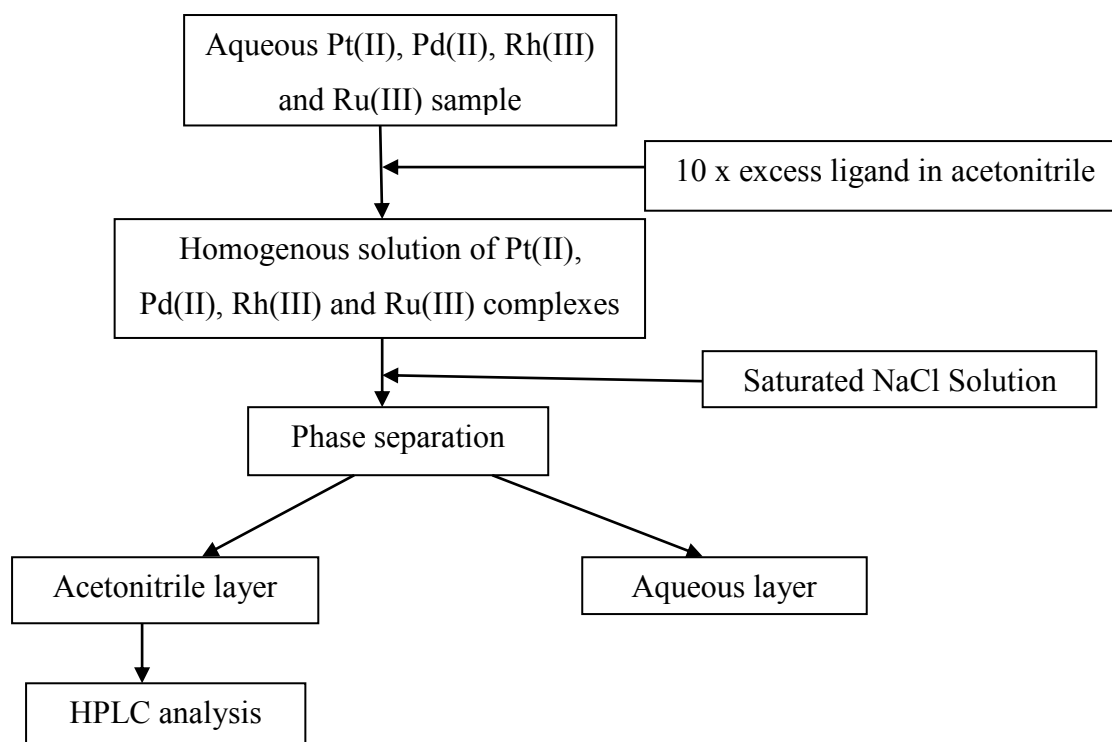


Figure 3.7. A salt-induced sample preparation scheme for pre-concentration of Pt(II), Pd(II), Rh(III) and Ru(III) *N,N*-diethyl-*N'*-benzoylthiourea in aqueous solutions.¹⁰

This involves an initial complex formation step, in which excess ligand solution in acetonitrile is added to aqueous solution of a mixture of Pt(II), Pd(II), Rh(III) and Ru(III) in HCl. This is then followed by warming of the homogenous mixture formed and an addition of a saturated sodium chloride solution which causes a phase separation. The addition of sodium chloride solution results in two phases: an acetonitrile layer in which the metal complexes pre-concentrate and an aqueous layer. The acetonitrile phase of the mixture is then filtered and directly injected for HPLC analysis. The chromatogram obtained (Figure 3.8) shows a similar elution order and retention times for all the metal complexes as when solutions of a mixture of

the pure complexes were injected (Figure 3.1). The excess free ligand in solution elutes at *ca.* 3 minutes of separation.

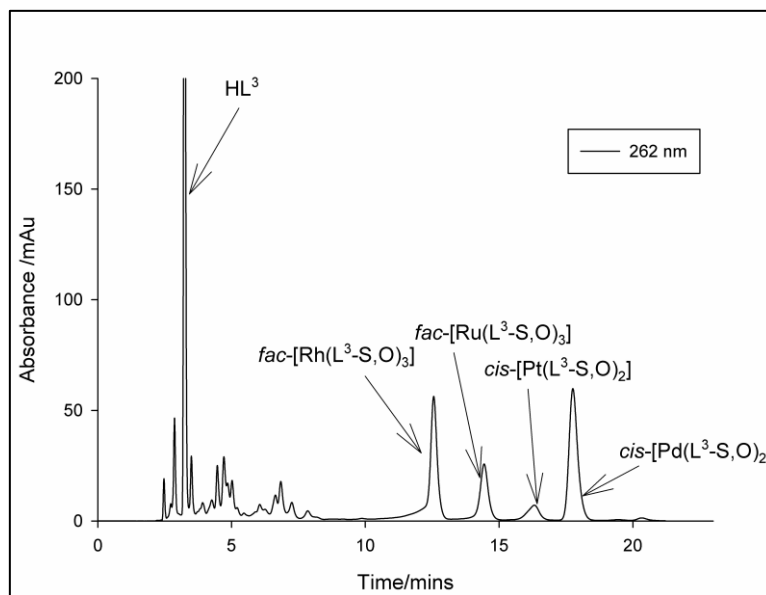


Figure 3.8. Chromatogram obtained for separation of Pd(II), Pt(II), Rh(III) and Ru(III) complexes with *N,N*-diethyl-*N'*-benzoylthiourea after a salt-induced pre-concentration method; conditions: Column GEMINI C₁₈, 5 μ m, 150 mm x 4.6 mm, mobile phase 90:10 (%v/v) acetonitrile:0.1 M acetate buffer (pH 6), flow rate 1 ml min⁻¹, 20 μ l injection volume, 262 nm detection.

Similar to the observations made in the previous section, an additional peak is formed at $t_R = 21$ minutes, after that for the *cis*-[Pd(L³-S,O)₂] complex. In this case, the additional peak which could have resulted from the formation of the *trans*-[Pd(L³-S,O)₂] complex upon exposure to light, is well separated from that of the *cis* isomer. The photo-induced isomerisation of such *cis*-[M(L-S,O)₂] (M = Pd(II), Pt(II)) complexes and separation of the resulting *cis/trans* isomers using reversed-phase HPLC are discussed in detail in the next chapter.

3.6. Conclusions

N,N-diethyl-*N'*-benzoylthiourea (**HL**³) is a suitable ligand for forming easily separable complexes with Pt(II), Pd(II), Rh(III) and Ru(III) using reversed-phase HPLC. Hence the *cis*-[Pd(L³-S,O)₂], *cis*-[Pt(L³-S,O)₂], *fac*-[Rh(L³-S,O)₃] and [Ru(L³-S,O)₃] are well separated in a mobile phase containing a 0.1M acetate buffer with either acetonitrile or methanol. However, separations involving Ir(III) produced additional unidentified peaks other than [Ir(L³-S,O)₃] synthesised.

Depending on the electronic effect of the ligand substituent, reversed-phase HPLC is also useful for the separation of a series of *cis*-[Pd(Lⁿ-S,O)₂] complexes with different ligands. The electron-withdrawing effect of the chloro substituent on *N,N*-diethyl-*N'*-*p*-chloro-benzoylthiourea (**HL**⁷) appears to increase the retention time of the corresponding *cis*-[Pd(L⁷-S,O)₂] complex. A similar effect is observed for the relatively longer hydrophobic butyl substituents on *N,N*-dibutyl-*N'*-(2,2-dimethylpropanoyl)thiourea (**HL**²) leading to a higher retention time for *cis*-[Pd(L²-S,O)₂] compared to *cis*-[Pd(L¹-S,O)₂]. On the other hand, electron-donating methoxy groups on *N,N*-diethyl-*N'*-3,4,5-trimethoxy-benzoylthiourea (**HL**⁶) appear to increase the polarity and hence decrease the retention time of the resulting *cis*-[Pd(L⁶-S,O)₂] complex.

A salt-induced pre-concentration method is effective for sample preparation of the complexes *cis*-[Pd(L³-S,O)₂], *cis*-[Pt(L³-S,O)₂], *fac*-[Rh(L³-S,O)₃] and [Ru(L³-S,O)₃] in aqueous solutions prior to their separation by reversed-phase HPLC.

CHAPTER IV

Photo-induced isomerisation of palladium(II) and platinum(II) complexes

Square planar complexes of Pt(II) and Pd(II) and those of other platinum group metal complexes are liable to undergo re-arrangement reactions such as photo-isomerisation when irradiated. As mentioned earlier, the factors governing such reactions and the mechanism by which they occur for *cis*-[M(Lⁿ-S,O)₂] (M = Pd(II), Pt(II)) complexes with the *N,N*-dialkyl-*N'*-acyl(aryl)thioureas have not yet been investigated in detail. Except for *trans*-bis(*N,N*-dibutyl-*N'*-naphthoylthioureato)platinum(II) as the only example of a *trans* isomer of this type of complexes isolated,⁵⁶ and the investigations carried out using *N,N*-diethyl-*N'*-3,4,5-trimethoxybenzoylthiourea with different light sources,⁵⁸ there have been very few reports on such reactions. In the study involving *N,N*-diethyl-*N'*-3,4,5-trimethoxybenzoylthiourea, it was found that *cis/trans* isomerisation for the *cis*-[M(Lⁿ-S,O)₂] complexes was induced by light of a given wavelength range (320–570 nm).⁵⁸ Monitored by reversed-phase HPLC, the resulting *trans*-[Pt(Lⁿ-S,O)₂] complexes were formed even when the *cis*-[Pd(Lⁿ-S,O)₂] complexes were exposed to ambient daylight. The *cis/trans* isomerisation of the complexes occurred when white or blue light (radiation cut-off at 300 nm) and yellow light (radiation cut-off at *ca.* 480 nm) were used for irradiation, but when red light (radiation cut-off of 600 nm) was used, no isomerisation took place.

In the previous chapter, as the *cis*-[M(Lⁿ-S,O)₂] (M = Pt(II), Pd(II)) complexes were separated using reversed-phase HPLC, additional peaks were also observed close to the main peaks for some of these complexes, and these were tentatively attributed to *trans*-[M(Lⁿ-S,O)₂] formed when solutions of the *cis*-[M(Lⁿ-S,O)₂] complexes were exposed to sunlight.

In this chapter, the *cis/trans* isomerisation of *cis*-[M(Lⁿ-S,O)₂] complexes will be investigated in more detail with the view to investigate the influence of the nature of the ligands on this

process. In an attempt not only to trap and isolate the *trans*-[M(Lⁿ-S,O)₂] complexes after isomerisation, but also to understand the mechanism of isomerisation, particular interest will be devoted to the use of reversed-phase HPLC as a means of monitoring the *cis/trans* isomerisation and to determine the qualitative rate of isomerisation. The *cis/trans* isomerisation reactions could generally be represented by equation 1.



Hence irradiation of the *cis*-[M(Lⁿ-S,O)₂] complexes by a suitable light source leads to a corresponding *trans*-[M(Lⁿ-S,O)₂] and in the dark, the *cis* isomer is reversibly formed from that of the *trans*. Throughout this section, the qualitative rate of *cis/trans* isomerisation will be estimated relatively by comparing the ratios of the peak areas of the *trans* and *cis* isomers determined by reversed-phase HPLC as given by equation 2.

$$Ratio = \frac{[Peak\ area]_{trans}}{[Peak\ area]_{cis}} \quad (2)$$

When the system represented by equation 1 reaches a steady state, the rate of *cis*→*trans* isomerisation should be equal to the rate of *trans*→*cis* isomerisation. When this occurs, the ratio defined by equation 2 corresponds to an equilibrium value K_e which represents the *trans/cis* peak area ratio obtained at steady state. It should therefore be noted that the rates of *cis/trans* isomerisation determined for all complexes in this chapter are only qualitative and not quantitative and all K_e values are obtained at steady state using equation 2.

4.1. Irradiation setup for *cis/trans* isomerisation

Some of the classical light sources which could be used for irradiating a sample resulting in photo-induced isomerisation include mercury lamps, halogen lamps or even lasers.⁸⁵ Unlike lasers, when light sources such as Hg UV and halogen lamps are used, direction of light into the sample in a defined way is rendered difficult. This could lead to a loss in some of the light intensity used for irradiation and consequently it would be difficult to determine the quantity of absorbed light or quantum yields. Intense white light such as sunlight or that from a tungsten lamp have previously been shown to result in the *cis/trans* isomerisation of *cis*-[Pd(Lⁿ-S,O)₂] complexes.⁵⁸ The results also showed that for such complexes, a cut-off wavelength of light of *ca.* < 450 nm could result in the *cis/trans* isomerisation. Hence, choosing a laser with a suitable wavelength (< 450 nm) could also in principle result to such changes.

In order to study this phenomenon, one could therefore irradiate a solution of the sample with a Hg UV lamp, tungsten lamp or with a laser ($\lambda < 450$ nm) and then rapidly inject an aliquot for reversed-phase HPLC analysis. An advantage of this direct irradiation and injection is that it is possible to irradiate the sample at different time intervals and with successive injections, the extent of isomerisation as a function of time of irradiation can be determined. Hence in this study, both white light from a tungsten lamp and a blue violet laser pointer ($\lambda = 405$ nm) were used for irradiation of the sample to determine the extent of *cis/trans* isomerisation.

Alternatively, a simple device involving simultaneous irradiation and determination was designed to study these processes. This system (Figure 4.1) consists of a photocell with a Hg UV lamp for irradiation connected directly to a reversed-phase HPLC column. A Teflon coil was then wound round the lamp in the cell and the sample flows from the pump, through the coil to the column and finally to the detector. When the Hg UV lamp is switched on, solution of the sample is irradiated by the emission from the lamp. The irradiated solution flows through the coil to the column prior to separation and detection and when the lamp is switched off, the solution flows in the dark.



Figure 4.1. Simultaneous irradiation and determination setup used to study *cis/trans* isomerisation of *cis*-[M(Lⁿ-S,O)₂] complexes.

The setup has several advantages which include:

1. The Hg UV lamp used for irradiation tends to be more convenient for use in the cell compared to other classical light sources.
2. Simultaneous irradiation and detection is possible.
3. Variation of photon flux intensity emitted from the lamp and hence determination of relative rate of *cis/trans* isomerisation can still be achieved by simply changing the length of the coil.
4. It can be used as a simple, practical and readily available device for determining the relative rates of isomerisation with HPLC determination.
5. It is compatible with the HPLC pump used and can withstand high pressures without disruption of sample flow.

4.2. *cis/trans* isomerisation of palladium(II) and platinum(II) *N,N*-dialkyl-*N'*-acyl(aroyl)thioureas

The *cis*-[M(L-S,O)₂] (M = Pt(II), Pd(II)) complexes were found to undergo a reversible *cis/trans* isomerisation when exposed to light of wavelength < 450 nm with reversed-phase HPLC suitable for separation of the *cis/trans* complexes. To investigate the effect of light on these complexes, a mixture of 200 mg/L solutions of *cis*-[Pd(L⁶-S,O)₂] and *cis*-[Pt(L⁶-S,O)₂] in acetonitrile was freshly prepared and 20 μl of the aliquot was injected onto the HPLC

column using the setup in Figure 4.1. When the sample was kept in subdued light and the Hg UV lamp was switched off, two peaks resulted as shown in Figure 4.2. The peak having a retention time of 22 minutes is assigned to *cis*-[Pd(L⁶-S,O)₂] while the other peak eluting earlier at 21 minutes results from *cis*-[Pt(L⁶-S,O)₂]. Assignment of the peaks was done by first injecting 20 μl each of solutions of the pure complexes for HPLC analysis from which their respective retention times were obtained.

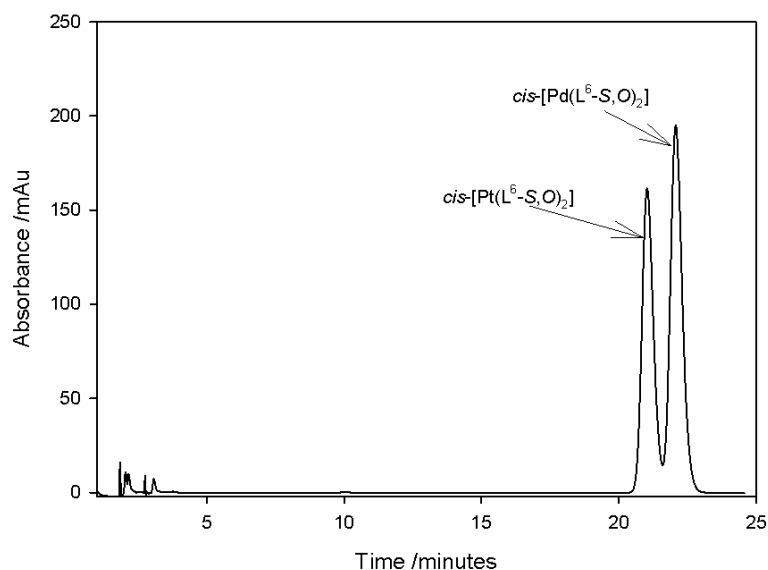


Figure 4.2. Chromatogram representing the separation of acetonitrile solutions of *cis*-[Pd(L⁶-S,O)₂] and *cis*-[Pt(L⁶-S,O)₂] in the dark; Conditions: C₁₈ ODS, 5 μm, 150 x 4.6 mm column; mobile phase 85:15 (% v/v) acetonitrile:0.1M acetate buffer (pH 6); flow rate 1 ml min⁻¹, 262 nm detection.

When the mixture of *cis*-[Pd(L⁶-S,O)₂] and *cis*-[Pt(L⁶-S,O)₂] was irradiated by switching on the Hg UV lamp, an additional peak was formed for each complex. The additional peaks formed were attributed to the formation of *trans*-[Pd(L⁶-S,O)₂] and *trans*-[Pt(L⁶-S,O)₂] as shown in the chromatogram in Figure 4.3. From the peak areas of the *trans* and *cis* complexes obtained, the ratio of the peak areas was determined using equation 2. A higher ratio of 0.4 was obtained for [Pd(L⁶-S,O)₂] compared to 0.3 for [Pt(L⁶-S,O)₂] suggesting that the extent of isomerisation is higher for *cis*-[Pd(L⁶-S,O)₂] when irradiated with the Hg UV lamp.

One way to confirm that the additional peaks formed are stereoisomers of the same complex is by comparing the absorbance profiles for the *cis*-[M(Lⁿ-S,O)₂] and *trans*-[M(Lⁿ-S,O)₂] complexes obtained using a diode array photometric detector. Similar absorbance profiles

were obtained for the *cis*-[M(L⁶-S,O)₂] (M = Pt(II), Pd(II)) and *trans*-[M(L⁶-S,O)₂] complexes (Appendix IV) confirming that these were indeed stereoisomers of the same complexes.

After irradiation, additional peaks were formed at retention times of 3 minutes, 4 minutes and 7 minutes. These additional peaks were found to be due to photo-decomposition of the *cis*-[Pt(L⁶-S,O)₂] as no such peaks were formed when a solution of pure *cis*-[Pd(L⁶-S,O)₂] was irradiated. Photo-decomposition of *cis*-[Pt(L⁶-S,O)₂] could occur especially when irradiated with a highly intensified UV light such as the Hg lamp used, leading to such additional peaks. When the Hg UV lamp was switched off once again and the irradiated solutions of *cis*-[Pd(L⁶-S,O)₂] and *cis*-[Pt(L⁶-S,O)₂] were allowed to stay in subdued light for a long period of time, the *trans* isomers of both complexes reverted back to the *cis* complexes and only single peaks were once again formed for both complexes. This indicates that the *cis/trans* isomerisation reactions are photoreversible.

Using the same setup in Figure 4.1 and with the Hg UV lamp switched off, single and well separated peaks were also obtained when 20 µl of an aliquot of a mixture of *fac*-[Rh(L³-S,O)₃] and [Ru(L³-S,O)₃] was injected. However, when this mixture was irradiated by switching the lamp on, no additional peak was observed for both complexes, suggesting that isomerisation of these complexes did not take place under the conditions used.

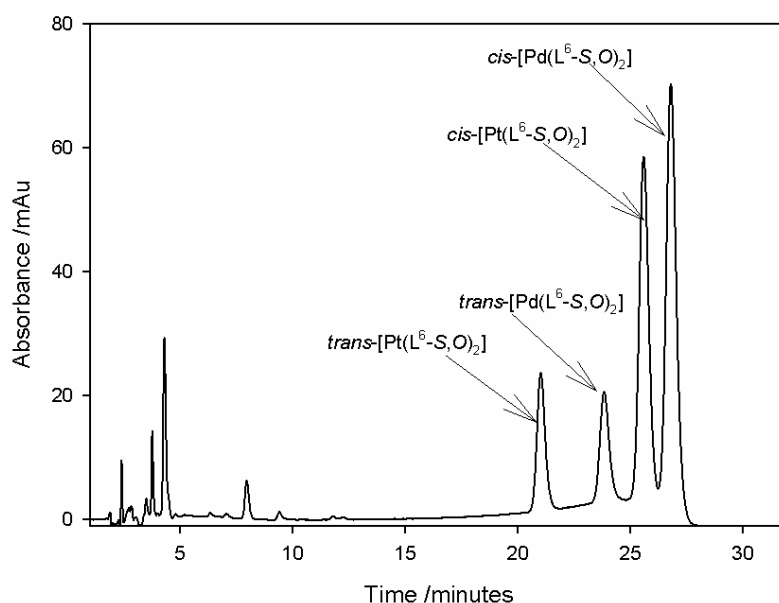


Figure 4.3. Chromatogram representing the separation of *cis* and *trans* complexes of [Pd(L⁶-S,O)₂] and [Pt(L⁶-S,O)₂] in acetonitrile upon irradiation with a Hg UV lamp; Conditions: C₁₈ ODS, 5 µm, 150 x 4.6 mm column; mobile phase 85:15 (% v/v) acetonitrile:0.1M acetate buffer (pH 6); flow rate 1 ml min⁻¹, 262 nm detection.

4.3. UV-VIS spectroscopy for monitoring *cis/trans* isomerisation

With the light sources for irradiation briefly discussed earlier in this chapter, reversed-phase HPLC was used for separation of the *cis/trans* isomers formed. UV-VIS spectroscopy was also used to monitor the changes resulting to *cis/trans* isomerisation of *cis*-[M(Lⁿ-S,O)₂] (M = Pt(II), Pd(II)) complexes. In such complexes, strong UV absorption bands could arise which could be caused by possible MLCT electronic transitions within the metal complexes.

In order to monitor the transformation from *cis*→*trans* using UV-VIS spectroscopy, solutions of *cis*-[Pd(L⁶-S,O)₂] and *cis*-[Pt(L⁶-S,O)₂] were prepared in acetonitrile and scanned using a diode array spectrophotometer in subdued light. The solutions were then irradiated at various time periods using a blue violet laser pointer ($\lambda = 405$ nm) and scanned by the UV spectrometer. The electronic absorption spectrum of *cis*-[Pd(L⁶-S,O)₂] (Figure 4.4) shows a major band with maximum absorbance at 300 nm and this could possibly arise from MLCT transitions. The blue line represents the absorbance profile of the complex when allowed in subdued light and this could be assigned to *cis*-[Pd(L⁶-S,O)₂]. Upon irradiation with the laser, after 3 minutes (green line) and 6 minutes (red line), a very slight change in absorbance is observed over the range 300 to 350 nm as a result of *cis/trans* isomerisation. Between this range, an isosbestic point is observed at *ca.* 330 nm indicating that two species (*cis*-[Pd(L⁶-S,O)₂] and *trans*-[Pd(L⁶-S,O)₂]) could be present in the solution. Over the range 280–400 nm, a very similar absorbance profile is obtained for all the lines confirming that the two species formed are stereoisomers of the sample complex [Pd(L⁶-S,O)₂].

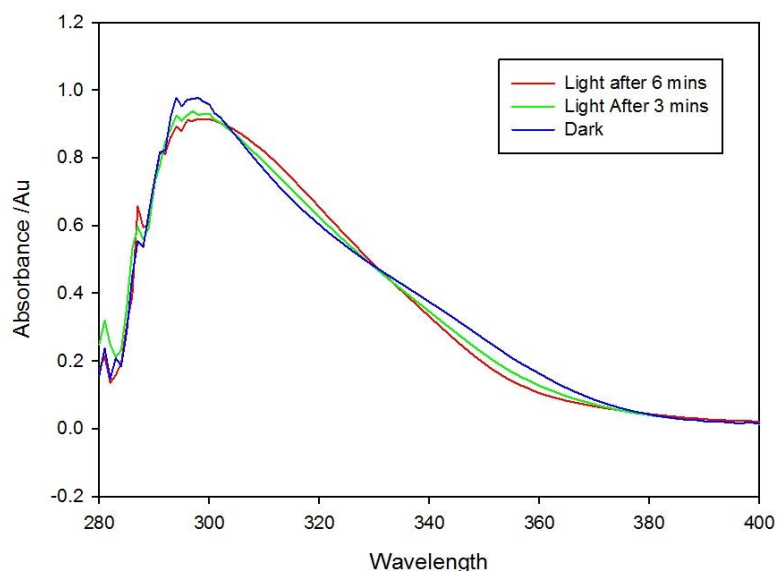


Figure 4.4. Electronic absorption spectrum obtained in the dark and after irradiation of cis -[Pd(L⁶-S,O)₂] in acetonitrile with a blue violet laser pointer ($\lambda = 405$ nm) at room temperature.

Similar changes were observed when an acetonitrile solution of cis -[Pt(L⁶-S,O)₂] was analysed. The UV-VIS absorbance profile of this complex in the dark and the spectral changes obtained upon irradiation are shown in Figure 4.5. Again, the similar absorbance profiles of the lines and an isosbestic point indicate the presence of two species, in this case cis -[Pt(L⁶-S,O)₂] and $trans$ -[Pt(L⁶-S,O)₂].

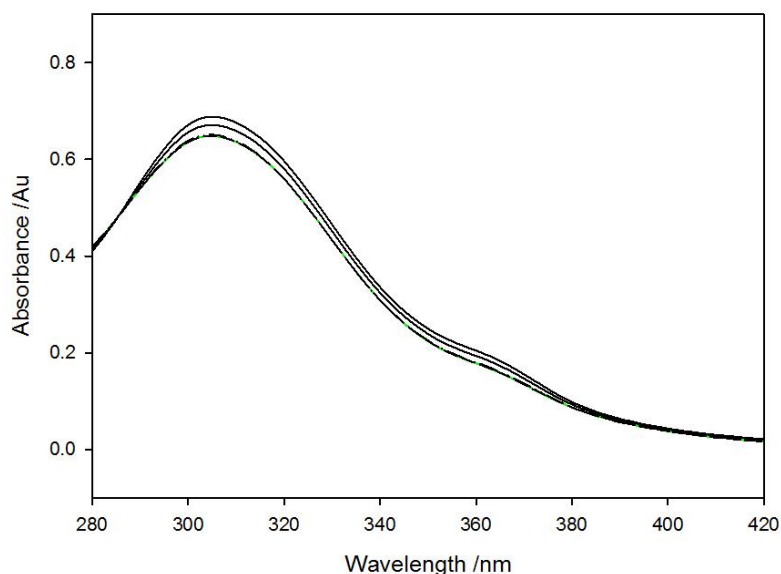


Figure 4.5. Electronic absorption spectrum in the dark and upon irradiation of a solution of [Pt(L⁶-S,O)₂] in acetonitrile with a blue violet laser ($\lambda = 405$ nm) and at room temperature.

However, compared to the changes observed for *cis*-[Pd(L⁶-S,O)₂] in Figure 4.4, the spectral changes observed for *cis*-[Pt(L⁶-S,O)₂] in Figure 4.5 are quite small suggesting that the extent of *cis/trans* isomerisation is greater for *cis*-[Pd(L⁶-S,O)₂] when both solutions are irradiated with the same light source. It can also be observed that the spectral changes for both complexes are smaller, compared to the changes in peak areas and peak separation obtained during reversed-phase HPLC. Hence HPLC is a more suitable technique for monitoring *cis/trans* isomerisation of *cis*-[M(Lⁿ-S,O)₂] compared to UV-VIS spectroscopy and further determination of the extent of *cis/trans* isomerisation will be carried out using reversed-phase HPLC.

4.4. Photo-induced isomerisation of *cis*-[Pd(Lⁿ-S,O)₂] complexes

For the series of complexes *cis*-[Pd(L³-S,O)₂], *cis*-[Pd(L⁴-S,O)₂], *cis*-[Pd(L⁶-S,O)₂] and *cis*-[Pd(L⁷-S,O)₂] the nature of different ligand substituents was shown to have an effect on the separation of these complexes by reversed-phase HPLC (Chapter 3, Figure 3.6). Since the *cis*-[Pd(Lⁿ-S,O)₂] complexes isomerise to *trans*-[Pd(Lⁿ-S,O)₂] under the influence of light, it could then be possible with a suitable choice of chromatographic conditions, to separate the *cis* and *trans* isomers involved after irradiating a mixture of *cis*-[Pd(Lⁿ-S,O)₂] complexes with different groups attached to the ligand.

By determining the ratios of the peak areas of the *trans* and *cis* isomers from reversed-phase HPLC, the complexes *cis*-[Pd(L³-S,O)₂], *cis*-[Pd(L⁴-S,O)₂], *cis*-[Pd(L⁶-S,O)₂] and *cis*-[Pd(L⁷-S,O)₂] were used to determine the effect of ligand substituents on the extent of isomerisation. Irradiation of solutions of the complexes and reversed-phase HPLC determination was first carried out using the setup in Figure 4.1, with Hg UV lamp used for illumination. In subdued light, when the lamp was switched off, four well-separated peaks were obtained as was shown in Figure 3.6 and these peaks are assigned to the respective *cis* complexes. When 20 µl of an aliquot of a mixture of the four complexes was irradiated by switching on the lamp, additional peaks were formed for each complex which are assigned to their respective *trans* isomers as shown in Figure 4.6. From the chromatogram (Figure 4.6), it can be observed that a poor separation is obtained between *cis*-[Pd(L⁷-S,O)₂] and *trans*-[Pd(L⁷-S,O)₂] with both complexes retained at *ca.* 68 minutes. Due to the poor separation, a ratio for the peak areas of *trans*-[Pd(L⁷-S,O)₂] and *cis*-[Pd(L⁷-S,O)₂] could not be obtained. It however appears that the presence of electron-withdrawing chloro substituent on the aryl moiety in [Pd(L⁷-S,O)₂] does

not favour the formation of the *trans* complex and also its separation from the *cis* complex. Due to the poor separation of the *cis/trans* isomers of $[\text{Pd}(\text{L}^7\text{-S},\text{O})_2]$, a further study on the isomerisation of this complex was not pursued.

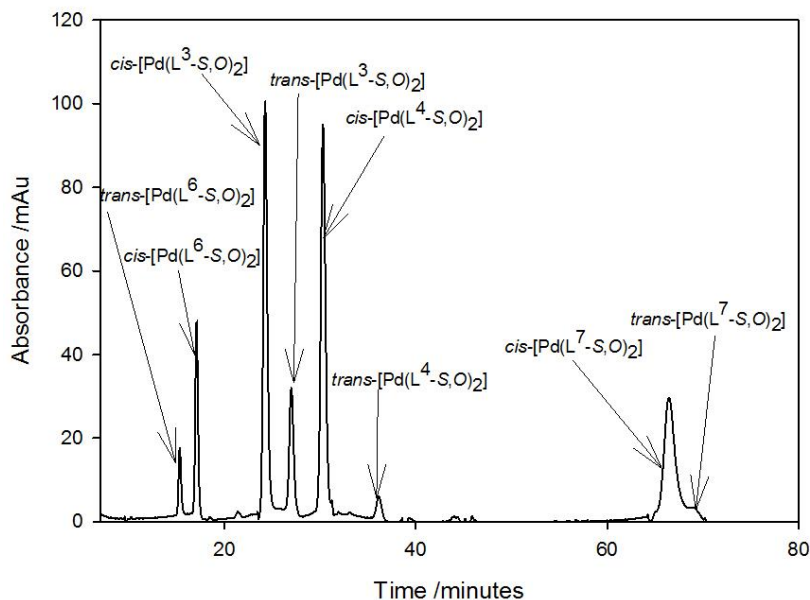


Figure 4.6. Chromatogram representing the separation of *cis* and *trans* isomers of $[\text{Pd}(\text{L}^7\text{-S},\text{O})_2]$, $[\text{Pd}(\text{L}^6\text{-S},\text{O})_2]$, $[\text{Pd}(\text{L}^4\text{-S},\text{O})_2]$ and $[\text{Pd}(\text{L}^3\text{-S},\text{O})_2]$ in acetonitrile, upon irradiation with Hg UV lamp; Conditions: C_{18} ODS, $5 \mu\text{m}$, $150 \times 4.6 \text{ mm}$ column; mobile phase 85:15 (% v/v) acetonitrile:0.1M acetate buffer (pH 6); flow rate 1 ml min^{-1} .

The *cis* and *trans* isomers of the other complexes $[\text{Pd}(\text{L}^4\text{-S},\text{O})_2]$, $[\text{Pd}(\text{L}^3\text{-S},\text{O})_2]$ and $[\text{Pd}(\text{L}^6\text{-S},\text{O})_2]$ were well separated as shown in Figure 4.6. Ratios of 0.2, 0.41 and 0.31 were obtained from the *trans/cis* peak areas of the *trans* and *cis* isomers of $[\text{Pd}(\text{L}^4\text{-S},\text{O})_2]$, $[\text{Pd}(\text{L}^3\text{-S},\text{O})_2]$ and $[\text{Pd}(\text{L}^6\text{-S},\text{O})_2]$ respectively. A lower ratio for $[\text{Pd}(\text{L}^4\text{-S},\text{O})_2]$ indicates that the extent of *cis/trans* isomerisation for this complex is lower compared to the other two complexes. This suggests that the presence of a piperidine ring on the ligand does not greatly favour the formation of the *trans* isomer upon irradiation of the complex with a Hg UV lamp. A lower ratio for $[\text{Pd}(\text{L}^6\text{-S},\text{O})_2]$ compared to $[\text{Pd}(\text{L}^3\text{-S},\text{O})_2]$ suggest that the presence of three electron-donating methoxy groups on $[\text{Pd}(\text{L}^6\text{-S},\text{O})_2]$ could have resulted in a decrease in the extent of *cis/trans* isomerisation.

A closer look at Figure 4.6 shows a correlation between ligand structure of the complexes and the retention time of the *cis* and *trans* isomers. A lower retention time was obtained for *trans*- $[\text{Pd}(\text{L}^6\text{-S},\text{O})_2]$ ($t_{\text{R}} = 16$ minutes) compared to *cis*- $[\text{Pd}(\text{L}^6\text{-S},\text{O})_2]$ ($t_{\text{R}} = 18$ minutes). However, for $[\text{Pd}(\text{L}^3\text{-S},\text{O})_2]$, a higher retention time ($t_{\text{R}} = 28$ minutes) is obtained for the *trans* complex

compared to $t_R = 25$ minutes for the *cis* complex. The lower retention time of *trans*-[Pd(L⁶-S,O)₂] relative to the *cis* isomer suggests that the presence of electron-donating methoxy groups on the ligands could have increase the polarity of the *trans* complex, thereby making it less retained to the HPLC column. This was confirmed by the fact that with one of these electron-donating methoxy groups present in [Pd(L⁵-S,O)₂], and upon separation after irradiation, the retention time of the *trans* complex was lower than that of the *cis* (Figure 4.11, page 71).

From the absorbance profiles of the *cis* and *trans* complexes (Appendix IV) obtained from the diode array photometric detector, the difference in wavelength at maximum absorbance for *cis* and *trans* isomers for each complex was also measured. Table 6 gives this difference as well as *trans/cis* peak area ratios and retention times for [Pd(L³-S,O)₂], [Pd(L⁴-S,O)₂], [Pd(L⁵-S,O)₂] and [Pd(L⁶-S,O)₂]. The table shows a trend in the difference in wavelength at maximum absorbance with respect to the different ligands attached to [Pd(L³-S,O)₂], [Pd(L⁵-S,O)₂] and [Pd(L⁶-S,O)₂]. A difference of 13 nm was obtained for both [Pd(L³-S,O)₂] and [Pd(L⁵-S,O)₂]. This suggests that the energy for electronic transitions resulting to *cis/trans* isomerisation for these two complexes could be similar. If this is so, then these two complexes are expected to have a very similar extent of isomerisation as can be seen from the *trans/cis* peak area ratios obtained (0.41 for [Pd(L³-S,O)₂] and 0.40 for [Pd(L⁵-S,O)₂]). A small difference of 2 nm was obtained for [Pd(L⁶-S,O)₂], suggesting that the extent of isomerisation of this complex could be much lower compared to [Pd(L³-S,O)₂] and [Pd(L⁵-S,O)₂] and this could be further confirmed by the smaller *trans/cis* peak area ratio of 0.31 obtained for [Pd(L⁶-S,O)₂].

Table 6. Table showing the difference in wavelengths at maximum absorbance, retention times and peak areas of *cis* and *trans* complexes of [Pd(L³-S,O)₂], [Pd(L⁴-S,O)₂], [Pd(L⁵-S,O)₂] and [Pd(L⁶-S,O)₂] in acetonitrile upon irradiation with a Hg UV lamp.

Complex	Peak Area/ mAu	t_r /mins	<i>trans/cis</i> peak area ratio	$\Delta\lambda$ /nm
<i>trans</i> -[Pd(L ³ -S,O) ₂]	4666.7	23.246	0.41	13
<i>trans</i> -[Pd(L ⁴ -S,O) ₂]	760.3	30.512	0.12	11
<i>trans</i> -[Pd(L ⁶ -S,O) ₂]	1548.2	14.262	0.31	2
<i>trans</i> -[Pd(L ⁵ -S,O) ₂]	5325.77	24.728	0.40	13

The trends observed in Table 6 for $[\text{Pd}(\text{L}^3\text{-S},\text{O})_2]$, $[\text{Pd}(\text{L}^5\text{-S},\text{O})_2]$ and $[\text{Pd}(\text{L}^6\text{-S},\text{O})_2]$ led to further investigations to estimate their relative rates of *cis/trans* isomerisation. This was initially carried out by using the setup in Figure 4.1 in which Hg UV lamp was used for irradiation. With this setup, it was possible to estimate the extent and relative rate of *cis/trans* isomerisation of *cis*- $[\text{Pd}(\text{L}^6\text{-S},\text{O})_2]$. This was done by using Teflon coils of different length and by irradiation through the coils with the Hg UV lamp, different extent of isomerisation could occur leading to different peak areas for the *cis* and *trans* isomers determined by reversed-phase HPLC. When the Hg lamp was switched on at minimum coil length (1 cm), and 20 μl of an acetonitrile solution of *cis*- $[\text{Pd}(\text{L}^6\text{-S},\text{O})_2]$ was injected onto the column, two peaks were formed corresponding to *cis*- $[\text{Pd}(\text{L}^6\text{-S},\text{O})_2]$ and *trans*- $[\text{Pd}(\text{L}^6\text{-S},\text{O})_2]$, with a *trans/cis* peak area ratio of 0.05. As the coil length was increased and the sample irradiated, the photon flux intensity from the Hg lamp increased, leading to an increase in the peak area of the *trans*- $[\text{Pd}(\text{L}^6\text{-S},\text{O})_2]$ and a corresponding decrease in the peak area of the *cis*- $[\text{Pd}(\text{L}^6\text{-S},\text{O})_2]$ as shown in Figure 4.7. A steady state was obtained after irradiation with a 10 cm coil, with a K_e value of 0.31.

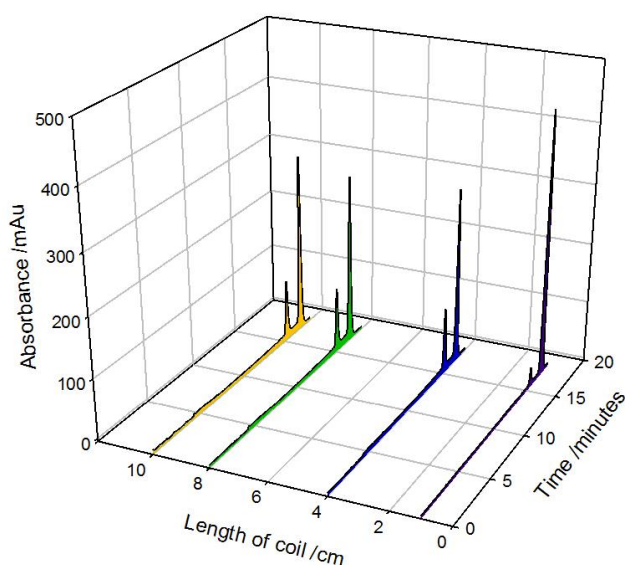


Figure 4.7. Overlaid chromatograms representing the separation of *cis* and *trans* complexes of $[\text{Pd}(\text{L}^6\text{-S},\text{O})_2]$ in acetonitrile both in the dark and upon irradiation with a Hg UV lamp; conditions: GEMINI C 18 $5\mu\text{m}$, 150×4.6 mm, mobile phase 90:10 (% v/v) acetonitrile:0.1M acetate buffer (pH 6), flow rate 1 ml min^{-1} , injection volume $20 \mu\text{l}$, 262 nm detection.

Figure 4.8 shows a plot of changes in peak areas for the *cis* and *trans* isomers of $[\text{Pd}(\text{L}^6\text{-S},\text{O})_2]$ with the different coil lengths used for irradiation. It can be seen from the plots that the

peak area for the *cis*-[Pd(L⁶-S,O)₂] decreased while that of the *trans*-[Pd(L⁶-S,O)₂] increased as the coil length was increased. With a 10 cm coil length used, the *cis/trans* isomerisation almost reached a steady state and at this point, the *trans/cis* ratio of peak areas is referred to as K_e and has a value of 0.31.

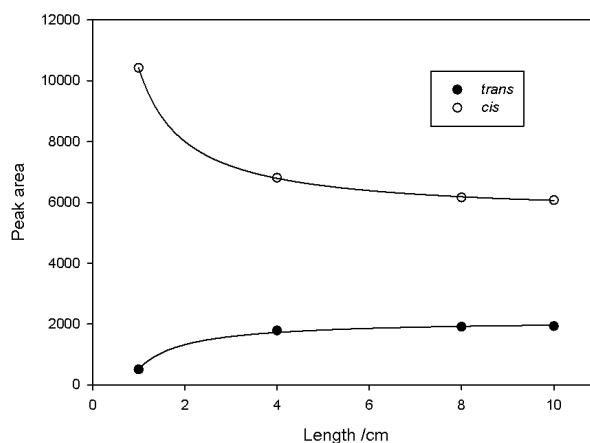


Figure 4.8. Plots of peak area for *cis* and *trans*-[Pd(L⁶-S,O)₂] in acetonitrile with length of coil upon irradiation with Hg UV lamp.

4.5. Effect of nature of ligands on relative rate of isomerisation of *cis*-[Pd(Lⁿ-S,O)₂] complexes

In the previous section, the extent and relative rate of *cis/trans* isomerisation was estimated by determining the peak areas of the *cis* and *trans* isomers of [Pd(L⁶-S,O)₂] using reversed-phase HPLC with the setup in Figure 4.1 during which a Hg UV lamp was used for irradiation. As was explained earlier, determination of the relative rates at which *cis/trans* isomerisation occurs using this setup was carried out by varying the intensity of photons emitted from the Hg UV lamp as a function of length of a Teflon coil. Although a simultaneous irradiation and determination could be carried out with this setup, it should be pointed out however that it has a disadvantage in that the length of coil could be limited for irradiation with the Hg UV lamp. It would however be much better to determine the relative rate of isomerisation for *cis*-[Pd(L⁶-S,O)₂] as well as that for the other complexes *cis*-[Pd(L³-S,O)₂] and *cis*-[Pd(L⁵-S,O)₂] as a function of time of irradiation. Hence by irradiating an acetonitrile solution of these complexes using either a tungsten lamp or a blue violet laser ($\lambda = 405$ nm) for certain periods of time followed by injection of the sample for HPLC analysis, their extent and relative rates of *cis/trans* isomerisation were also determined.

4.5.1. Ligand effect on relative rate of forward (*cis*→*trans*) isomerisation of [Pd(Lⁿ-S,O)₂] complexes

A 200 mg/L each of solutions of *cis*-[Pd(L³-S,O)₂], *cis*-[Pd(L⁵-S,O)₂] and *cis*-[Pd(L⁶-S,O)₂] were prepared and 20 μl of *cis*-[Pd(L⁶-S,O)₂] was injected onto the HPLC column in a dark room. This resulted in a single peak corresponding to *cis*-[Pd(L⁶-S,O)₂]. The sample was first irradiated with a tungsten lamp for different periods of time followed by subsequent injection onto the column. Upon irradiation, an additional peak was formed corresponding to *trans*-[Pd(L⁶-S,O)₂] and the area of this peak was found to increase with time of irradiation while that of *cis*-[Pd(L⁶-S,O)₂] was found to decrease. At *ca.* 20 minutes of irradiation, a steady state was reached when no further changes in peak area was observed for both *cis/trans* isomers of the complex. A plot of *trans/cis* peak area ratio against time of irradiation of *cis*-[Pd(L⁶-S,O)₂] is shown in Figure 4.9. This shows that the ratio initially increases until a steady state was reached at *ca.* 20 minutes. At this time, the *trans/cis* peak area ratio is given by K_e and has a value of 0.22.

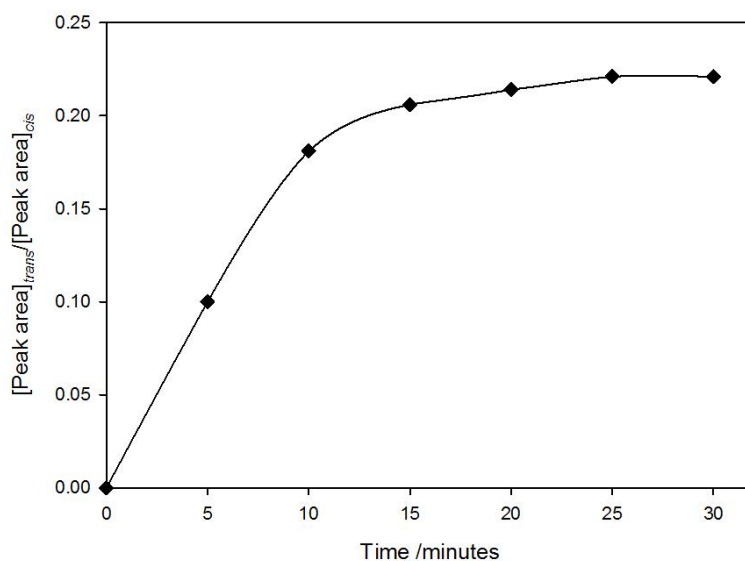


Figure 4.9. A plot of *trans/cis* peak area ratio with time for *cis*-[Pd(L⁶-S,O)₂] in acetonitrile upon irradiation with tungsten lamp.

Although these results are consistent to the that obtained when similar solutions were irradiated using a tungsten lamp from previous studies,⁵⁸ it should be noted that the K_e value obtained (0.22) is much lower compared to when a similar solution was irradiated with a Hg UV lamp. In the case of a Hg UV lamp, a K_e value of 0.31 was obtained as discussed in the

previous section. The lower K_e value (0.22) upon irradiation with the tungsten lamp could have resulted from an instrumental error as the solution of *cis*-[Pd(L⁶-S,O)₂] was automatically injected onto the HPLC system for analysis. This was accompanied by time lapses (*ca.* 1 minute) between irradiation of sample and its injection onto the HPLC column. With these time lapses, it is possible that some of the *trans*-[Pd(L⁶-S,O)₂] present at steady state could revert back to *cis*-[Pd(L⁶-S,O)₂] hence decreasing the *trans/cis* peak area ratio which could have resulted to a lower K_e value. To eliminate this error in order to obtain a more consistent K_e value, it was necessary to use a setup in which the sample could be irradiated as a function of time and then quickly and manually injected for HPLC analysis. Thus a new setup was developed with a 2 ml glass syringe coupled to the HPLC injector. After irradiation of a certain volume of sample in the syringe for a certain period of time, the sample was then injected as quickly as possible onto the HPLC column.

When a 0.5 ml solution of *cis*-[Pd(L⁶-S,O)₂] measured with the glass syringe was now irradiated with a blue violet laser ($\lambda = 405$ nm) and then manually injected onto the HPLC column, similar changes in peak areas of the *cis* and *trans* isomers of the complex were observed as when either a tungsten lamp or Hg UV lamp were used for irradiation. Figure 4.10 shows an overlaid chromatogram of the changes in peak area for *cis*-[Pd(L⁶-S,O)₂] and *trans*-[Pd(L⁶-S,O)₂] upon irradiation with the blue violet laser pointer. The *cis* isomer which elutes after 13 minutes experiences a decrease in peak area as irradiation time increases, while the peak area of the *trans* complex increases. At steady state, a K_e value of 0.30 was obtained after 3 minutes of irradiating *cis*-[Pd(L⁶-S,O)₂] with the blue violet laser pointer. This value is very close to the K_e value of 0.31 that was obtained when the same solution was irradiated with the Hg UV lamp.

Upon irradiation with the tungsten lamp earlier, a steady state was reached after *ca.* 20 minutes of irradiation meanwhile a much lesser time of *ca.* 3 minutes was needed for the same solution to reach a steady state when irradiated with the blue violet laser pointer. This difference in time for a steady state to be achieved suggests that the light from the blue violet laser could be much more intense compared to that emitting from the tungsten lamp. Hence compared to the tungsten lamp, the blue violet laser pointer was selected as a suitable irradiation source added to its advantage that a specific wavelength (405 nm) of light from it resulted in photo-isomerisation of the complexes investigated.

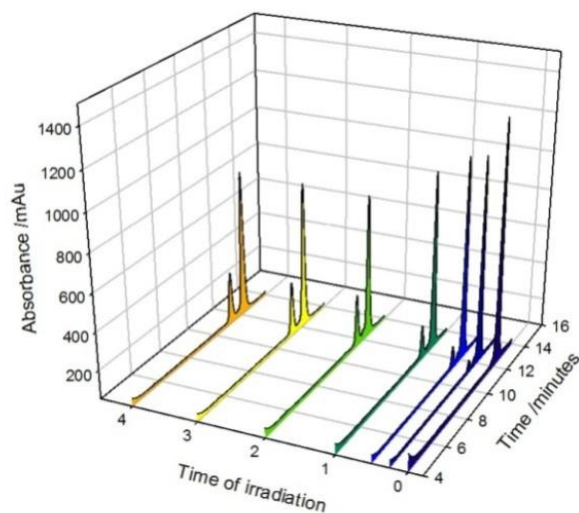


Figure 4.10. Overlaid chromatograms representing the forward isomerisation of a solution of $[\text{Pd}(\text{L}^6\text{-S},\text{O})_2]$ in acetonitrile upon irradiation with a 405 nm blue violet laser; Conditions: GEMINI C18 ODS, 5 μm , 150 x 4.6 mm column; mobile phase 95:5 (% v/v) acetonitrile:0.1M acetate buffer (pH 6); 1 ml min^{-1} flow rate.

To determine the extent and relative rate of *cis/trans* isomerisation of *cis*- $[\text{Pd}(\text{L}^5\text{-S},\text{O})_2]$, an acetonitrile solution of the complex was also irradiated with the blue violet laser pointer at different periods of time and manually injected onto the HPLC column. Figure 4.11 shows the changes in peak area of the *cis* and *trans* complexes with different times of irradiation. The peak area of *cis*- $[\text{Pd}(\text{L}^5\text{-S},\text{O})_2]$ appears to decrease at a relatively faster rate while that of the *trans*- $[\text{Pd}(\text{L}^5\text{-S},\text{O})_2]$ increases and a steady state was achieved at *ca.* 2.5 minutes of irradiation.

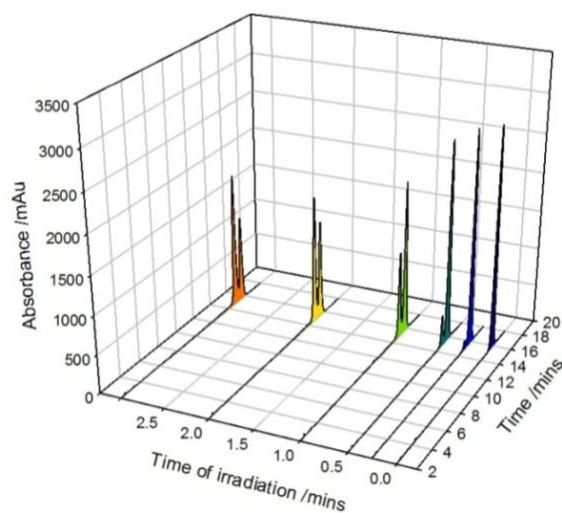


Figure 4.11. Overlaid chromatograms representing the forward isomerisation of a solution of $[\text{Pd}(\text{L}^5\text{-S},\text{O})_2]$ in acetonitrile upon irradiation with a 405 nm blue violet laser; Conditions: GEMINI C18 ODS, 5 μm , 150 x 4.6 mm column; mobile phase 95:5 (% v/v) acetonitrile:0.1M acetate buffer (pH 6); 1 ml min^{-1} flow rate.

Finally, an acetonitrile solution of cis -[Pd(L³-S,O)₂] was also irradiated with the blue violet laser pointer at different time periods and then injected onto the HPLC column. Figure 4.12 shows the changes in the peak areas of cis -[Pd(L³-S,O)₂] and $trans$ -[Pd(L³-S,O)₂]. The changes suggests that the relative rate of $cis/trans$ isomerisation of cis -[Pd(L³-S,O)₂] is much higher than that of cis -[Pd(L⁶-S,O)₂]. A steady state was achieved for this complex after *ca.* 3 minutes of irradiation.

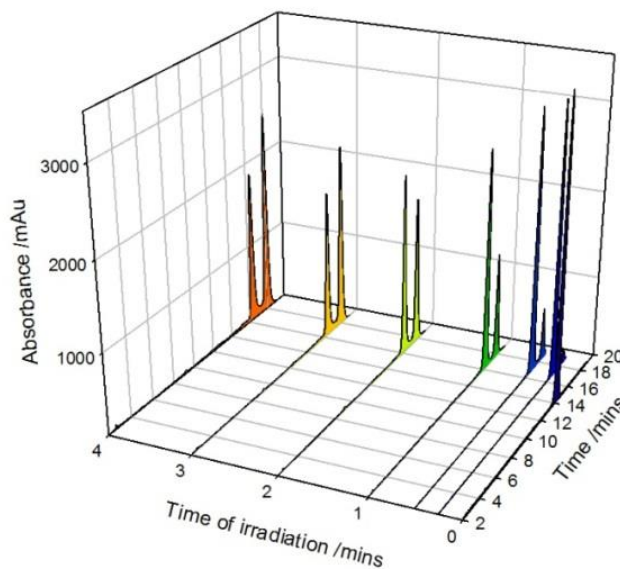


Figure 4.12. Overlaid chromatograms representing the forward isomerisation of a solution of [Pd(L³-S,O)₂] in acetonitrile upon irradiation with a 405 nm blue violet laser; Conditions: GEMINI C₁₈ ODS, 5 μ m, 150 x 4.6 mm column; mobile phase 95:5 (% v/v) acetonitrile:0.1M acetate buffer (pH 6); 1 ml min⁻¹ flow rate.

The $trans/cis$ peak area ratios of the 3 complexes cis -[Pd(L³-S,O)₂], cis -[Pd(L⁵-S,O)₂] and cis -[Pd(L⁶-S,O)₂] were plotted against time of irradiation (Figure 4.13). From the plots, it can be seen that the $trans/cis$ peak area ratio initially increases for all 3 complexes and then attains a constant value (K_e) when a steady state is reached for each complex. A similar K_e value of *ca.* 1.4 was obtained for cis -[Pd(L³-S,O)₂] and cis -[Pd(L⁵-S,O)₂], but slightly higher for cis -[Pd(L⁵-S,O)₂] suggesting that the extent of $cis/trans$ isomerisation for both complexes are similar. Also a similar increase in the $trans/cis$ peak area ratio with time for both cis -[Pd(L³-S,O)₂] and cis -[Pd(L⁵-S,O)₂] was obtained but slightly higher for cis -[Pd(L⁵-S,O)₂] also suggesting that the relative rate of $cis/trans$ isomerisation for cis -[Pd(L⁵-S,O)₂] is slightly higher. A much lower K_e value (*ca.* 0.30) was obtained for cis -[Pd(L⁶-S,O)₂] indicating a lower extent of isomerisation compared to either cis -[Pd(L³-S,O)₂] or cis -[Pd(L⁵-S,O)₂].

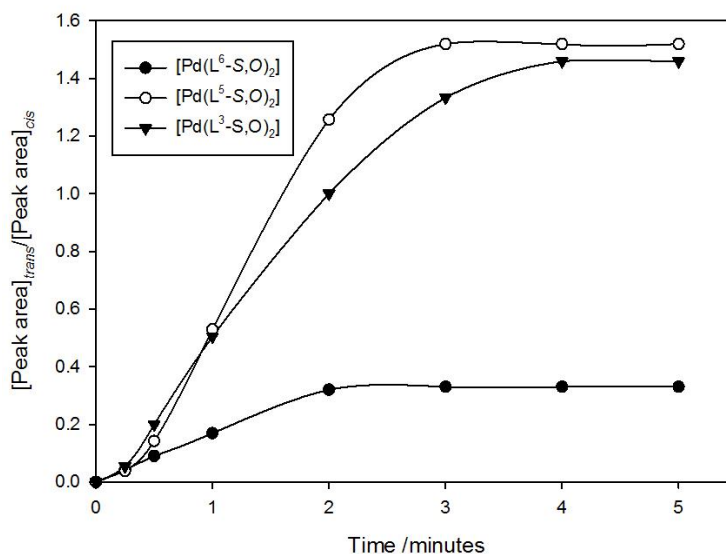


Figure 4.13. A plot of *trans/cis* peak area ratio vs time of irradiation for *cis*→*trans* isomerisation of [Pd(L³-S,O)₂], [Pd(L⁵-S,O)₂] and [Pd(L⁶-S,O)₂] in acetonitrile upon irradiation with blue violet laser pointer ($\lambda = 405$ nm).

4.5.2. Ligand effect on relative rate of reverse (*trans*→*cis*) isomerisation for [Pd(Lⁿ-S,O)₂] complexes

The relative rates of reverse (*trans*→*cis*) isomerisation of [Pd(Lⁿ-S,O)₂] complexes were also studied. This was done by irradiating a constant volume of a solution of the complexes using a blue violet laser pointer until a steady state was reached. The irradiated solutions were then allowed to stay in a dark room at a certain temperature for different periods of time during which the *trans* complexes are expected to revert back to the corresponding *cis* complexes.

The relative rates of reverse isomerisation for [Pd(L³-S,O)₂] and [Pd(L⁶-S,O)₂] were determined by irradiating acetonitrile solutions of the complexes for 3 minutes using a blue violet laser pointer. The irradiated solutions were then left in the dark at 17.4 °C for different periods of time and then quickly and manually injected for HPLC analysis. For both complexes, irradiation of their solutions led to a steady state at which there were no further changes in the peak areas of their *cis* and *trans* isomers. When the irradiated solutions were allowed to stay in the dark for some time, the peak areas of the *trans* isomers were found to decrease while that of the *cis* isomers increase until the *cis* complexes were completely restored.

Figure 4.14 shows overlaid chromatograms indicating the changes in peak areas of the *cis* and *trans* isomers of $[\text{Pd}(\text{L}^6\text{-S},\text{O})_2]$ when the irradiated solution was allowed to stay in a dark room for a certain period of time and at 17.4°C . From the chromatograms, it can be seen that in the dark and from a steady state, the peak area of the *cis*- $[\text{Pd}(\text{L}^6\text{-S},\text{O})_2]$ decreases with time while that of the *trans*- $[\text{Pd}(\text{L}^6\text{-S},\text{O})_2]$ increases and at *ca.* 4 minutes in the dark, all of the *trans* complex completely reverts back to the *cis* complex.

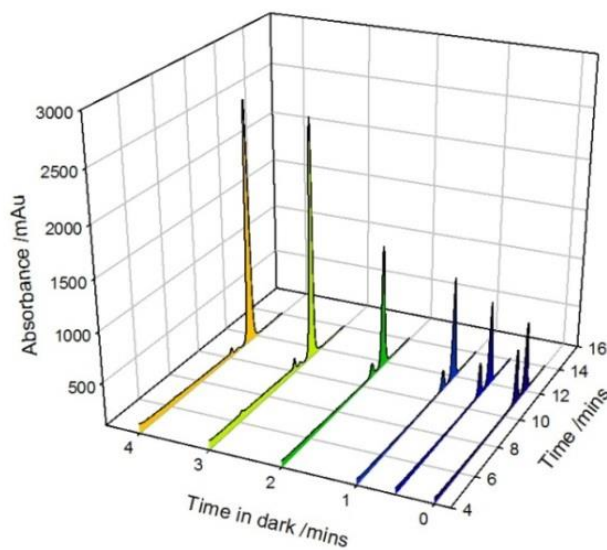


Figure 4.14. Overlaid chromatograms representing changes in isomerisation for $[\text{Pd}(\text{L}^6\text{-S},\text{O})_2]$ when an irradiated acetonitrile solution of sample is allowed in the dark at 17.4°C ; conditions: GEMINI C 18 ODS $5\mu\text{m}$, $150 \times 4.6 \text{ mm}$ column, mobile phase 95:5 (% v/v) acetonitrile:0.1M acetate buffer (pH 6), flow rate 1 ml min^{-1} .

Figure 4.15 shows a plot of *trans/cis* peak area ratio against time when an acetonitrile solution of $[\text{Pd}(\text{L}^6\text{-S},\text{O})_2]$ was kept in the dark. It can be seen from the plot that from a K_e value of *ca.* 0.30 obtained after irradiation for 3 minutes, the *trans/cis* peak area ratio rapidly decreases and approaches zero at *ca.* 4 minutes of time in the dark. At this time, almost all of *trans*- $[\text{Pd}(\text{L}^6\text{-S},\text{O})_2]$ should have reverted back to *cis*- $[\text{Pd}(\text{L}^6\text{-S},\text{O})_2]$.

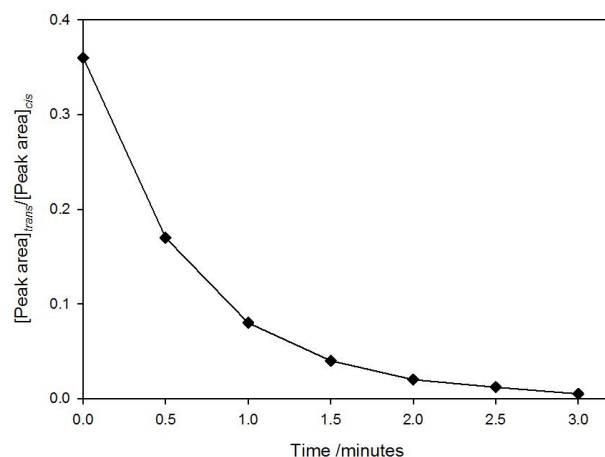


Figure 4.15. A plot of *trans/cis* peak area ratio against time in dark when a solution of $[\text{Pd}(\text{L}^6\text{-S},\text{O})_2]$ in acetonitrile is irradiated with a 405 nm blue violet laser and allowed to stay in the dark at different times at 17.4 °C.

For the *trans*→*cis* isomerisation of $[\text{Pd}(\text{L}^3\text{-S},\text{O})_2]$, after a steady state was achieved upon irradiation for 3 minutes, the peak area of *trans*- $[\text{Pd}(\text{L}^3\text{-S},\text{O})_2]$ was also found to decrease with time of the solution in the dark while a corresponding increase in peak area occurred for *cis*- $[\text{Pd}(\text{L}^3\text{-S},\text{O})_2]$. However, as shown in the overlaid chromatograms in Figure 4.16, the relative rate of *trans*→*cis* isomerisation appears to be much slower compared to that observed for $[\text{Pd}(\text{L}^6\text{-S},\text{O})_2]$ and up to 8 hours of time in the dark was needed for *trans*- $[\text{Pd}(\text{L}^3\text{-S},\text{O})_2]$ to completely revert back to *cis*- $[\text{Pd}(\text{L}^3\text{-S},\text{O})_2]$.

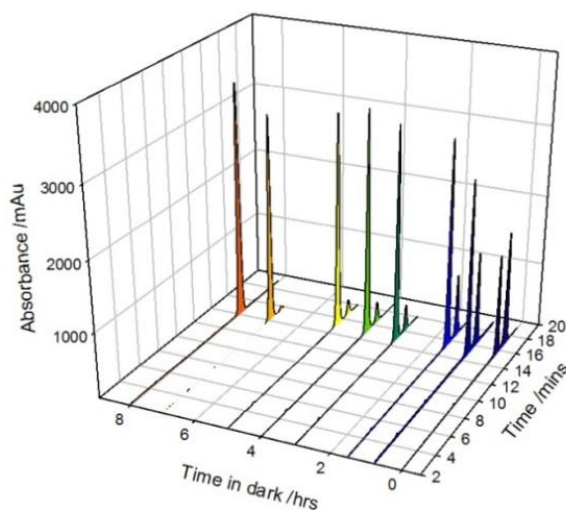


Figure 4.16. Overlaid chromatograms representing the changes in peak areas for both *cis* and *trans* complexes of $[\text{Pd}(\text{L}^3\text{-S},\text{O})_2]$ in acetonitrile after irradiation with 405 nm blue violet laser and allowed to stay in the dark at 17.4 °C; conditions: GEMINI C 18 ODS 5 μm , 150 x 4.6 mm column, mobile phase 95:5 (% v/v) acetonitrile:0.1M acetate buffer (pH 6), flow rate 1 ml min⁻¹.

Figure 4.17 shows a plot of the *trans/cis* ratio of peak areas against time of allowing an irradiated solution of $[\text{Pd}(\text{L}^3\text{-S},\text{O})_2]$ to stay in a dark room for different time periods. After the solution was irradiated for 3 minutes, a steady state K_e value of *ca.* 1.4 was obtained. When the solution was allowed to stay in the dark, the *trans/cis* peak area ratio slowly decreased as a result of changes from *trans*- $[\text{Pd}(\text{L}^3\text{-S},\text{O})_2]$ to *cis*- $[\text{Pd}(\text{L}^3\text{-S},\text{O})_2]$. The *trans/cis* peak area ratio decreases with time in the dark for $[\text{Pd}(\text{L}^3\text{-S},\text{O})_2]$ and after *ca.* 8 hours (420 minutes) in the dark, the ratio approaches zero when all of *cis*- $[\text{Pd}(\text{L}^3\text{-S},\text{O})_2]$ was completely restored.

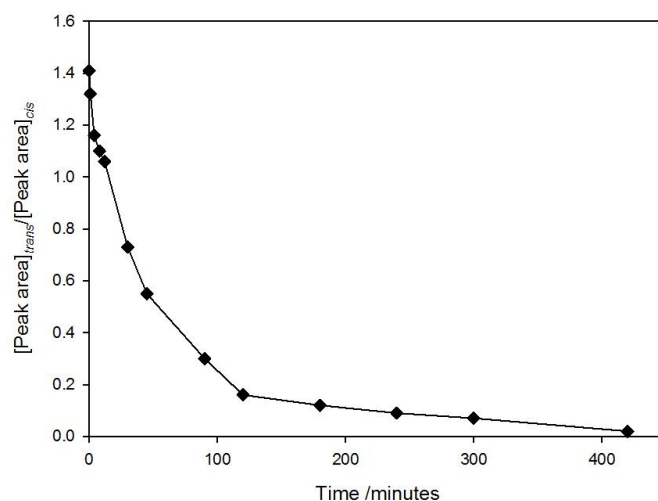


Figure 4.17. Variation of *trans/cis* peak area ratio with time for $[\text{Pd}(\text{L}^6\text{-S},\text{O})_2]$ after an acetonitrile solution of the complex is irradiated with a blue violet laser pointer (405 nm) and allowed for stay in the dark at 17.4 °C.

4.6. Photo-induced Isomerisation of *cis*- $[\text{Pt}(\text{L}^n\text{-S},\text{O})_2]$ complexes

In the previous section the relative rates and extents of *cis/trans* isomerisation of *cis*- $[\text{Pd}(\text{L}^n\text{-S},\text{O})_2]$ have been estimated. To investigate the effect of metal center on the relative isomerisation rates, a similar procedure was used to estimate the relative rate of *cis/trans* isomerisation of *cis*- $[\text{Pt}(\text{L}^6\text{-S},\text{O})_2]$ compared to that of *cis*- $[\text{Pd}(\text{L}^6\text{-S},\text{O})_2]$ already determined. A solution of *cis*- $[\text{Pt}(\text{L}^6\text{-S},\text{O})_2]$ (200 mg/L) in acetonitrile was prepared and 0.5 ml of the sample in a glass syringe was irradiated with a blue violet laser ($\lambda = 405$ nm) at different periods of time. The irradiated solution was then manually injected for HPLC analysis.

In the dark, only a single peak was observed at a retention time of 14.8 minutes which was attributed to *cis*- $[\text{Pt}(\text{L}^6\text{-S},\text{O})_2]$. Upon irradiation, the *cis*- $[\text{Pt}(\text{L}^6\text{-S},\text{O})_2]$ complex isomerises to *trans*- $[\text{Pt}(\text{L}^6\text{-S},\text{O})_2]$ as seen by the formation and growth of an additional peak at a lower retention time of 12.5 minutes (Figure 4.18). As was observed in the case of *cis*- $[\text{Pd}(\text{L}^6\text{-S},\text{O})_2]$

(Figure 4.10), the peak area of *trans*-[Pt(L⁶-S,O)₂] increases while that of *cis*-[Pt(L⁶-S,O)₂] decreases with increase in time of irradiation. However, there are certain differences which could be observed between the chromatograms of these two complexes. Firstly, the changes observed in Figure 4.18 suggest a lower relative rate of *cis/trans* isomerisation of *cis*-[Pt(L⁶-S,O)₂] compared to *cis*-[Pd(L⁶-S,O)₂]. Also, Figure 4.18 shows that additional peaks are also formed at retention times of 4 and 6 minutes by irradiating the solution of *cis*-[Pt(L⁶-S,O)₂] with a blue violet laser. Note that in Figure 4.3, these additional peaks were also formed when the same solution of *cis*-[Pt(L⁶-S,O)₂] was irradiated with a Hg UV lamp. Although these additional peaks could not be assigned, they could have resulted from the photo-decomposition of *cis*-[Pt(L⁶-S,O)₂] upon irradiation with high intensity light sources such as Hg UV lamp or the blue violet laser. The additional peaks due to photo-decomposition are absent in the chromatogram (Figure 4.10) when a solution of *cis*-[Pd(L⁶-S,O)₂] was irradiated. This suggests the relative stability of *cis*-[Pd(L⁶-S,O)₂] to photo-decomposition compared to *cis*-[Pt(L⁶-S,O)₂] upon irradiation with highly intensified light emitted from either a Hg UV lamp or a blue violet laser.

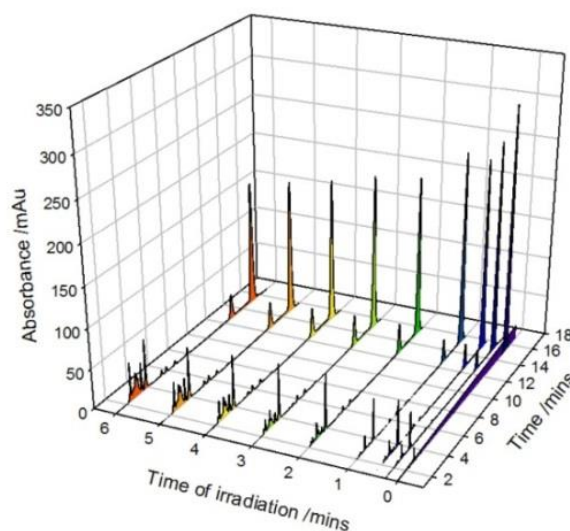


Figure 4.18. Overlaid chromatograms representing the reversed-phase HPLC separation of acetonitrile solution of *cis*-[Pt(L⁶-S,O)₂] and *trans*-[Pt(L⁶-S,O)₂] with increase in time of irradiation with blue violet laser pointer (405 nm); conditions: GEMINI C 18 ODS, mobile phase 90:10 (% v/v) acetonitrile:0.1M acetate buffer (pH 6), flow rate 1 ml min⁻¹.

Furthermore, from Figure 4.18, it can be seen that the peak areas of the photo-decomposition products formed upon irradiation of *cis*-[Pt(L⁶-S,O)₂] increases as irradiation time increases. A steady state was achieved after *ca.* 6 minutes of irradiation with K_e value of 0.182 obtained.

Hence after 6 minutes of irradiation, no further change in peak area was observed for *cis*-[Pt(L⁶-S,O)₂], *trans*-[Pt(L⁶-S,O)₂] as well as that of the photo-decomposition products.

The relative rate of reverse (*trans*→*cis*) isomerisation of *cis*-[Pt(L⁶-S,O)₂] was also estimated by irradiating an acetonitrile solution of the complex for 6 minutes using a blue violet laser and allowing the irradiated solution to stay in a dark room at 17.4 °C for different periods of time. After each time period in the dark, the solution was quickly and manually injected for HPLC analysis. Figure 4.19 shows the chromatogram for the pattern observed in the various peak areas when the solution was left in the dark and Table 7 gives the values for the change in peak areas for both the *cis* and *trans* isomers as well as the *trans/cis* peak area ratios.

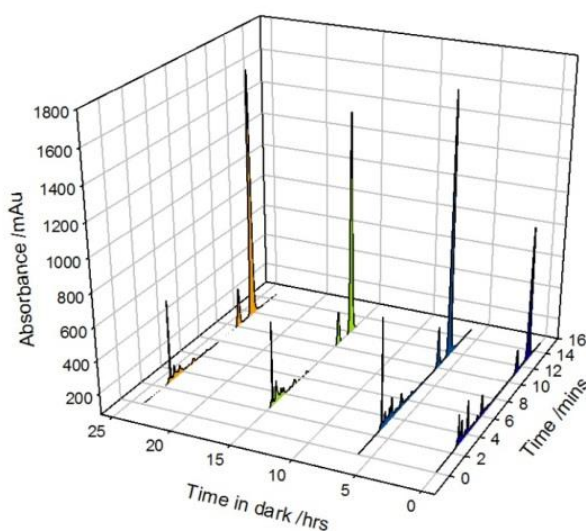


Figure 4.19. Overlaid chromatograms representing the changes in peak areas of *cis* and *trans* complexes of [Pt(L⁶-S,O)₂] when an acetonitrile solution of the *cis* complex was irradiated with a 405 nm laser and the allowed to stay in the dark at different time intervals; conditions: GEMINI C 18 ODS, mobile phase 95:5 (% v/v) acetonitrile:0.1M acetate buffer (pH 6), flow rate 1 ml min⁻¹.

After irradiating the solution of *cis*-[Pt(L⁶-S,O)₂] for 6 minutes, a steady state was achieved for the *cis* and *trans* isomers with a K_e value of 0.182 (Table 7). When the irradiated solution was allowed to stay in the dark for *ca.* 5 hours, the *trans/cis* peak area ratio decreased slightly from K_e to a value of 0.135. From Figure 4.19, it can be seen that this decrease in the *trans/cis* peak area ratio is associated with an increase in peak areas of *cis*-[Pt(L⁶-S,O)₂] and *trans*-[Pt(L⁶-S,O)₂] and a corresponding decrease in the peak areas of the photo-decomposition products formed. Hence the decrease in the *trans/cis* peak area ratio observed in Table 7 could be due to a reversible formation *cis*-[Pt(L⁶-S,O)₂] and *trans*-[Pt(L⁶-S,O)₂] from the photo-

decomposition products when the irradiated solution of cis -[Pt(L⁶-S,O)₂] was left in the dark for 5 hours. When the irradiated solution was left in the dark for a longer period of time, even after 24 hours, the value for the $trans/cis$ peak area ratio remained fairly constant. It can be seen from Figure 4.19 that after allowing the irradiated solution of cis -[Pt(L⁶-S,O)₂] in the dark for 24 hours, the additional peaks that were formed at retention time of 6 minutes almost disappeared. This could mean that at this time, almost all of the photo-decomposition products which resulted to these peaks should have reverted back to give either cis -[Pt(L⁶-S,O)₂] or $trans$ -[Pt(L⁶-S,O)₂] leading to a fairly constant value in the $trans/cis$ peak area ratios. This very small changes in the $trans/cis$ peak area ratios compared to that observed in Figure 4.14 leads to a conclusion that the relative rate of reverse ($trans \rightarrow cis$) isomerisation is much lower for [Pt(L⁶-S,O)₂] compared to [Pd(L⁶-S,O)₂].

Table 7. Table showing the changes in peak areas and relative rate of reverse isomerisation for [Pd(L⁶-S,O)₂] upon irradiation of an acetonitrile solution with a blue violet laser ($\lambda = 405$ nm).

Time/hrs	cis -[Pt(L ⁶ -S,O) ₂]	$trans$ -[Pt(L ⁶ -S,O) ₂]	$trans/cis$ ratio of peak areas
0	383.8	69.8	0.182
1	486.3	66.4	0.135
6	521.8	69.8	0.134
15	451.9	60.5	0.134
24	510.5	68.9	0.135

4.7. Conclusions

A simultaneous irradiation and determination setup was developed to estimate the extent of isomerisation of cis -[Pd(L⁶-S,O)₂] and cis -[Pt(L⁶-S,O)₂] as well as for other complexes cis -[Pd(L³-S,O)₂], cis -[Pd(L⁴-S,O)₂] and cis -[Pd(L⁵-S,O)₂], using a Hg UV lamp for irradiation. Although UV-VIS spectroscopy also led to monitoring of the $cis/trans$ isomerisation of these complexes, the changes observed were small compared to when reversed-phase HPLC was used. By determining the extent of isomerisation from $trans/cis$ peak area ratios determined from reversed-phase HPLC, the order cis -[Pd(L⁴-S,O)₂] < cis -[Pd(L⁶-S,O)₂] < cis -[Pd(L³-S,O)₂] < cis -[Pd(L⁵-S,O)₂] was obtained for the extent of $cis/trans$ isomerisation of these complexes. A remarkable difference was observed in the retention times of the cis and $trans$

isomers of $[\text{Pd}(\text{L}^3\text{-S},\text{O})_2]$ and $[\text{Pd}(\text{L}^6\text{-S},\text{O})_2]$. For $[\text{Pd}(\text{L}^3\text{-S},\text{O})_2]$, the *cis* isomer was less retained than the *trans* isomer meanwhile an opposite effect was observed for $[\text{Pd}(\text{L}^6\text{-S},\text{O})_2]$.

Alternative irradiation with a tungsten lamp or a blue violet laser pointer ($\lambda = 405 \text{ nm}$) also led to *cis/trans* isomerisation with relative rate of isomerisation determined as a function of time of irradiation using these light sources. Upon irradiation of an acetonitrile solution with a tungsten lamp and a blue violet laser pointer, *cis*- $[\text{Pd}(\text{L}^6\text{-S},\text{O})_2]$ isomerises to *trans*- $[\text{Pd}(\text{L}^6\text{-S},\text{O})_2]$, determined by the changes in peak areas for these isomers by reversed-phase HPLC. This eventually led to a steady state after 3 minutes of irradiation with a blue violet laser pointer, much lower than 20 minutes needed for the same complex to reach steady state when a tungsten lamp was used.

Using a blue violet laser pointer for irradiation, a similar relative rate of *cis*→*trans* isomerisation was observed for *cis*- $[\text{Pd}(\text{L}^3\text{-S},\text{O})_2]$ and *cis*- $[\text{Pd}(\text{L}^5\text{-S},\text{O})_2]$ but slightly higher for *cis*- $[\text{Pd}(\text{L}^5\text{-S},\text{O})_2]$, meanwhile a much lower relative rate of *cis*→*trans* isomerisation was obtained for *cis*- $[\text{Pd}(\text{L}^6\text{-S},\text{O})_2]$. In the dark, a solution of *cis*- $[\text{Pd}(\text{L}^6\text{-S},\text{O})_2]$ experiences a higher relative rate of reverse or *trans*→*cis* isomerisation compared to *cis*- $[\text{Pd}(\text{L}^3\text{-S},\text{O})_2]$.

The relative rates of both forward and reverse isomerisation of *cis*- $[\text{Pt}(\text{L}^6\text{-S},\text{O})_2]$ were found to be lower than that of *cis*- $[\text{Pd}(\text{L}^6\text{-S},\text{O})_2]$. Irradiation of the solution of *cis*- $[\text{Pt}(\text{L}^6\text{-S},\text{O})_2]$ with highly intensified light from Hg UV lamp as well as from a blue violet laser pointer resulted to photo-decomposition products which in the dark after *ca.* 24 hours reverted back to either *cis*- $[\text{Pt}(\text{L}^6\text{-S},\text{O})_2]$ or *trans*- $[\text{Pt}(\text{L}^6\text{-S},\text{O})_2]$.

4.8. Experimental section

4.8.1. General procedure

All chemicals used for synthesis and HPLC separation were purchased from Sigma Aldrich. Acetone solvent used for ligand synthesis was distilled and potassium thiocyanate was dried in a heated vacuum before use.

^1H and ^{13}C NMR spectra of ligands and complexes were recorded at 25°C in CDCl_3 solutions using Varian VNMRS 300 MHz, Varian UNITY INOVA 400 MHz or 600 MHz NMR spectrometers.

Mass spectrometry data were obtained using ESI positive in Waters Synapt G2 instrument with acetonitrile, 0.1% formic acid during injection.

Melting points were obtained using Electrothermal IA 9000 series digital melting point apparatus.

FT-IR analyses were performed on a Thermo Nicolet Avatar 330 Smart Performer ATR instrument using a ZnSe crystal.

Thin Layer Chromatography (TLC) was carried out using silica plates in dichloromethane/hexane mixtures of varying compositions and visualisation was performed using a UV lamp.

Reversed-phase chromatographic analysis was done using two systems: an Agilent system with Quat pump equipped with automatic sampling meanwhile subsequent analysis were performed with a Varian Polaris system equipped with a 20 μl sampling loop. A GEMINI C₁₈ 150 x 4.6 mm, 5 μm column was used at all times with photometric detection at 262 nm using a UV150 Photo-diode array (PDA) detector. The mobile phase composition was adjusted at various times using an acetonitrile:acetate buffer (pH 6) mixture and an isocratic flow rate of 1 ml min⁻¹ and 20 μl sample injection volume were used at all times. Only de-ionised water and HPLC grade acetonitrile filtered through a 0.45 μm was used to make up the mobile phase.

4.8.2. Preparation of acetate buffer for HPLC separation

Acetate buffer of pH 6 was prepared by mixing 25 ml of 0.1M acetic acid and 475 ml of 0.1M sodium acetate solutions, making up a total volume of 500 ml. All solutions were made up with de-ionised water and the resulting buffer solution was filtered through a 0.45 μm pore size filter.

CHAPTER V

Conclusions, proposed isomerisation mechanism and future work

5.1. Discussions and proposed mechanism of *cis/trans* isomerisation

From the results, it has been shown that *N,N*-diethyl-*N'*-benzoylthiourea (**HL**³) co-ordinates to Pt(II), Pd(II), Rh(III), Ru(III) and Ir(III) resulting to complexes which can be well separated in a 85:15 (% v/v) methanol:acetate buffer mixture by reversed-phase HPLC. The small difference in retention times of *cis*-[Pd(L³-S,O)₂] and *cis*-[Pt(L³-S,O)₂] as well as for [Rh(L³-S,O)₃] and [Ir(L³-S,O)₃] leading to overlap of peaks and poor separation in some cases illustrates the isostructural similarity between the two complexes in both cases.

A series of *cis*-[Pd(Lⁿ-S,O)₂] complexes with different ligands were also well separated by reversed-phase HPLC. The different retention times of the complexes are as a result of difference in polarity as different groups are attached to the ligands. Hence *cis*-[Pd(L⁶-S,O)₂] with 3 electron-donating methoxy groups attached to the ligand was found to have a lower retention time whereas *cis*-[Pd(L⁷-S,O)₂] having an electron-withdrawing chloro substituent was more retained during separation. The electron-donating methoxy groups could have thus resulted in an increase in polarity in *cis*-[Pd(L⁶-S,O)₂] whereas the electron-withdrawing chloro substituents could have decrease the polarity in *cis*-[Pd(L⁷-S,O)₂].

The square planar *cis*-[M(Lⁿ-S,O)₂] (M = Pd(II), Pt(II)) complexes were found to undergo *cis/trans* isomerisation upon absorption of light emitted from a Hg UV lamp, a tungsten lamp and a blue violet laser pointer. The absorption bands from these complexes upon light absorption could have resulted from electronic transitions from ground states to MLCT excited states. The excited states could be singlet (¹MLCT) or triplet (³MLCT) in character

but absorption could occur mainly to the $^1\text{MCLT}$ states. The energy difference between the MLCT states and the ground states could therefore depend on the nature of the metal center and the co-ordinating ligand bound to the metal. This difference in energy could be used to explain the different extent and relative rates of isomerisation observed for the $\text{cis-}[\text{Pd}(\text{L}^3\text{-S},\text{O})_2]$, $\text{cis-}[\text{Pd}(\text{L}^5\text{-S},\text{O})_2]$, $\text{cis-}[\text{Pd}(\text{L}^6\text{-S},\text{O})_2]$ and $\text{cis-}[\text{Pt}(\text{L}^6\text{-S},\text{O})_2]$ complexes. For $\text{cis-}[\text{Pd}(\text{L}^6\text{-S},\text{O})_2]$, $\text{cis-}[\text{Pt}(\text{L}^6\text{-S},\text{O})_2]$ and $\text{cis-}[\text{Pd}(\text{L}^5\text{-S},\text{O})_2]$, the presence of electron-donating methoxy groups on the ligands increased the polarity of the *trans* complexes and as a result, these were less retained onto the HPLC column compared to their respective *cis* complexes.

The relatively lower rate of $\text{cis}\rightarrow\text{trans}$ isomerisation for $\text{cis-}[\text{Pd}(\text{L}^6\text{-S},\text{O})_2]$ is due to the presence of electron-donating methoxy groups on the aryl moiety of the ligands. The presence of these groups could possibly stabilise the complex by increasing the energy gap between the ground state and the excited state, thereby decreasing the relative rate of *cis/trans* isomerisation. This also could have resulted in a comparatively small difference in the wavelength at maximum absorbance (2 nm) measured using the diode array photometric detector between the $\text{cis-}[\text{Pd}(\text{L}^6\text{-S},\text{O})_2]$ and $\text{trans-}[\text{Pd}(\text{L}^6\text{-S},\text{O})_2]$ isomers. A similar relative rate of $\text{cis}\rightarrow\text{trans}$ isomerisation was obtained for $\text{cis-}[\text{Pd}(\text{L}^3\text{-S},\text{O})_2]$ and $\text{cis-}[\text{Pd}(\text{L}^5\text{-S},\text{O})_2]$ suggesting that the energy gaps between the ground and excited states are similar for transitions leading to *cis/trans* isomerisation to occur. The similar difference in wavelength (13 nm) at maximum absorbance for the *cis* and *trans* isomers of these two complexes further confirms their similar relative rates as well as extent of isomerisation.

When irradiated solutions of $\text{cis-}[\text{Pd}(\text{L}^3\text{-S},\text{O})_2]$ and $\text{cis-}[\text{Pd}(\text{L}^6\text{-S},\text{O})_2]$ were left in a dark room, a reverse ($\text{trans}\rightarrow\text{cis}$) isomerisation occurred for both complexes but at different relative rates. This *trans* to *cis* isomerisation in the dark could possibly involve deactivation from excited MLCT states by different pathways which could be radiative or non radiative. A relatively higher rate of reverse ($\text{trans}\rightarrow\text{cis}$) isomerisation was determined for $\text{cis-}[\text{Pd}(\text{L}^6\text{-S},\text{O})_2]$ compared to $\text{cis-}[\text{Pd}(\text{L}^3\text{-S},\text{O})_2]$. This could have resulted from a destabilising effect on the MLCT state relative to the other states for deactivation to occur, caused by the presence of the three electron-donating methoxy groups on $\text{cis-}[\text{Pd}(\text{L}^6\text{-S},\text{O})_2]$. In the absence of these electron-donating groups in $\text{cis-}[\text{Pd}(\text{L}^3\text{-S},\text{O})_2]$, a much lower rate of *trans* to *cis* isomerisation was obtained suggesting that a longer time was needed for deactivation from MLCT states to occur, which could lead to a different pathway from that of $\text{cis-}[\text{Pd}(\text{L}^6\text{-S},\text{O})_2]$.

The fact that the presence of electron-donating groups have been shown to decrease the relative rate of *cis*→*trans* isomerisation could provide an insight on a possible mechanism by which the *cis/trans* isomerisation occurs. In such *cis*-[M(Lⁿ-S,O)₂] complexes, the metal center is co-ordinated to the ligands through the sulfur and oxygen atoms. Excitation upon light absorption could possibly lead to weakening of either the M-O or M-S bonds. The groups directly attached to these bonds could play a role in affecting the strength of these bonds and consequently the overall stability to light and relative rates of *cis/trans* isomerisation of the complexes involved. Since the presence of three electron-donating methoxy groups decreased the rate of *cis*→*trans* isomerisation, it suggests that the methoxy groups have a stabilising effect on the metal center and this should be associated with strengthening of the M-O bond if determined. This leads to a suggestion that that the *cis/trans* isomerisation could partly occur by an intramolecular mechanism involving both M-O bond breaking and a subsequent M-O bond forming.

Preliminary studies using ¹H NMR spectroscopy showed that in chloroform, *cis/trans* isomerisation of *cis*-[Pd(L⁶-S,O)₂] did not take place when a solution of the complex was irradiated with a blue violet laser. This also suggests that the *cis/trans* isomerisation reactions are solvent dependent, that is, the energy of the MLCT state could also be affected by the solvent polarity which could change the dipole moment of the complex. Since the solvents could play a role in the *cis/trans* isomerisation, the mechanism by which they occur could also involve an intermolecular pathway in which the solvent is co-ordinated to the metal center by association, after which a subsequent dissociation of the solvent molecule could occur leading to the *trans* complexes. With these suggestions, the mechanism illustrated in Figure 5.1 is postulated for the *cis/trans* isomerisation of the *cis*-[M(Lⁿ-S,O)₂] complexes in acetonitrile when irradiated.

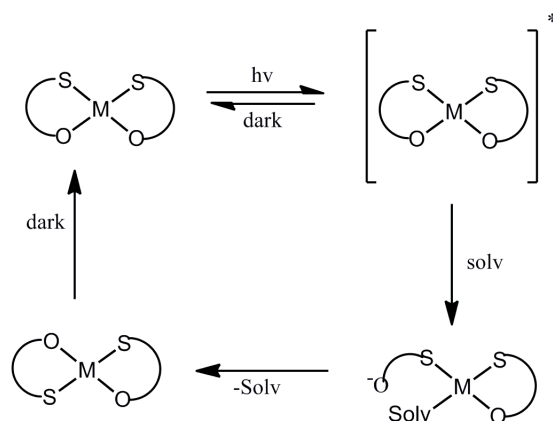


Figure 5.1. Proposed Mechanism for the photo-induced isomerisation of cis - $[M(L^n-S,O)_2]$ complexes in acetonitrile, Solv = solvent.

5.2. General conclusion

The complexes cis - $[Pd(L^3-S,O)_2]$, cis - $[Pt(L^3-S,O)_2]$, fac - $[Rh(L^3-S,O)_3]$, $[Ru(L^3-S,O)_3]$ and $[Ir(L^3-S,O)_3]$ were successfully synthesised. Characterisation of the $[Ru(L^3-S,O)_3]$ and $[Ir(L^3-S,O)_3]$ were mainly done by positive Electrospray Ionisation Mass spectrometry due to the paramagnetic nature of these complexes. A modified synthetic procedure for $[Ru(L^3-S,O)_3]$ led to higher reaction yields and N,N -diethyl- N' -benzoylthiourea (**HL**³) was found to form more stable complexes with Ru(III) which could easily be isolated compared to the N,N -dialkyl- N' -acylthioureas (**HL**¹ and **HL**²) used.

The use of reversed-phase HPLC led to the separation of cis - $[Pd(L^3-S,O)_2]$, cis - $[Pt(L^3-S,O)_2]$, fac - $[Rh(L^3-S,O)_3]$ and $[Ru(L^3-S,O)_3]$ while the relatively unstable $[Ir(L^3-S,O)_3]$ which was closely retained to fac - $[Rh(L^3-S,O)_3]$ gave rise to other unassigned peaks. The effects of methanol and acetonitrile solvents on separation were investigated and it was found that a methanol/acetate buffer (pH 6) mixture was more suitable for separation of all five metal complexes. With the pure complexes separated, a salt-induced sample preparation method was also found to be suitable for pre-concentration of cis - $[Pt(L^3-S,O)_2]$, cis - $[Pd(L^3-S,O)_2]$, fac - $[Rh(L^3-S,O)_3]$ and $[Ru(L^3-S,O)_3]$ in aqueous solutions prior to their separation by reversed-phase HPLC. A series of cis - $[Pd(L^n-S,O)_2]$ complexes with different ligands were also synthesised and well separated by reversed-phase HPLC, with electron-donating methoxy group decreasing the retention time of cis - $[Pd(L^6-S,O)_2]$ compared to cis - $[Pd(L^7-S,O)_2]$ with electron-withdrawing chloro substituents in the ligands.

A series of photo-active *cis*-[M(Lⁿ-S,O)₂] (M =Pt(II), Pd(II)) complexes with a variety of *N,N*-dialkyl-*N'*-acyl(aroyl)thioureas were also synthesised and their relative rates of *cis*→*trans* isomerisation determined. Although reversed-phase HPLC and UV-VIS spectroscopy were used to monitor the *cis/trans* isomerisation, the latter technique was found to be less suitable for monitoring the isomerisation process as relatively very small changes in absorbance were obtained. With reversed-phase HPLC determination and upon irradiation of acetonitrile solutions of the complexes with a Hg UV lamp, a tungsten lamp as well as a blue violet laser pointer, the relative rates of isomerisation for the complexes were found to depend on the nature of the ligands.

The relative rates of forward *cis/trans* isomerisation of the *cis*-[M(Lⁿ-S,O)₂] complexes were obtained by determining the *trans/cis* peak area ratio at every time of irradiation. Similar relative rates of forward isomerisation were obtained for *cis*-[Pd(L³-S,O)₂] and *cis*-[Pd(L⁵-S,O)₂] but slightly higher for *cis*-[Pd(L⁵-S,O)₂] with similar K_e values (*ca.* 1.4) obtained for these complexes at steady states upon irradiation with a blue violet laser pointer. Compared to these two complexes, a much lower relative rate of *cis*→*trans* isomerisation was obtained for *cis*-[Pd(L⁶-S,O)₂] with a lower K_e value (0.31) obtained. Other differences in the separation *cis*-[Pd(L⁶-S,O)₂] included the lower retention time of the *trans* isomer compared to that of the *cis*, and also a small difference in wavelength (2 nm) at maximum absorbance between the *cis* and *trans* isomers. A much relatively higher rate of reverse (*trans*→*cis*) isomerisation was obtained for *cis*-[Pd(L⁶-S,O)₂] with the *trans* isomer needing *ca.* 4 minutes to completely revert back to the *cis* complex. The relative rate of reverse isomerisation for *cis*-[Pd(L³-S,O)₂] was however much lower compared to that of *cis*-[Pd(L⁶-S,O)₂] as up to 8 hours of time after which the irradiated solution was allowed in the dark was needed for the *trans*→*cis* process to be completed.

A lower relative rate of both forward and reverse *cis/trans* isomerisation was obtained for *cis*-[Pt(L⁶-S,O)₂] compared to *cis*-[Pd(L⁶-S,O)₂], illustrating the effect of metal center on the relative rate of *cis/trans* isomerisation. The relatively lower rate of forward isomerisation for *cis*-[Pt(L⁶-S,O)₂] which was attributed to the lower kinetic lability of this complex to *cis/trans* isomerisation also produced certain unassigned photo-decomposition products formed from the highly intensified light sources used. These photo-decomposition products slowly reverted back to either *cis*-[Pt(L⁶-S,O)₂] or *trans*-[Pt(L⁶-S,O)₂], leading to a much lower relative rate for the reverse isomerisation and hence an apparently no change in the *trans/cis* peak area

ratio was obtained even when an irradiated solution of the complex was allowed to stay in a dark room for 24 hours.

5.3. Future work

Since it was possible during this study to use reversed-phase HPLC for separation of *cis*-[Pd(L³-S,O)₂], *cis*-[Pt(L³-S,O)₂], *fac*-[Rh(L³-S,O)₃], [Ru(L³-S,O)₃], [Ir(L³-S,O)₃] as well as *cis* and *trans* isomers of [M(Lⁿ-S,O)₂] (M = Pt(II), Pd(II)) complexes, a possible area for further investigation would be to extend this study to the possible photo-induced isomerisation of *fac*-[M(Lⁿ-S,O)₃] (M = Rh(III)/Ru(III)) and separation by reversed-phase HPLC. Oxidative addition of the *cis*-[M(Lⁿ-S,O)₂] complexes have been reported previously to yield octahedral complexes of the form [M(Lⁿ-S,O)₂X₂] (X = halogen) in the presence of halogens.²⁹ Hence reversed-phase HPLC separation could also in the future be extended to such octahedral Pt(IV) or Pd(IV) complexes with a possible photo-induced isomerisation of the complexes .

Also, a proper setup consisting of irradiation and subsequent determination using ¹H NMR spectroscopy would also be possible not only for monitoring the *cis/trans* isomerisation of the *cis*-[M(Lⁿ-S,O)₂] complexes but also to determine absolute rate constants for both the forward and reverse isomerisation which have only been done qualitatively in this study.

Furthermore, the properties investigated so far in this study such as the relative photo-stability of the *cis*-[M(Lⁿ-S,O)₂] complexes and associated ligand effect are basis for the design of molecular switches and photo-catalysts. Since the reverse isomerisation of the *trans*-[M(Lⁿ-S,O)₂] complexes is thermally induced, which is one of the requirements for application as photochromic materials, this study could be extended in future to a possible use of the photo-switchable *cis*-[M(Lⁿ-S,O)₂] complexes as molecular switches.

Finally, this study has shown the promise for the possible design of a new class of [M(Lⁿ-S,O)₂] metal complexes such that the ligand structure could be tuned to obtain a color change upon irradiation, a property which could be useful for several photochemical applications.

References

1. G. G. Robson, "Platinum 1986", *Johnson Matthey plc*, 1986.
2. Johnson Matthey, www.matthey.com.
3. J. L. Grem, B. A. Chabner, J. M. Collins, *Cancer Chemotherapy, Principles and Practice*, 1990, 180.
4. Frank R. Hartley, *Chemistry of the Platinum Group Metals Recent developments*, Elsevier Science Publishers B.V. Amsterdam, 1991.
5. R. J. Kriek, W. J. Engelbrecht, J. J. Cruywagen, *J. S. Afr. Inst. Min. Metall.*, 1995, 75.
6. Neucki K., *Ber. Dtsch. Chem. Ges.*, 1873, **6**, 598.
7. A. Rodenstein, R. Ritcher and R. Kirmse, *Z. Anorg. Allg. Chem.*, 2007, **633**, 1713.
8. J. Imrich, T. Busova, P. Kristrian and J. Dzara, *Chem. Pap.*, 1994, **48**, 42.
9. L. Beyer, E. Hoyer, H. Hartman and J. Liebscher, *Z. Chem.*, 1981, **21**, 81.
10. K. R., Koch, S. A. Bourne, J. Miller, A. N. Mautjana, A. N. Westra, *Dalton Trans.*, 2003, 1952.
11. L. Beyer, R. Richter, and O. Seidelmann, *J. Prakt. Chem./Chem.-Ztg.*, 1999, **341**, 704.
12. M. Reinel, R. Richter and R. Kirmse, *Z. Anorg. Allg. Chem.*, 2002, **628**, 41.
13. R. Flores-Centurion, R. Ritcher, J. Angulo-Comejo and L. Beyer, *Bol. Soc. Quim. Peru*, 1999, **65**, 211.
14. R. Richter, f. Dietze, S. Schmidt, E. Hoyer, W. Poll and D. Mootz, *Z. Anorg. Allg. Chem.*, 1997, **623**, 135.
15. R. Richter, J. Sieler, L. Beyer, O. Lindqvist and L. Andersen, *Z. Anorg. Allg. Chem.*, 1985, **522**, 171.
16. R. del Campo, J. J. Criado, E. Garcia, E. Rodriguez-Fernandez and F. Sanz, *J. Inorg. Biochem.*, 2002, **89**, 74.
17. H. Perez, R. S. Correa, B. O'Reilly, A. M. Plutin, C. P. Silva and Y. P. Mascarenhas, *J. Struct. Chem.*, 2012, **53**, 921.
18. W. Hernandez, E. Spodine, L. Beyer, W. Schroder, R. Richter, J. Ferreira and M. Pavani, *Bioinorganic Chemistry and Applications*, 2005, **3**, 3.
19. S. Sieler, R. Richter, E. Hoyer, L. Beyer, O. Lindqvist, L. Andersen, *Z. Anorg. Allg. Chem.*, 1990, **580**, 167.
20. Schuster M. and Unterreitmaier E., *Fres. J. Anal. Chem.*, 1993, **346**, 630.
21. K. H. Konig, M. Schuster, B. Steinbrech, G. Schneeweis and R. Sclodder, *Fresenius Z. Anal. Chem.*, 1985, **321**, 457.

22. B. H. Abdullah and M. S. Yousif, *Orient. J. Chem.*, 2010, **26**, 763.
23. K. R. Koch, *Coord. Chem. Rev.*, 2001, **216**, 473.
24. K. R. Koch, C. Sacht, T. Grimmbacher, S. Bourne, *S. Afr. J. Chem.*, 1995, **48**, 71.
25. A. Dago, Yu Shepelev, F. Fajardo, F. Alvarez, R. Pomes, *Acta. Crystallogr.*, Sect. C **45**, 1989, 1192.
26. K. R. Koch, Y. Wang and A. Coetzee, *J. Chem. Soc. Dalton Trans.*, 1999, 1013.
27. K. R. Koch, C. Sacht, S. Bourne, *Inorg. Chim. Acta.*, 1995, **232**, 109.
28. K. R. Koch, T. Grimmbacher, C. Sacht, *Polyhedron*, 1998, **17**, 267.
29. A. N. Westra, S. Bourne, C. Esterhuysen and K. R. Koch, *Dalton Trans.*, 2005, 2162.
30. V. R. Meyer, *Practical High-Performance Liquid Chromatography, Fourth Edition*, Wiley, New York, 2005.
31. I.P. Alimarin, V. M. Ivanov, T. A. Bol'shova and E. M. Basova, *Fres. Z. Anal. Chem.*, 1989, **335**, 63.
32. L. Qi-ping, W. Yuan-Chao, C. Jie-Ke, *Anal. Sci.*, 1993, **9**, 523.
33. H. Quifen, X. Yang, Z. Huang, J. Cheng, Y. Guanyu, *J. Chromatogr. A*, 2005, 1094, 77.
34. X. Dong, Y. Han, H. Quifen, J. Cheng, Y. Guangyu, *J. Braz. Chem. Soc.*, 2006, **1**, 190.
35. L. Wuping and L. Qiping, *Fresenius J. Anal. Chem.*, 1994, **350**, 671.
36. H. S. Zhang, Y. W. Mou and J. K. Cheng, *Talanta*, 1994, **41**, 1459.
37. J. M. Sanchez, O. Obrezkov and V. Salvado, *J. Chromatogr. A* **871**, 2000, 217.
38. I. P. Alimarin, E. M. Basova, T. A. Bol'shova, V. M. Ivanov, *J. Anal. Chem.*, 1986, **41**, 1.
39. T. A. Bol'shova, P. N. Nesterenko, E. M. Basova, V. M. Ivanov and N. B. Morozova, *Zh. Anal. Khim.*, 1987, **42**, 1648.
40. E. M. Basova, T. A. Bol'shova, V. M. Ivanov, and N. B. Morozova, *Zh. Anal. Khim.*, 1988, **44**, 680.
41. Q. Liu, H. Zhang and J. Cheng, *Talanta*, 1991, **38**, 669.
42. P. Jones, and G. Schwedt, *Anal. Chim. Acta*, 1989, **220**, 195.
43. P.-H. Van Wyk, W. J. Gerber, K. R. Koch, *J. Anal. At. Spectrom.*, 2012, **27**, 577.
44. G. K. Anderson, R. J. Cross, *J. Chem. Soc. Rev.*, 1980, **9**, 185.
45. C. R. Barone, C. Coletti, R. J. McQuitty, N. J. Farrer, G. Lorusso, L. Maresca, A. Marrone, G. Natile, C. Pacifico, S. Parsons, R. Nazzareno, P. J. Sadler, and F. J. White, *Dalton Trans.*, 2013, **42**, 6840.

46. A. Gavriluta, G. E. Buchel, L. Freitag, G. Novitchi, J. B. Tommasino, E. Jeanneau, P.-S. Kuhn, L. Gonzalez, V. B. Arion, and D. Luneau, *Inorg. Chem.*, 2013, **52**, 6260.
47. P. Wang, H. K. Lee, *J. Chromatogr. A*, 1997, **789**, 437.
48. K. Yamaguchi, S. Kume, K. Namiki, M. Murata, N. Tamai, H. Nishihara, *Inorg. Chem.*, 2005, **44**, 9056.
49. R. J. Goodfellow, J. G. Evans, P. L. Goggin, and D. A. Duddell, *J. Chem. Soc. (A)*, 1968, 1604.
50. J. Chatt, and R. G. Wilkins, *J. Chem. Soc.*, 1952, 273.
51. J. Chatt, and R. G. Wilkins, *J. Chem. Soc.*, 1953, 70.
52. E. Turner, N. Bakken, and L. Jian, *Inorg. Chem.*, 2013, **52**, 7344.
53. B. L. Porter, B. A. McClure, E. R. Abrams, J. T. Engle, C. J. Ziegler, J. J. Rack, J. *Photochem. Photobiol.*, 2011, **217**, 341.
54. M. Sumitani, N. Nakashima, and K. Yoshihara, *Chem. Phys. Letters*, 1979, **68**, 255.
55. T. J. Meyer, *Pure & Appl. Chem.*, 1986, **58**, 1193.
56. K. R. Koch, J. du Toit, M. R. Caira and S. Sacht, *J. Chem. Soc., Dalton Trans.*, 1994, 785.
57. F. H. Allen, *Acta Crystallogr., Sect. B*, 2002, **58**, 380-388 CSC Version 5.25 updates (Jul 2004).
58. D. Hanekom, J. M. McKenzie, N. M. Derix and K. R. Koch, *Chem. Commun.*, 2005, 767.
59. F. Scandola, O. Traverso, V. Balzani, G. L. Zucchini, and V. Carassiti, *Inorg. Chim. Acta.*, 1967, 1.
60. V. Balzani, and V. Carassiti, *J. Phys. Chem.*, 1968, **72**, 383.
61. V. Balzani, V. Carassiti, L. Moggi, and F. Scandola, *Inorg. Chem.*, 1965, **4**, 1243.
62. V. Anbalagan, T. S. Srivastava, *J. Photochem. Photobiol. A. Chem.*, 1995, **89**, 113.
63. M. Bronislaw and E. Gonzalo, *J. Photochem. Photobiol.*, 1990, **52**, 1.
64. B. Durham, S. R. Wilson, D. J. Hodgson, T. J. Meyer, *J. Am. Chem. Soc.*, 180, **102**, 600.
65. R. W. Callahan, G. M. Brown, T. J. Meyer, *J. Am. Chem. Soc.*, 1974, 96, 7829.
66. D. A. Redfield and J. H. Nelson, *Inorg. Chem.*, 1973, 12, 15.
67. C. A. Tolman, *Chem. Rev.*, 1977, **77**, 313.
68. B. Centinkaya, E. Centinkaya, and M. F. Lappert, *J. C. S. Dalton*, 1973, 906.
69. J. Chatt and B. L. Shaw, *J. Chem. Soc.*, 1959, 705.
70. F. R. Hartley, *Chem. Soc. Rev.*, 1973, **2**, 63.

71. H. D. K. Drew and G. H. Wyatt, *J. Chem. Soc.*, 1934, 56.
72. D. G. Cooper and J. Powell, *Can. J. Chem.*, 1973, **51**, 1634.
73. W. J. Louw, *J. S. C. Chem. Comm.*, 1974, 353.
74. J. Powell and D. G. Cooper, *J. S. C. Chem. Comm.*, 1974, 749.
75. W. J. Louw, *Inorg. Chem.*, 1977, **16**, 2147.
76. L. Cattalini, and M. Martelli, *J. Am. Chem. Soc.*, 1969, **91**, 312.
77. C. R. Bock, E. A. Koerner, *Advances in Photochemistry, Interscience, New York*, 1974, 221.
78. I. B. Douglass and F. B. Dains, *J. Am. Chem. Soc.*, 1934, **56**, 719.
79. F. A. Cotton and G. Wilkinson, *Advanced Inorganic Chemistry 5th Edition*, John Wiley and Sons, New York, 1988.
80. S. A. Cotton, *Chemistry of Precious Metals 1st Edition*, Chapman and Hall, London, 1997.
81. K. R. Koch, A. Irving and M. Matoetoe, *Inorg. Chim. Acta.*, 1993, **206**, 193.
82. R. C. Gurira and P. W. Carr, *J. Chrom. Soc. Sc.*, 1982, **20**, 461.
83. B. J. Mueller, and R. J. Lovett, *Anal. Chem.*, 1985, **57**, 2693.
84. B. J. Mueller and R. J. Lovett, *Anal. Chem.*, 1987, **59**, 1405.
85. U. Megerle, R. Lechner, B. Konig, E. Riedle, *Photochem. Photobiol. Sci.*, 2010, **9**, 1400.

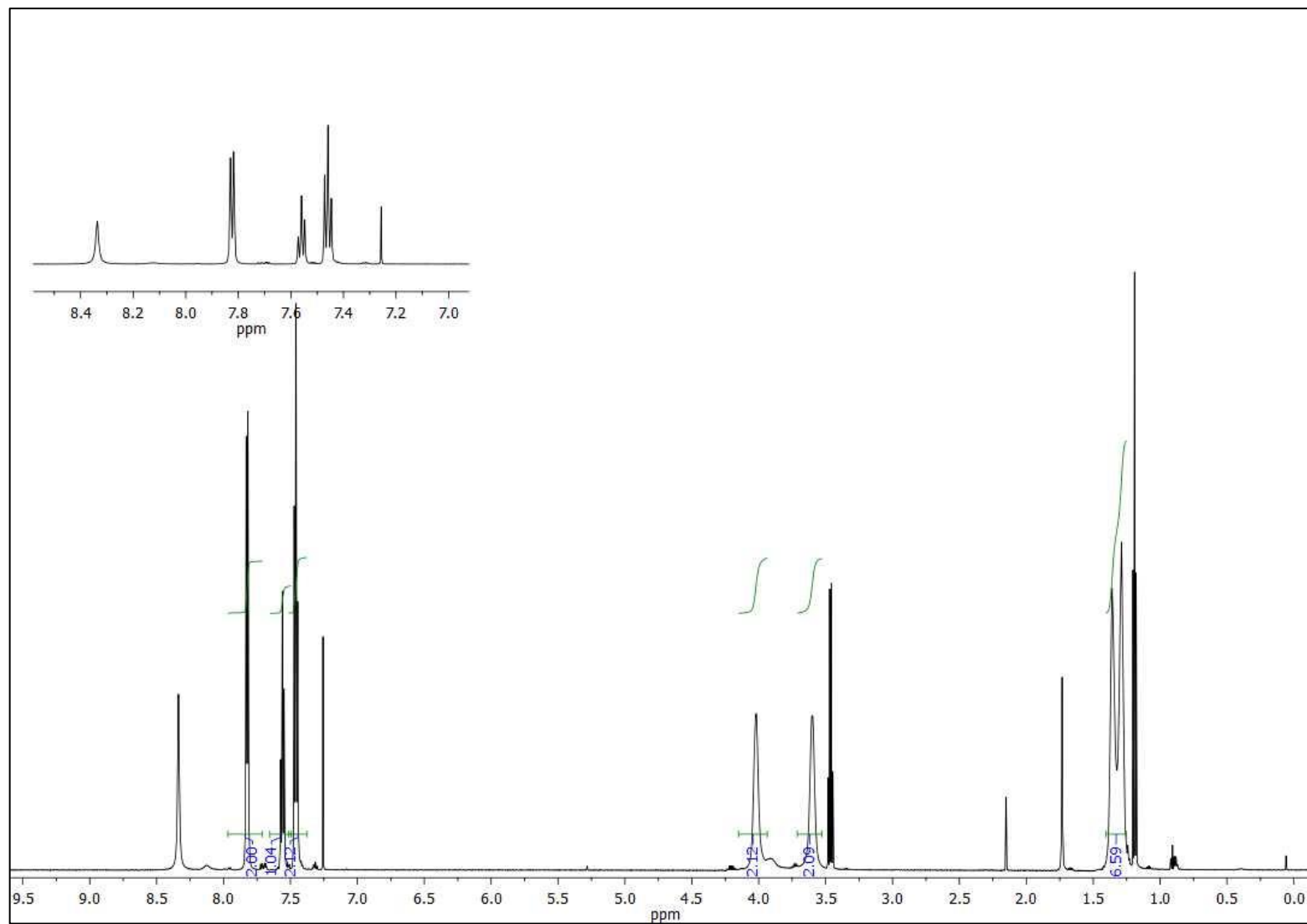


Figure 1 (Appendix). ^1H NMR spectrum of *N,N*-diethyl-*N'*-benzylthiourea (HL^3) in CDCl_3 and at 25°C .

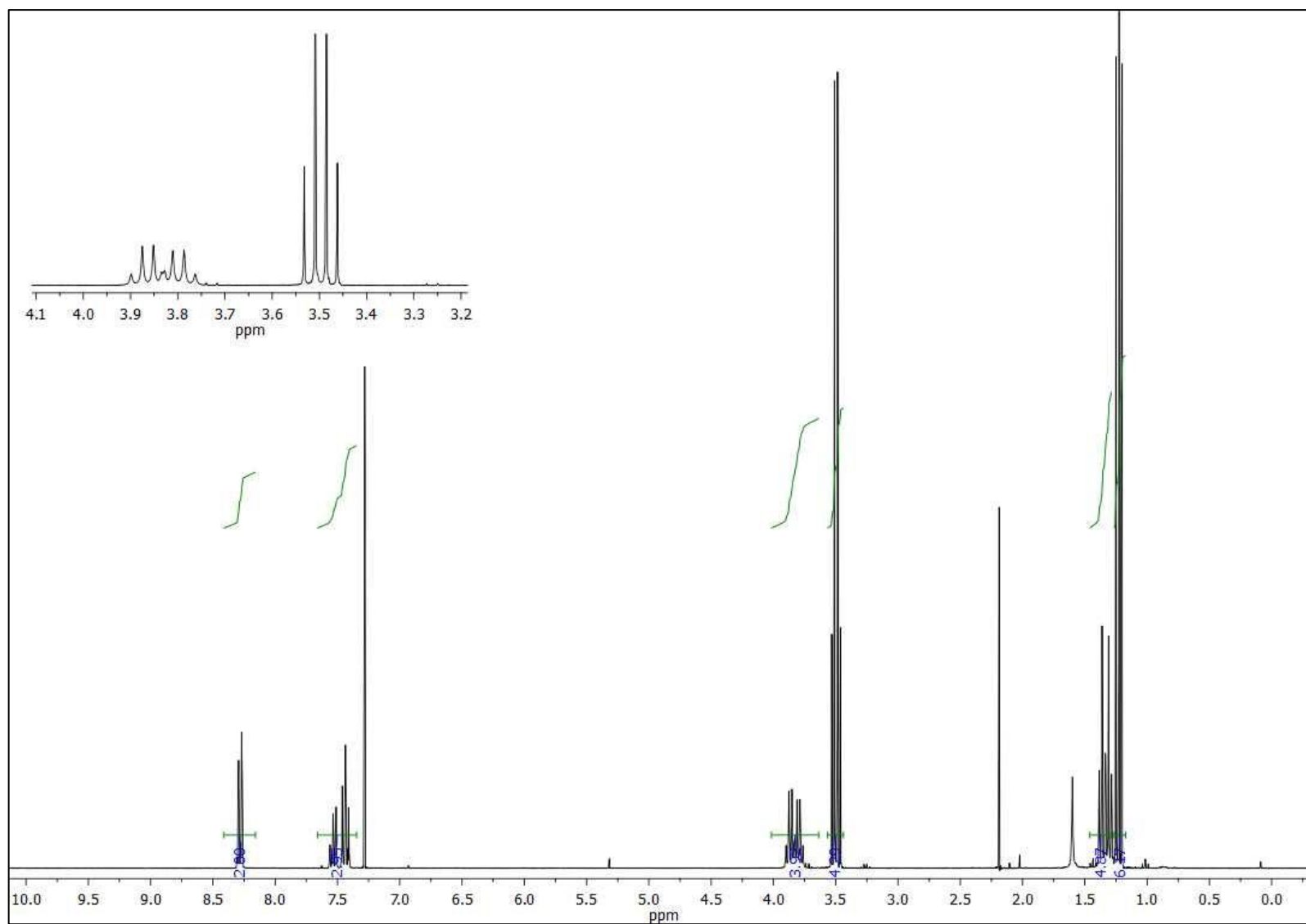


Figure 2 (Appendix). ^1H NMR spectrum of bis(*N,N*-diethyl-*N'*-benzoylthioureato)palladium(II) in CDCl_3 and at 25°C .

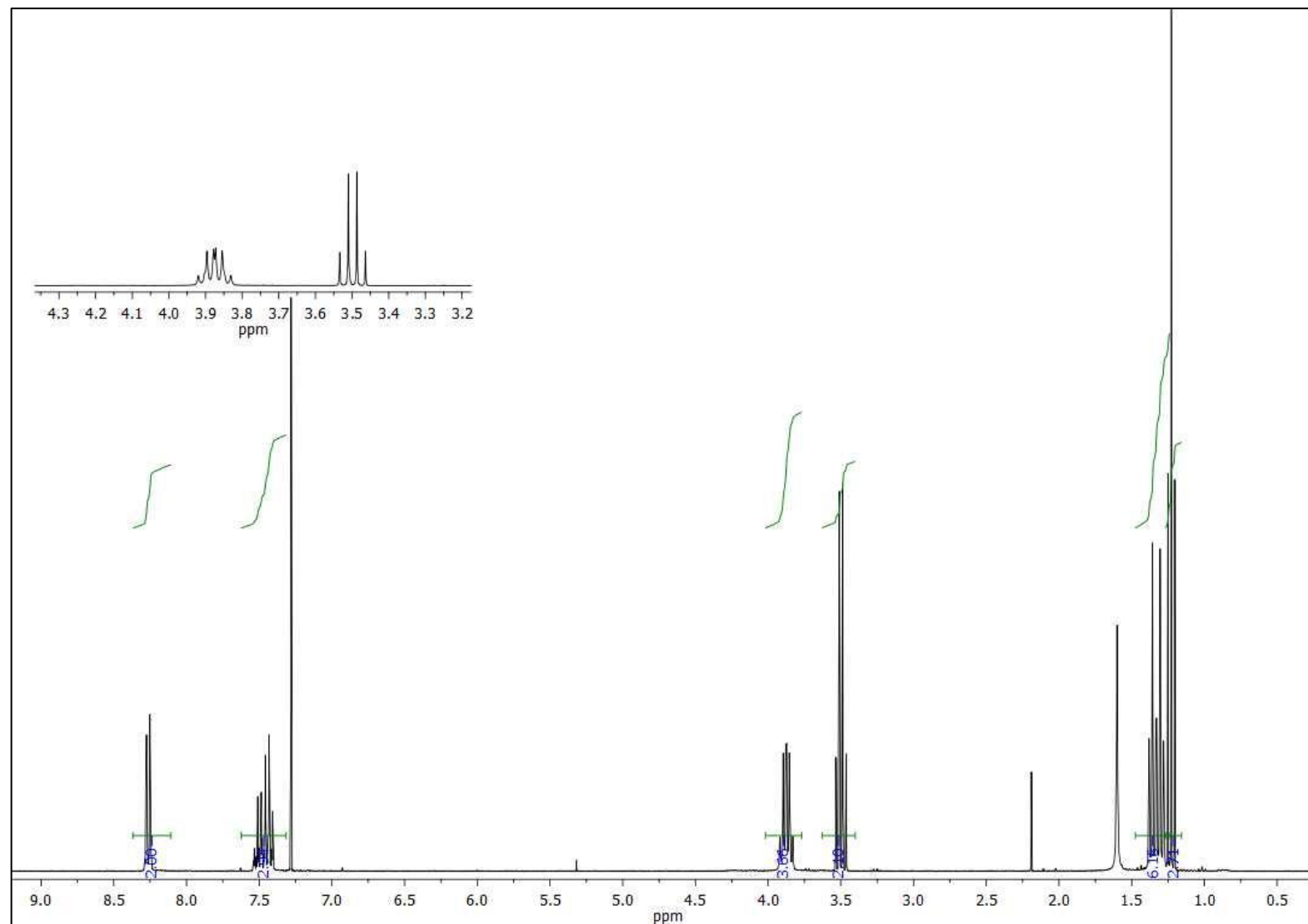


Figure 3 (Appendix). ^1H NMR spectrum of bis(*N,N*-diethyl-*N'*-benzoylthioureato)platinum(II) in CDCl_3 and at 25°C .

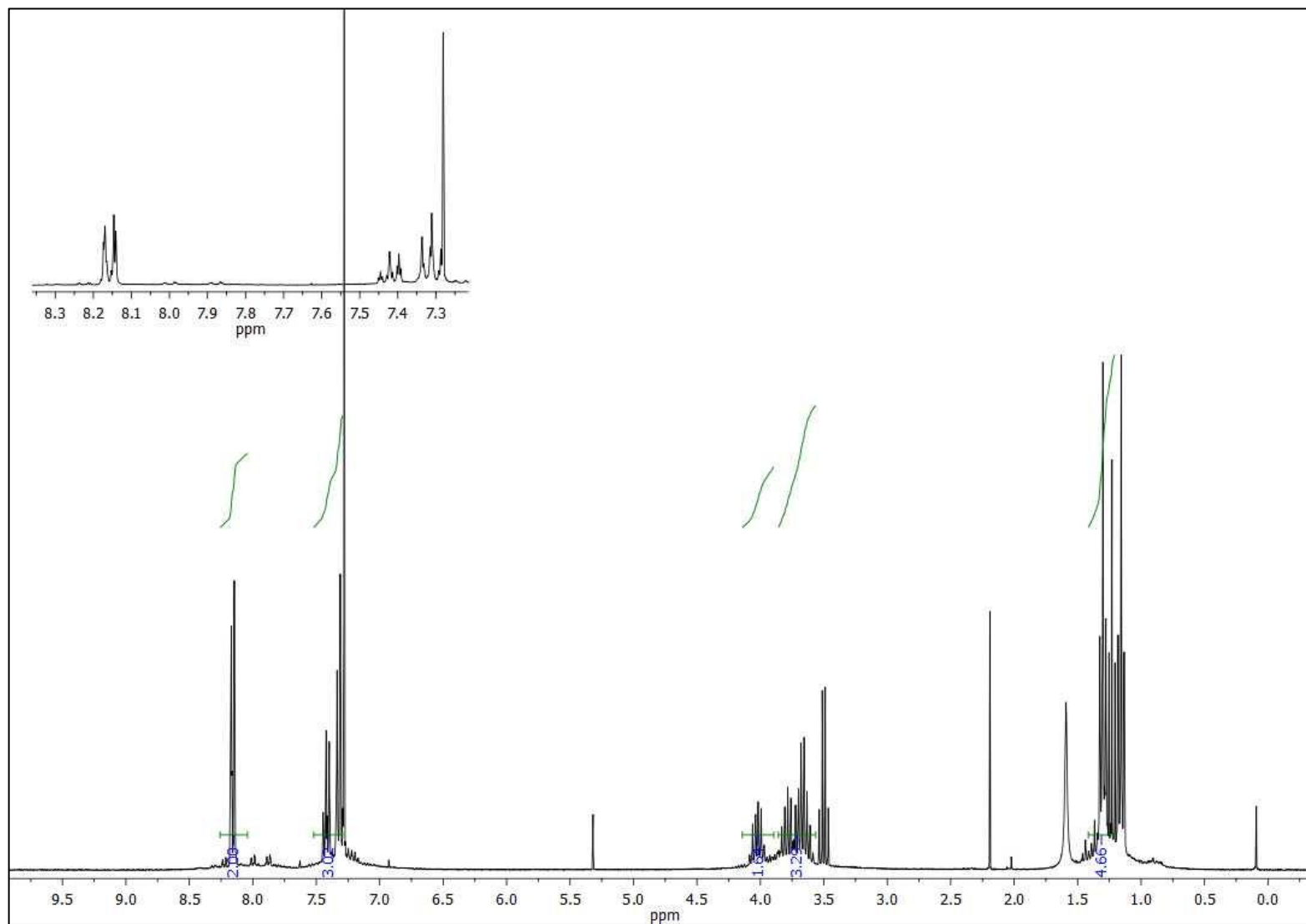


Figure 4 (Appendix). ^1H NMR spectrum of tris(*N,N*-diethyl-*N'*-benzoylthioureato)rhodium(III) in CDCl_3 and at 25°C .

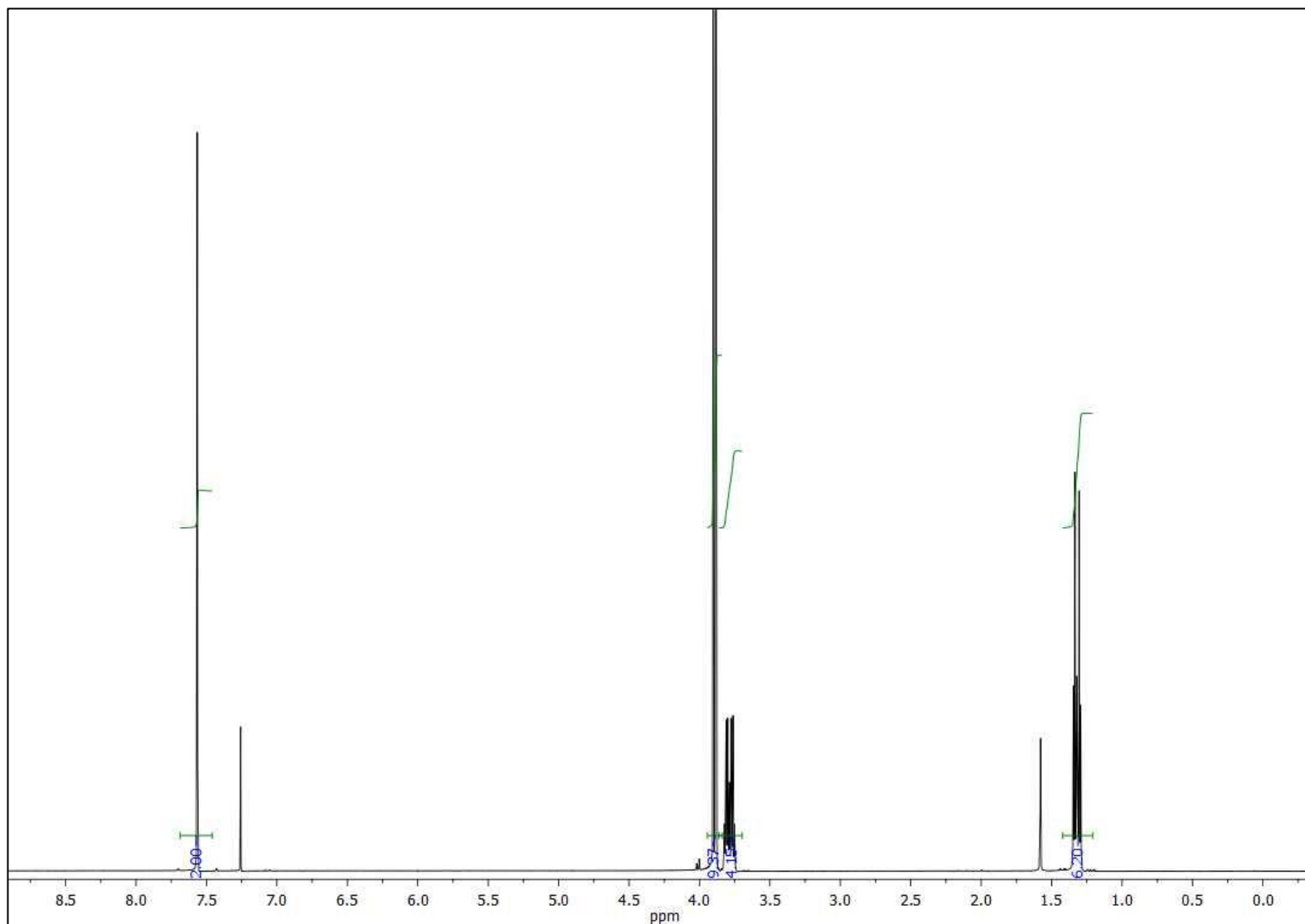


Figure 5 (Appendix). ^1H NMR spectrum of bis(*N,N*-diethyl-*N'*-3,4,5-trimethoxybenzoylthioureato)platinum(II) in CDCl_3 and at 25°C .

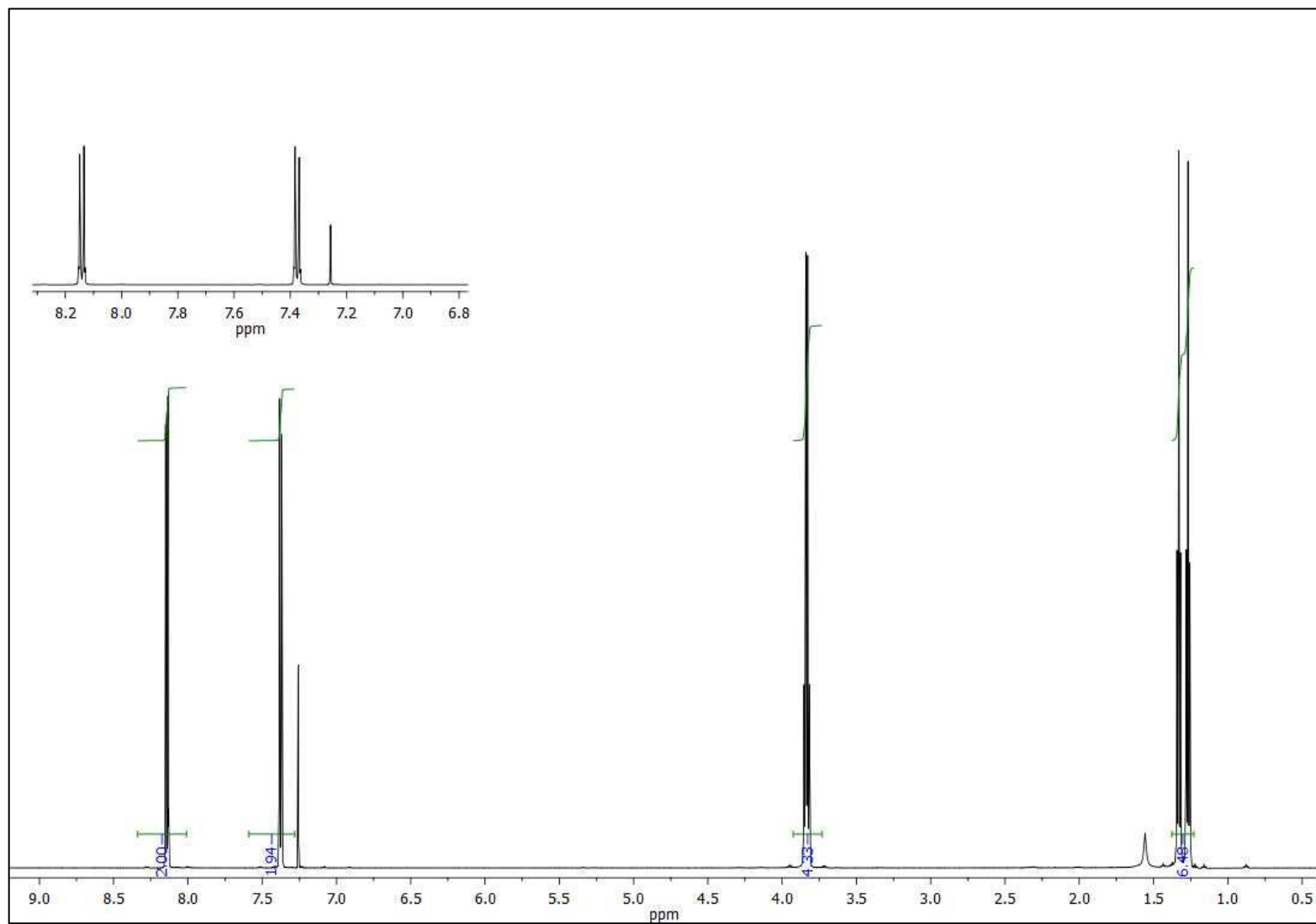


Figure 6 (Appendix). ^1H NMR spectrum of bis(*N,N*-diethyl-*N'*-*p*-chloro-benzoylthioureato)palladium(II) in CDCl_3 and at 25°C .

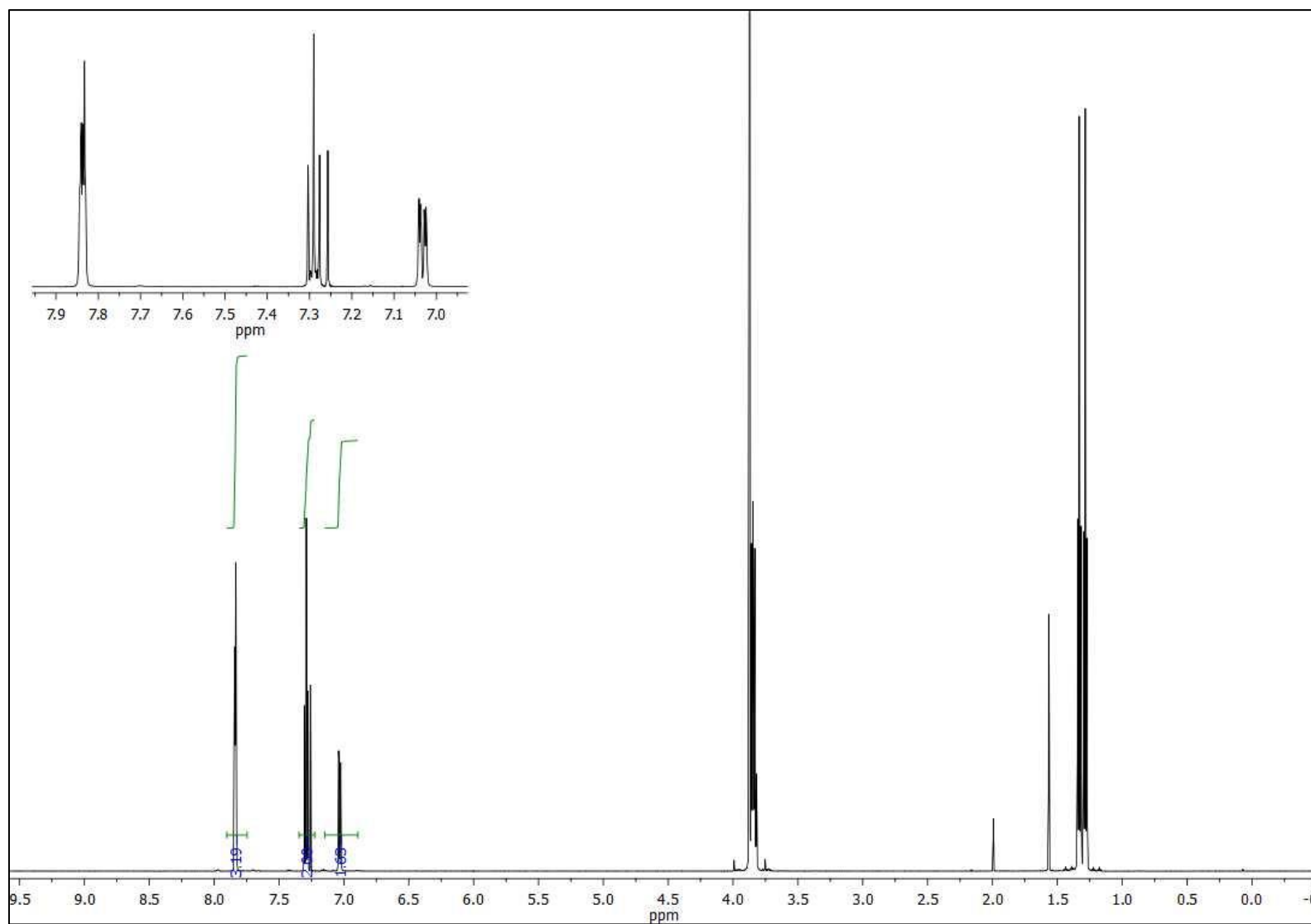


Figure 7 (Appendix). ^1H NMR spectrum of bis(*N,N*-diethyl-*N'*-*p*-methoxy-benzoylthioureato)palladium(II) in CDCl_3 and at 25°C .

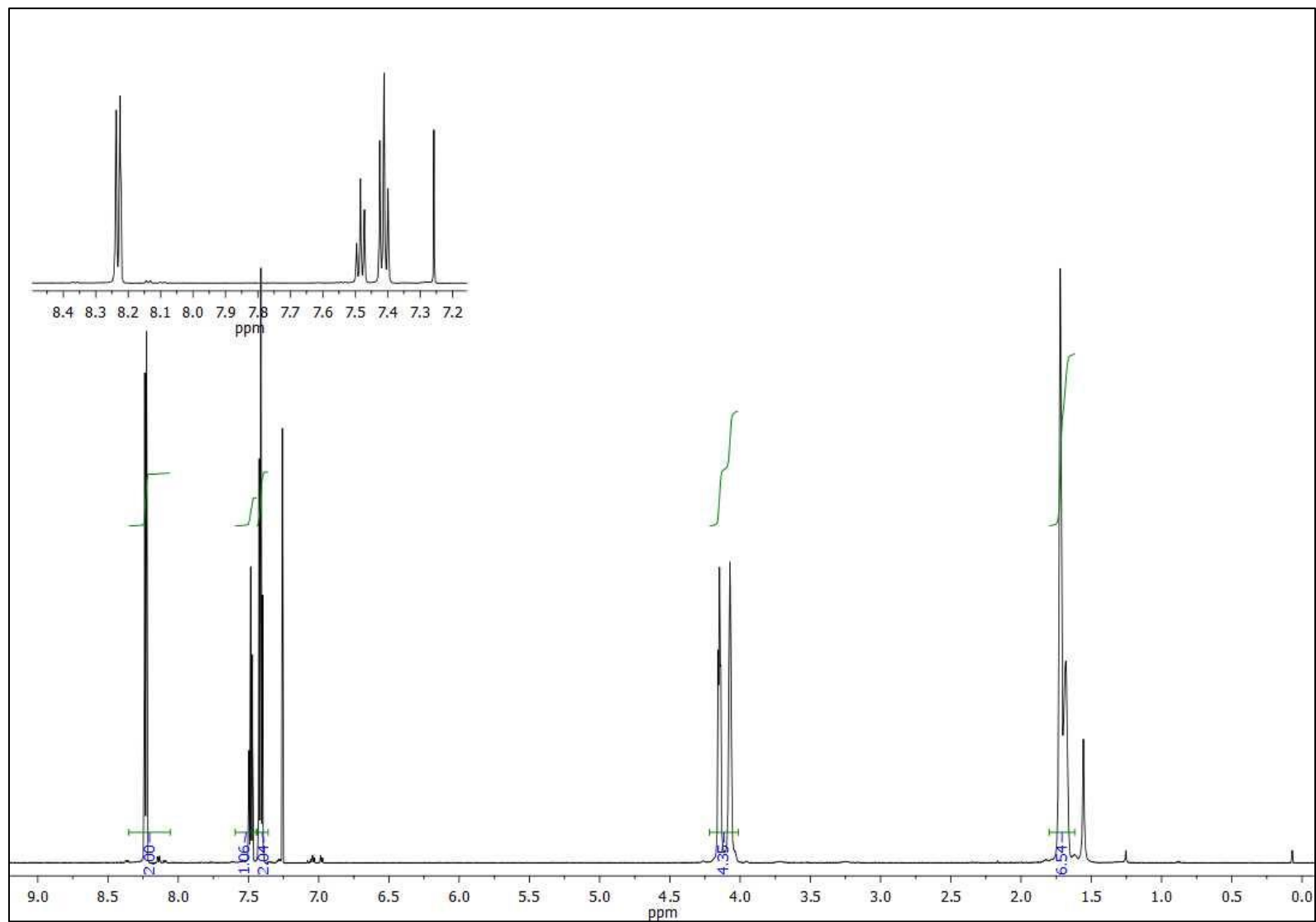


Figure 8 (Appendix). ^1H NMR spectrum of bis(*N*-piperidyl-*N'*-benzoylthioureato)palladium(II) in CDCl_3 and at 25°C .

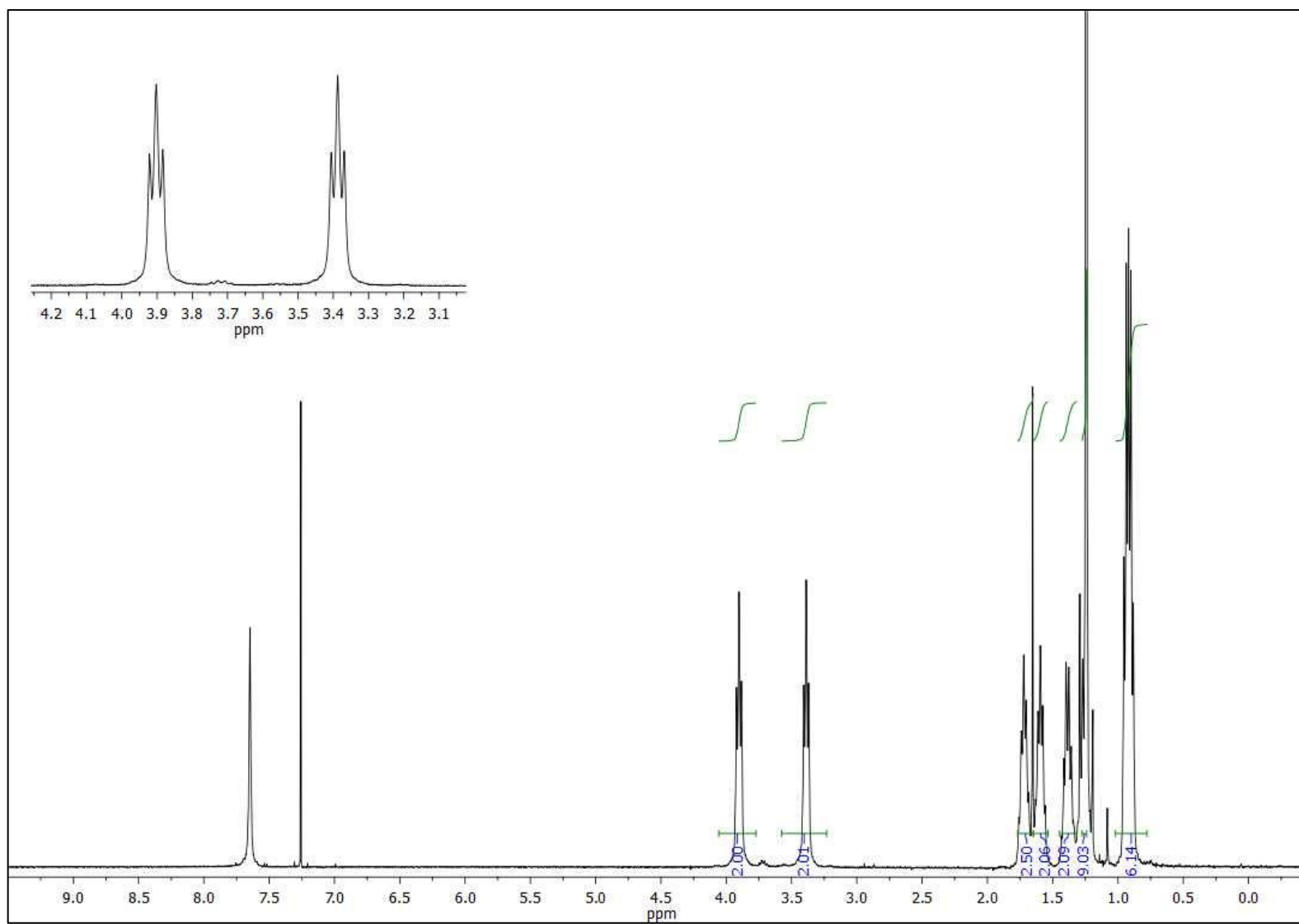


Figure 9 (Appendix). ^1H NMR spectrum of *N,N*-dibutyl-*N'*-(2,2-dimethylpropanoyl)thiourea in CDCl_3 and at 25°C .

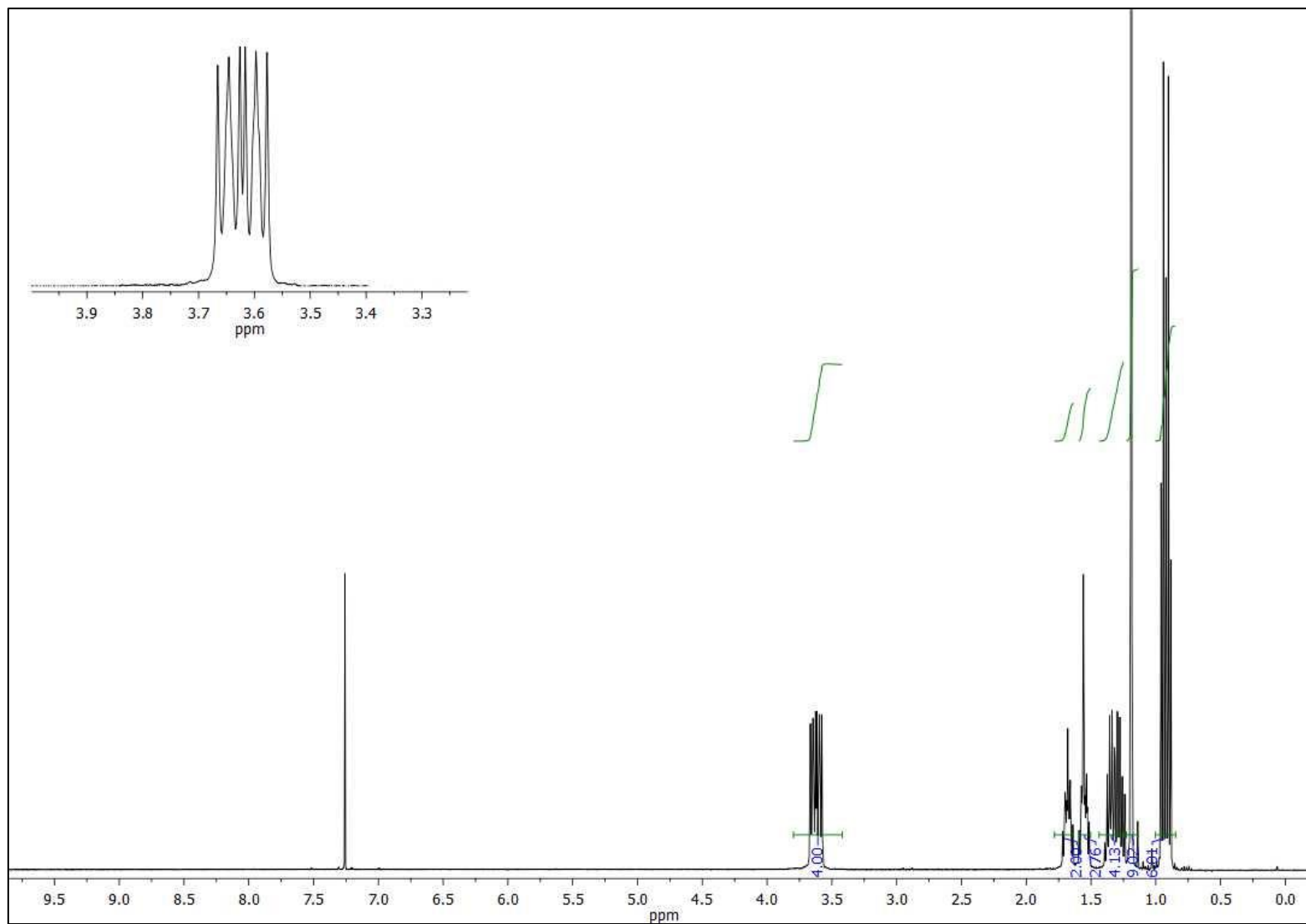


Figure 10 (Appendix). ^1H NMR spectrum of bis(*N,N*-dibutyl-*N'*-(2,2-dimethylpropanoyl)thioureato)palladium(II) in CDCl_3 and at 25°C .

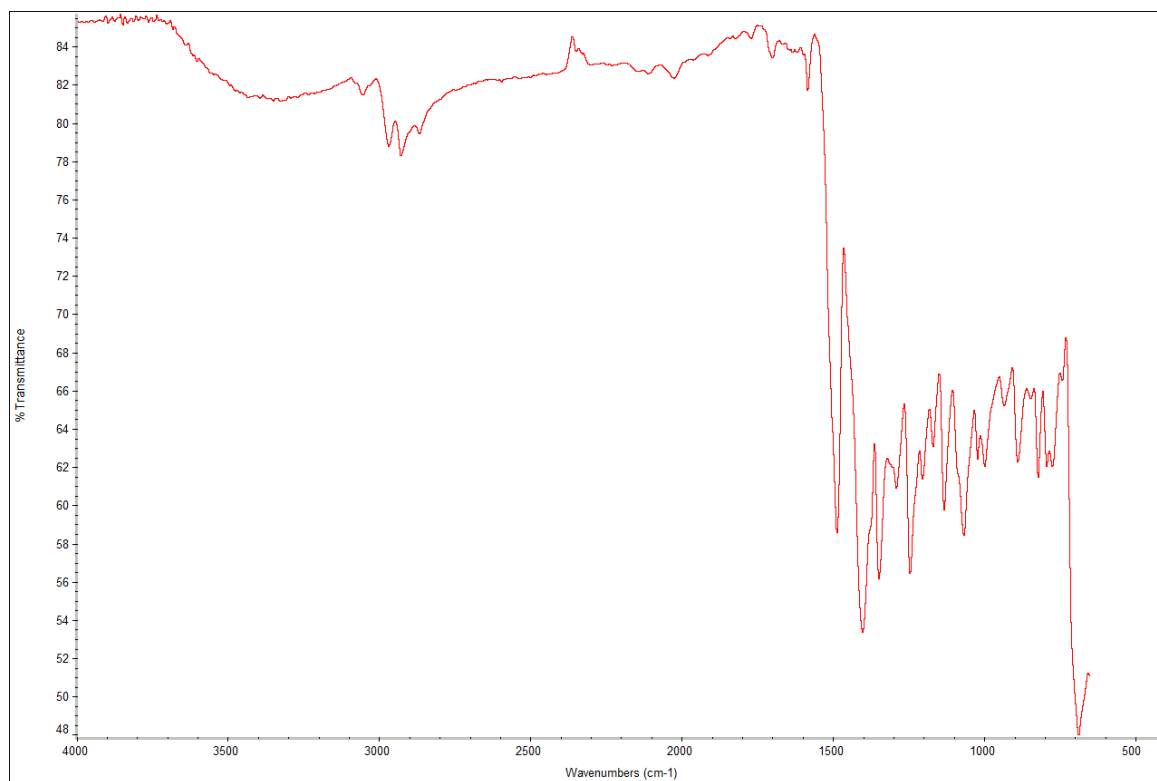


Figure 11 (Appendix). FT-IR spectrum of tris(*N,N*-diethyl-*N'*-benzoylthioureato)iridium(III).

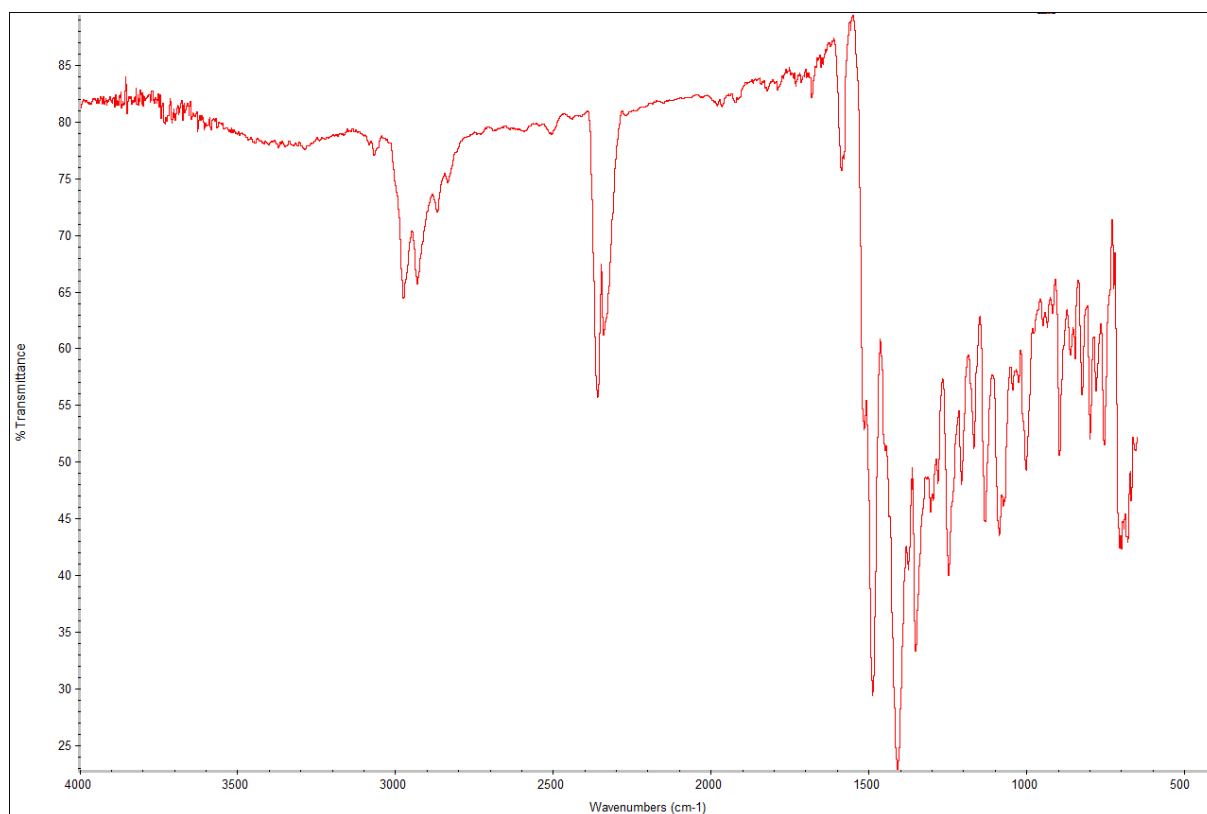


Figure 12 (Appendix). FT-IR spectrum of bis(*N,N*-diethyl-*N'*-benzoylthioureato)platinum(II).

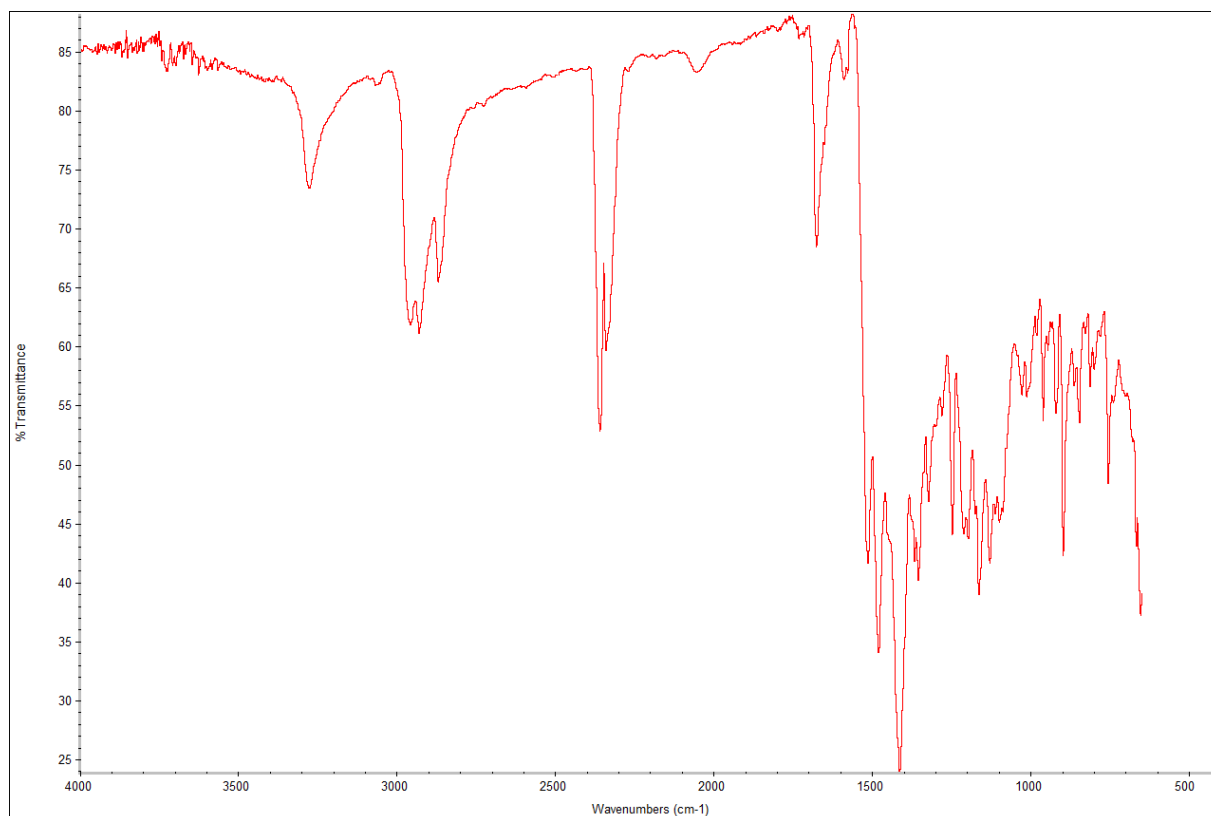


Figure 13 (Appendix). FT-IR spectrum of *N*-pirrolidyl-*N'*-(2,2-dimethylpropanoyl)thiourea.

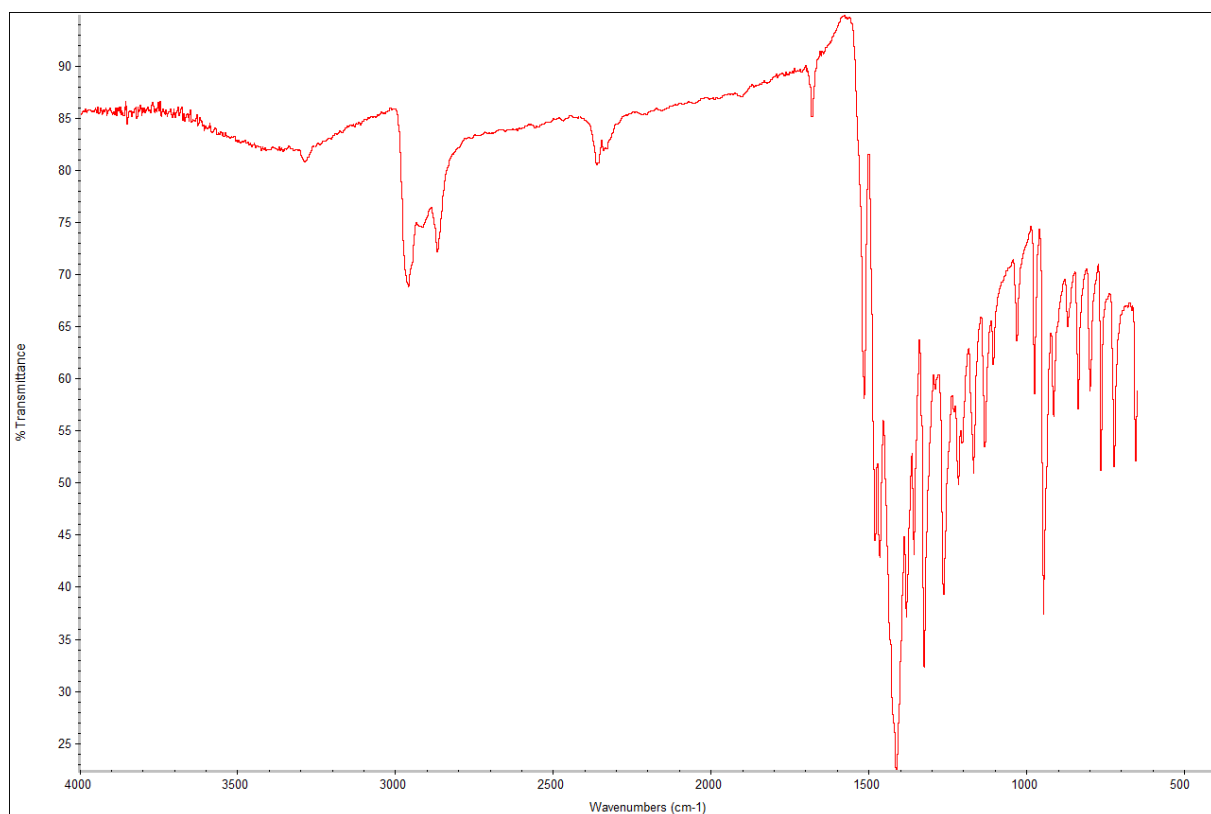


Figure 14 (Appendix). FT-IR spectrum of bis(*N*-pirrolidyl-*N'*-(2,2-dimethylpropanoyl)thioureato)palladium(II).

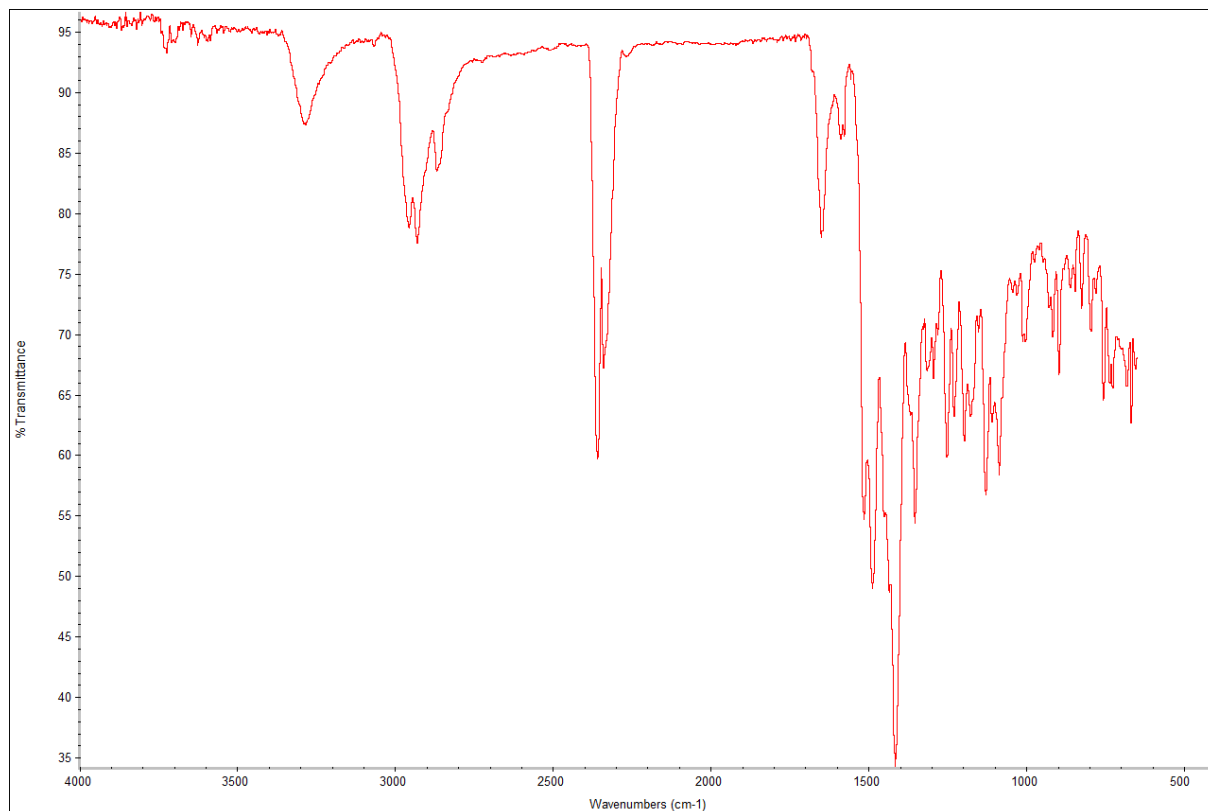


Figure 15 (Appendix). FT-IR spectra of *N,N*-dibutyl-*N'*-(2,2-dimethylpropanoyl)thiourea.

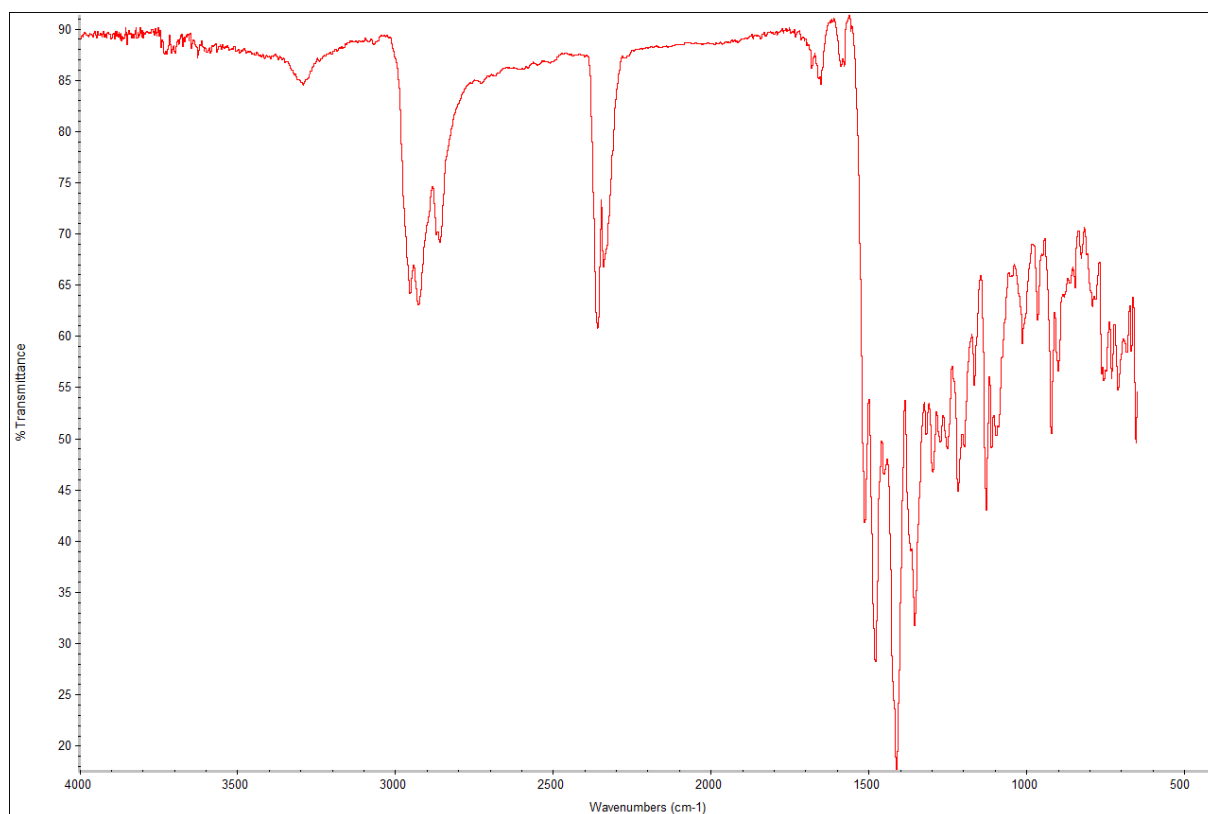


Figure 16 (Appendix). FT-IR spectrum of bis(*N,N*-dibutyl-*N'*-(2,2-dimethylpropanoyl)thioureato)palladium(II).

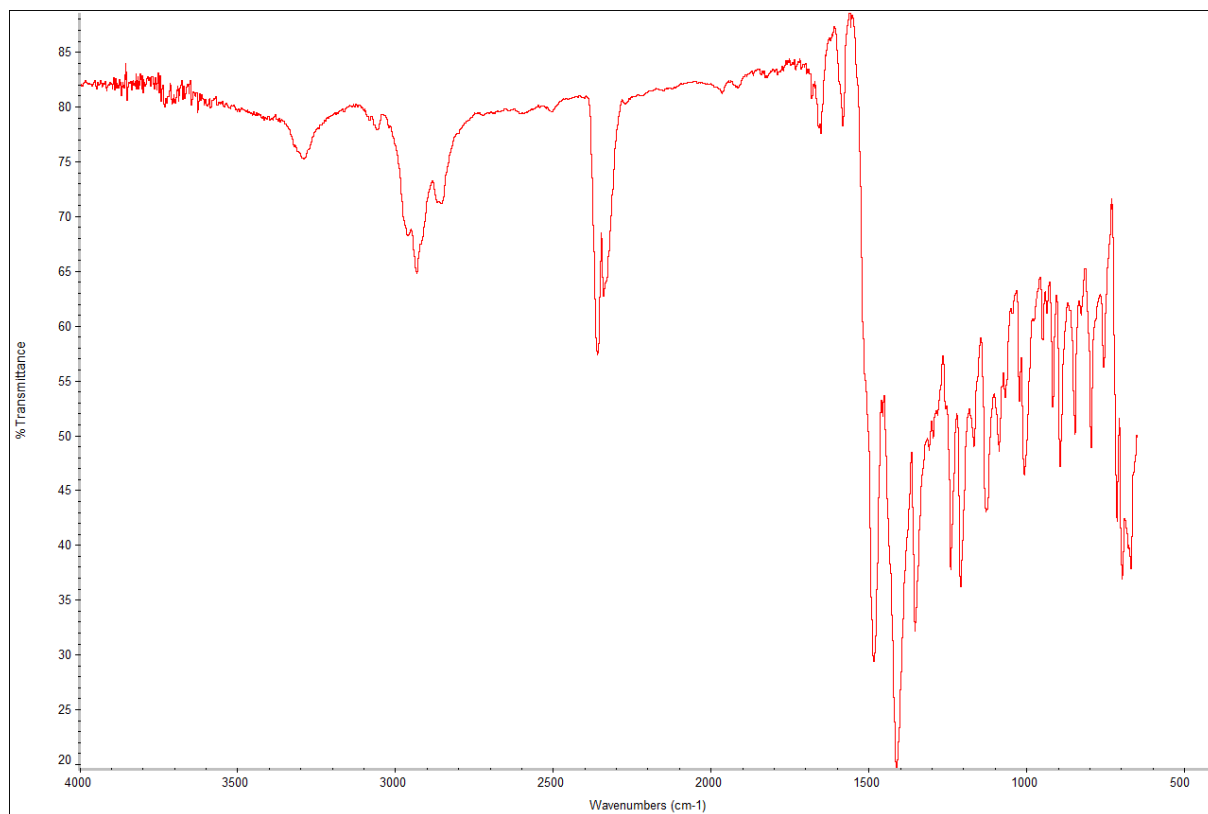


Figure 17 (Appendix). FT-IR spectrum of bis(*N*-piperidyl-*N'*-benzoylthioureato)palladium(II).

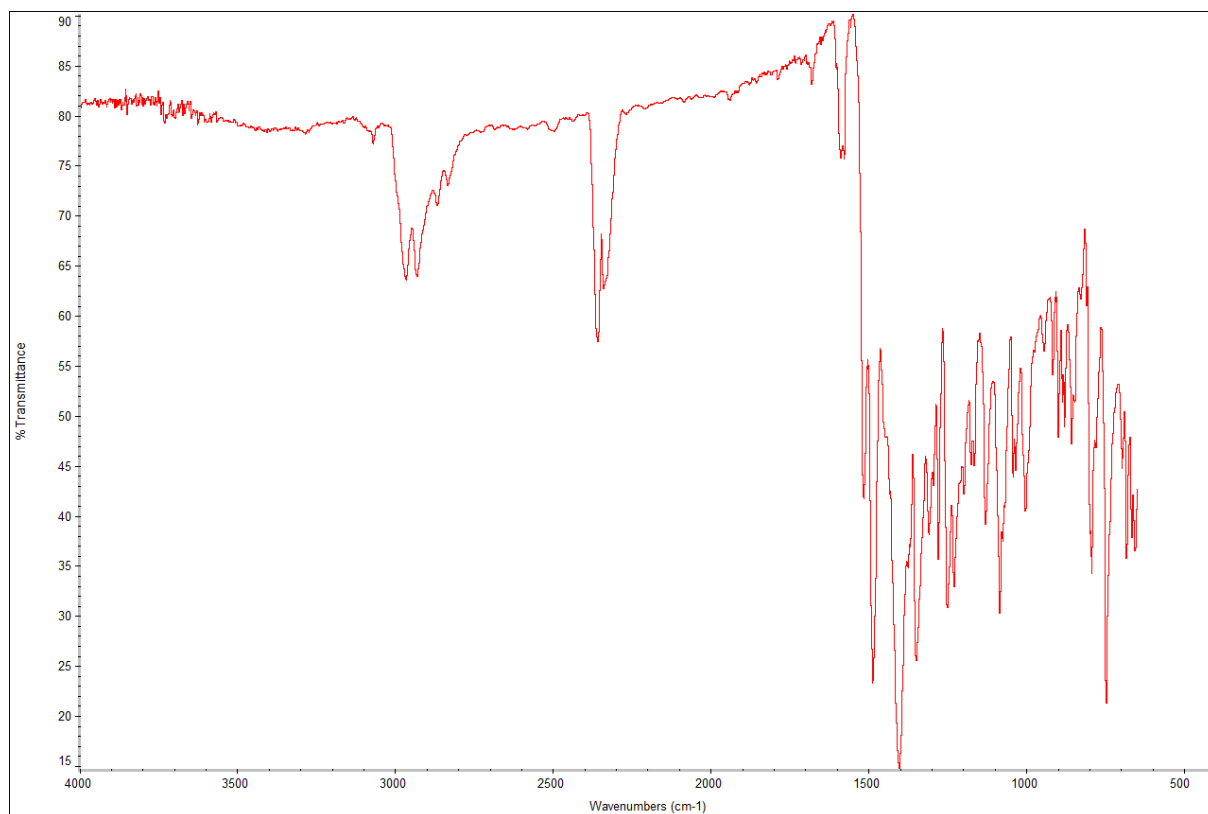


Figure 18 (Appendix). FT-IR spectrum of bis(*N,N*-diethyl-*N'*-*p*-methoxy-benzoylthioureato)palladium(II).

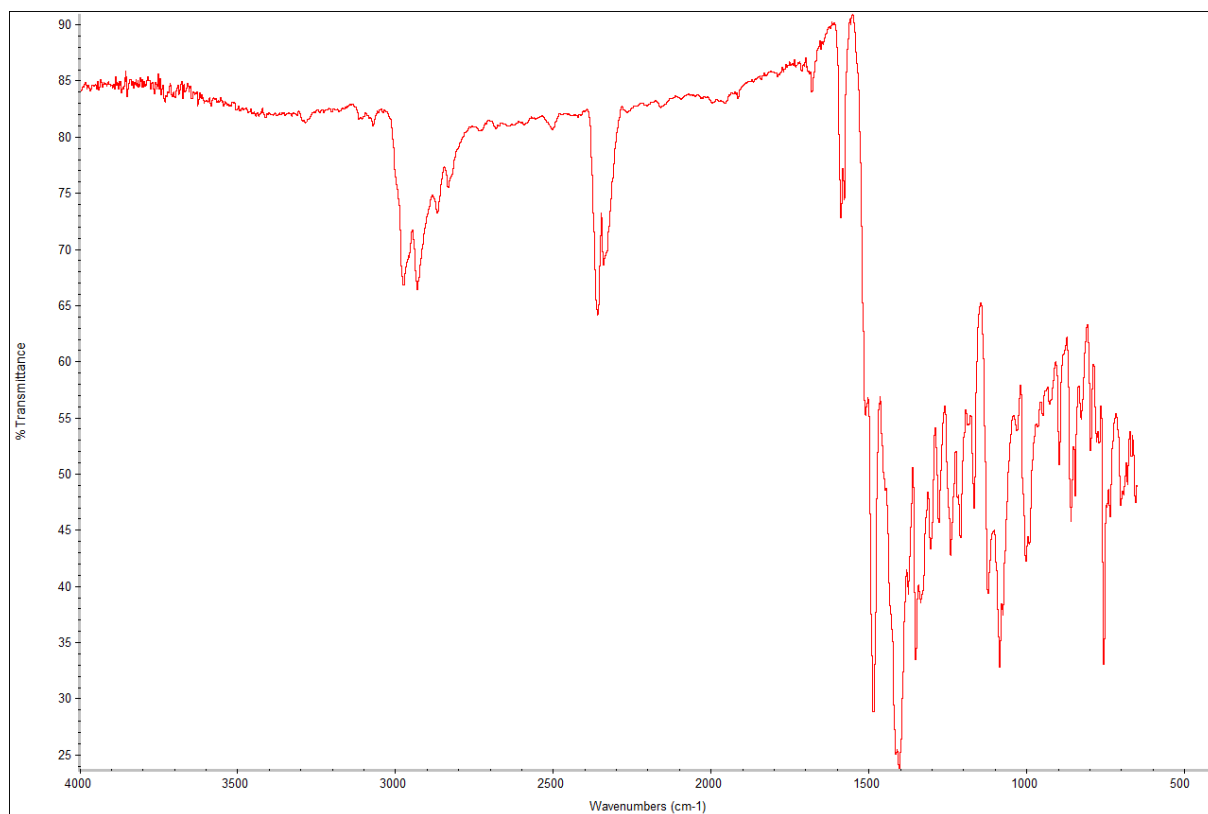


Figure 19 (Appendix). FT-IR spectra of bis(*N,N*-diethyl-*N'*-3,4,5-trimethoxybenzoylthioureato)palladium(II).

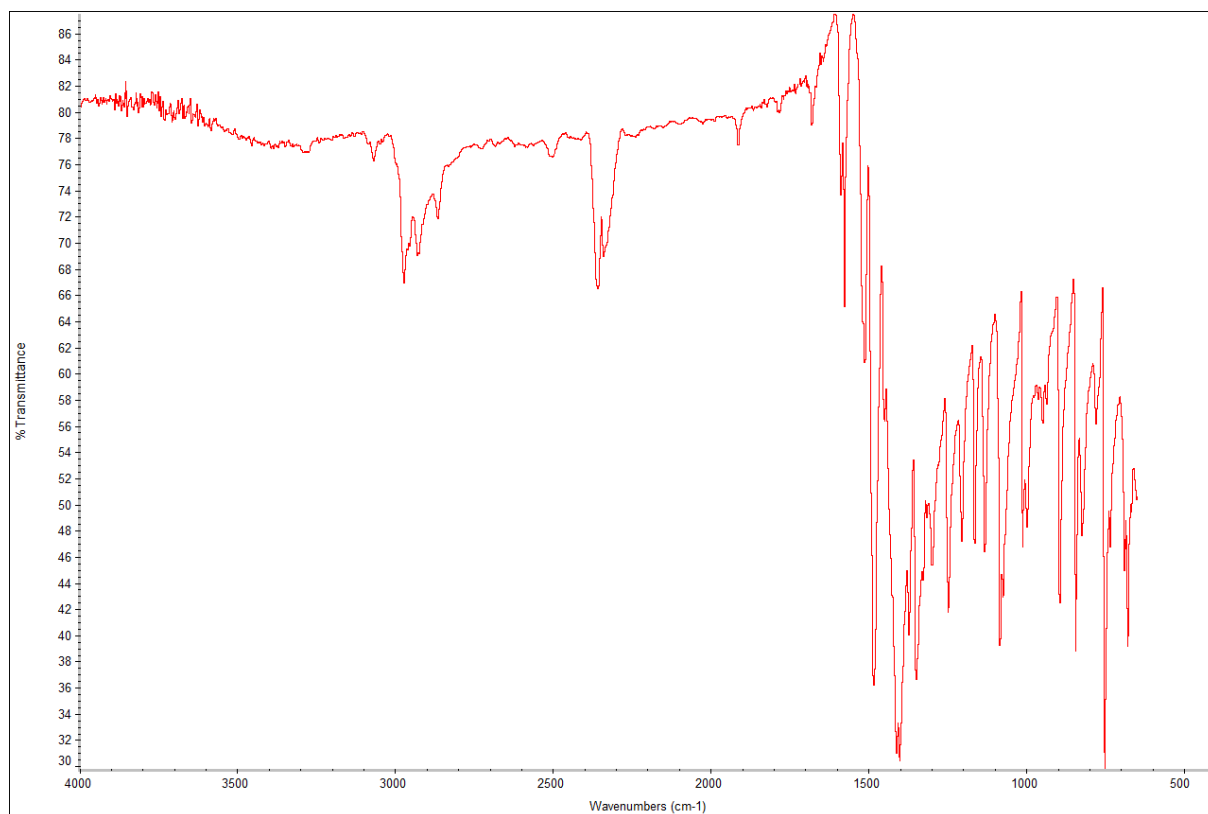


Figure 20 (Appendix). FT-IR spectrum of bis(*N,N*-diethyl-*N'*-*p*-chloro-benzoylthioureato)palladium(II).

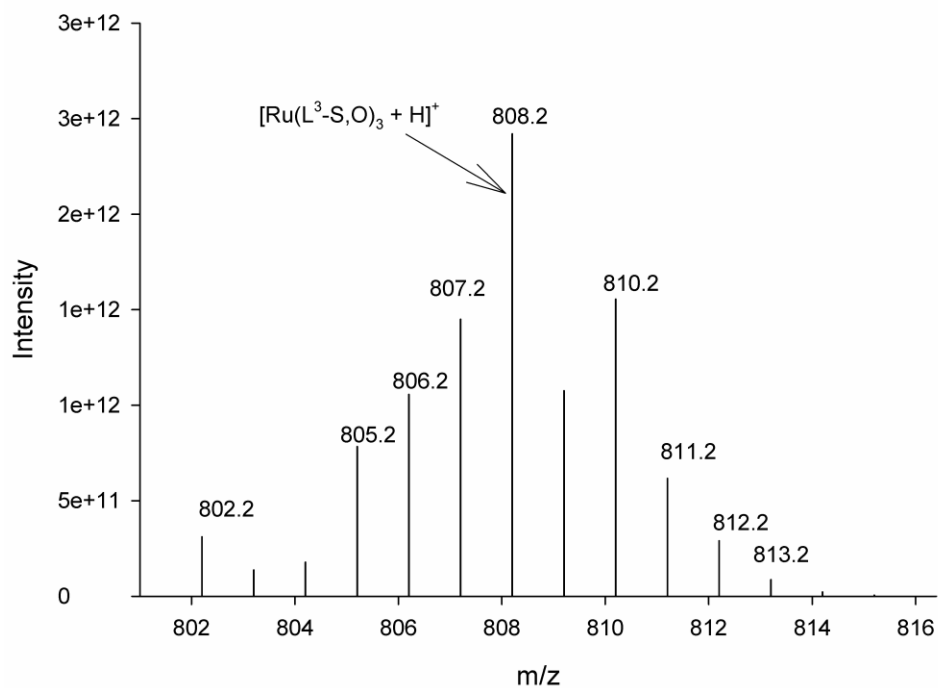


Figure 21 (Appendix). Simulated Mass spectrum of tris(*N,N*-diethyl-*N'*-benzoylthioureato)ruthenium(III).

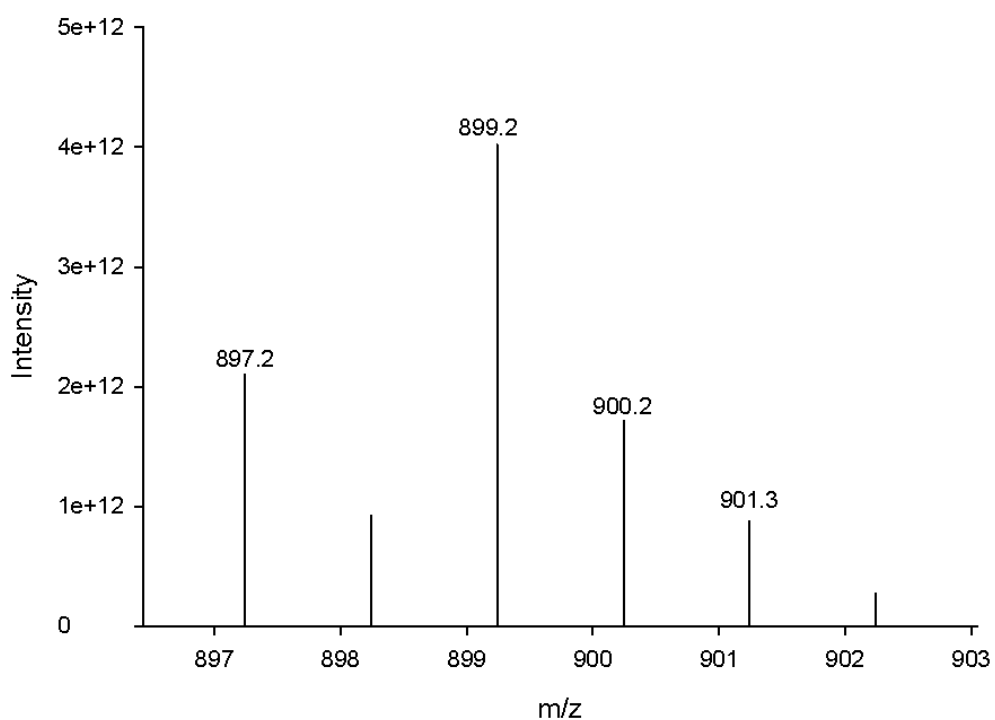


Figure 22 (Appendix). Simulated Mass spectrum of tris(*N,N*-diethyl-*N'*-benzoylthioureato)iridium(III).

